Published for SISSA by Springer

Received: December 23, 2019
Revised: February 28, 2020
Accepted: March 1, 2020
Published: March 30, 2020

Measurement of isolated-photon plus two-jet production in pp collisions at $\sqrt{s} = 13$ TeV with the ATLAS detector

The ATLAS collaboration

E-mail: atlas.publications@cern.ch

Abstract: The dynamics of isolated-photon plus two-jet production in pp collisions at a centre-of-mass energy of 13 TeV are studied with the ATLAS detector at the LHC using a dataset corresponding to an integrated luminosity of 36.1 fb^{-1}. Cross sections are measured as functions of a variety of observables, including angular correlations and invariant masses of the objects in the final state, $\gamma + \text{jet} + \text{jet}$. Measurements are also performed in phase-space regions enriched in each of the two underlying physical mechanisms, namely direct and fragmentation processes. The measurements cover the range of photon (jet) transverse momenta from 150 GeV (100 GeV) to 2 TeV. The tree-level plus parton-shower predictions from Sherpa and Pythia as well as the next-to-leading-order QCD predictions from Sherpa are compared with the measurements. The next-to-leading-order QCD predictions describe the data adequately in shape and normalisation except for regions of phase space such as those with high values of the invariant mass or rapidity separation of the two jets, where the predictions overestimate the data.

Keywords: Hadron-Hadron scattering (experiments), Hard scattering, Jets, Photon production

ArXiv ePrint: 1912.09866

https://doi.org/10.1007/JHEP03(2020)179

JHEP03(2020)179

Contents

JHEP03(2020)179

1 Introduction

The production of prompt photons[1] in association with two jets in proton-proton collisions, $pp \to \gamma + \text{jet} + \text{jet} + \text{X}$, provides a means of testing perturbative QCD (pQCD) predictions. Measurements of the angular correlations between the photon and each of the jets as well as between the two jets can be used to probe the dynamics of the hard-scattering process. In addition, measurements of the invariant-mass distributions of the dijet system and the photon plus dijet system are sensitive to the dynamics of the hard interaction. A comprehensive study of the observables describing this final state is of relevance for the development of pQCD calculations as well as for the tuning of Monte Carlo (MC) models.

Prompt-photon plus two-jet production proceeds via two mechanisms (see figure 1): direct processes, in which the photon originates from the hard interaction, and fragmentation processes, in which the photon arises from the fragmentation of a high transverse momentum[2] (p_{T}) parton [1, 2]. The direct and fragmentation contributions are well defined only at leading order (LO) in QCD; at higher orders this distinction is no longer possible. Furthermore, pure electroweak processes or electroweak virtual corrections are expected to play an important role for photon transverse energies at the TeV scale [3–6] and dijet configurations with large invariant mass and large separation in rapidity.

Measurements of prompt-photon production in a final state with accompanying hadrons necessitate an isolation requirement on the photon to minimise the large multi-jet background where hadrons in jets decay into photons. The production of isolated photons in association with jets in pp collisions at $\sqrt{s} = 7$, 8 and 13 TeV was studied by ATLAS [7–10] and CMS [11–15]. Previous measurements of the production cross sections of photons accompanied by two jets were done for angular correlations and the transverse momenta of the photon and the jets at $\sqrt{s} = 8$ TeV [9]. With the increase in centre-of-mass energy to 13 TeV, new observables have been introduced to explore the dynamics where electroweak contributions could be relevant, in particular, the invariant mass of the two jets and the invariant mass of the photon-jet-jet system.

Measurements of photon plus two-jet production provide a deeper understanding of the dynamics of the underlying processes and complement the recent measurements of photon plus one-jet production at 13 TeV [10]. The analysis presented here includes the study of the kinematics of the photon plus two-jet system via the measurement of the cross section as a function of the leading-photon transverse energy (E_{T}^{γ}), and of the transverse momentum ($p_{\text{T}}^{\text{jet}}$) and rapidity ($y^{\text{jet}}$) of each of the two jets. The dynamics of the photon plus two-jet system is studied by measuring the azimuthal angular separation between the photon and each of the jets ($\Delta\phi^{\gamma-\text{jet}}$), the difference in rapidity between the photon and each of the jets ($\Delta y^{\gamma-\text{jet}}$), the invariant mass of the dijet system ($m^{\text{jet–jet}}$), the azimuthal angular separation

[1] All photons that are not produced in hadron decays are considered to be 'prompt'.

[2] ATLAS uses a right-handed coordinate system with its origin at the nominal interaction point (IP) in the centre of the detector and the z-axis along the beam pipe. The x-axis points from the IP to the centre of the LHC ring, and the y-axis points upwards. Cylindrical coordinates (r, ϕ) are used in the transverse plane, ϕ being the azimuthal angle around the z-axis. The transverse energy is defined as $E_{\text{T}} = E \sin\theta$, where E is the energy and θ is the polar angle. The pseudorapidity is defined as $\eta = -\ln\tan(\theta/2)$ and the angular distance is measured in units of $\Delta R \equiv \sqrt{(\Delta\eta)^2 + (\Delta\phi)^2}$.

JHEP03(2020)179

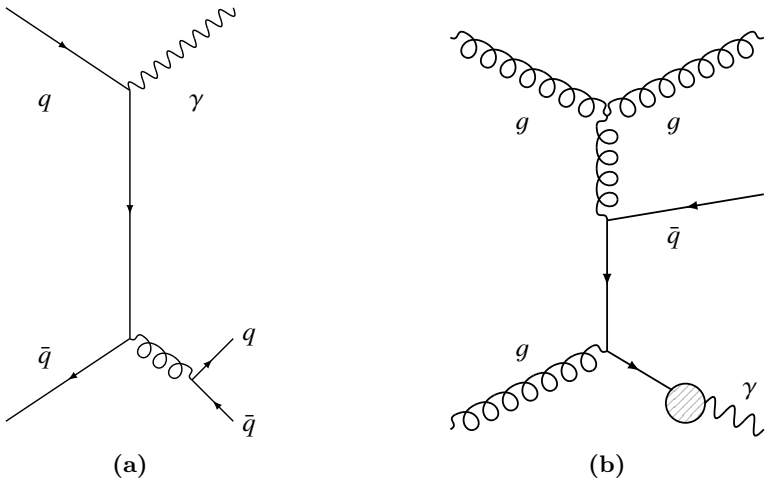

Figure 1. Examples of diagrams for γ + jet + jet production through (a) direct-photon and (b) fragmentation-photon processes.

between the two jets ($\Delta\phi^{\text{jet–jet}}$), the difference in rapidity between the two jets ($\Delta y^{\text{jet–jet}}$) and the invariant mass of the photon-jet-jet system ($m^{\gamma\text{–jet–jet}}$). Measurements of the final state γ + jet + jet have the advantage that the second jet is explicitly identified and the interplay between the two underlying production mechanisms can be tested more directly than in the γ + jet final state. The two underlying production mechanisms exhibit distinct features in kinematic variables as well as in angular correlations or invariant masses of the objects in the final state. For example, the spectrum in E_{T}^{γ} ($p_{\text{T}}^{\text{jet}}$, $m^{\text{jet–jet}}$) is expected to be harder (softer) for direct processes than for fragmentation processes; as another example, angular correlations such as $\Delta\phi^{\text{jet–jet}}$ are expected to be different for the two processes, with the two jets being closer to each other in direct processes than in fragmentation processes. These distinct features arise from the matrix elements of the two processes and the fraction of the centre-of-mass energy of the colliding partons carried away by the final-state photon [16]. In order to enhance the sensitivity to the two underlying mechanisms, measurements are performed in two complementary regions of phase space, in addition to the inclusive phase space, by selecting those events in which E_{T}^{γ} is larger (smaller) than the leading (sub-leading) jet p_{T}.[3] This separation allows a more in-depth study of the direct and fragmentation contributions since it is performed in terms of kinematic variables and, therefore, does not rely on distinguishing between direct and fragmentation processes using a MC generator. Furthermore, the photon is required to be isolated and the distance in the η–ϕ plane between the photon and each of the jets is required to be larger than 0.8; the region of phase space in which a jet is close to the photon is removed to avoid a bias in the photon isolation energy as well as to suppress the dependence on the modelling of the fragmentation component in that region. The analysis is performed using 36.1 fb^{-1} of ATLAS data at $\sqrt{s} = 13$ TeV taken during 2015 and 2016. The predictions of the tree-level plus parton shower models of Pythia [17] and Sherpa [18], as well as the next-to-leading-order (NLO) QCD predictions from Sherpa [19–23], are compared with the measurements.

[3]The leading (sub-leading) jet is the one with (next-to) highest $p_{\text{T}}^{\text{jet}}$.

JHEP03(2020)179

2 ATLAS detector

The ATLAS experiment uses a multipurpose particle detector [24] with a forward-backward symmetric cylindrical geometry. It consists of an inner tracking detector surrounded by a thin superconducting solenoid, electromagnetic and hadronic calorimeters, and a muon spectrometer incorporating three large superconducting toroidal magnets. The inner-detector system is immersed in a 2 T axial magnetic field and provides charged-particle tracking in the range $|\eta| < 2.5$. The high-granularity silicon pixel detector is closest to the interaction region and provides four measurements per track; the innermost layer, known as the insertable B-layer [25, 26], provides high-resolution hits at small radius to improve the tracking performance. The pixel detector is followed by a silicon microstrip tracker, which typically provides four three-dimensional space-point measurements per track. These silicon detectors are complemented by a transition radiation tracker, which enables radially extended track reconstruction up to $|\eta| = 2.0$. The calorimeter system covers the range $|\eta| < 4.9$. Within the region $|\eta| < 3.2$, electromagnetic (EM) calorimetry is provided by barrel and endcap high-granularity lead/liquid-argon (LAr) EM calorimeters, with an additional thin LAr presampler covering $|\eta| < 1.8$ to correct for energy loss in material upstream of the calorimeters; for $|\eta| < 2.5$, the EM calorimeter is divided into three layers in depth. Hadronic calorimetry is provided by a steel/scintillator-tile calorimeter, segmented into three barrel structures within $|\eta| < 1.7$, and two copper/LAr hadronic endcap calorimeters, which cover the region $1.5 < |\eta| < 3.2$. The solid-angle coverage is completed out to $|\eta| = 4.9$ with forward copper/LAr and tungsten/LAr calorimeter modules, which are optimised for EM and hadronic measurements, respectively. Events are initially selected using a first-level trigger implemented in custom electronics, which reduces the event-acceptance rate from the maximum bunch crossing rate of 40 MHz to a design value of 100 kHz using a subset of detector information. Software algorithms with access to the full detector information are then used in the high-level trigger to yield a recorded event rate of about 1 kHz [27].

3 Data selection

The data used in this analysis were collected with the ATLAS detector during the pp collision running periods of 2015 and 2016, when the LHC operated at a centre-of-mass energy of $\sqrt{s} = 13$ TeV. Only events taken during stable beam conditions and satisfying detector and data-quality requirements [28], which include the calorimeters and inner tracking detectors being in nominal operation, are considered. The total integrated luminosity of the collected sample amounts to $36.1 \pm 0.8\,\text{fb}^{-1}$. The uncertainty in the combined 2015–2016 integrated luminosity of 2.1% [29] is obtained using the LUCID-2 detector [30] for the primary luminosity measurements.

3.1 Event selection

Events were recorded using a single-photon trigger, with a transverse energy threshold of 140 GeV; 'loose' identification criteria for the photon, which are based on the shower

JHEP03(2020)179

shapes in the second layer of the electromagnetic calorimeter and on the fraction of energy deposited in the hadronic calorimeter, were also applied [31]. Events are required to have a reconstructed primary vertex [32]. If multiple primary vertices are reconstructed, the one with the highest sum of the p_{T}^2 of the associated tracks is selected as the primary vertex.

3.2 Photon selection

The photon-candidate reconstruction, selection and calibration closely follow those reported in ref. [33] and are summarised in the following. Photon candidates are reconstructed from clusters of energy deposited in the electromagnetic calorimeter and classified [34] as unconverted photons (those candidates without a matching track or reconstructed conversion vertex in the inner detector) or converted photons (those candidates with a matching reconstructed conversion vertex or a matching track consistent with originating from a photon conversion).

The photon identification is primarily based on shower shapes in the calorimeter [34]. The information from the hadronic calorimeter and the lateral shower shape in the second layer of the EM calorimeter are used in an initial selection. The final 'tight' selection comprises more stringent criteria for these variables as well as requirements on the shower shapes in the first layer of the EM calorimeter. Small differences are observed in the average values of the shower-shape variables between data and simulation and are corrected for in simulated events before applying the photon identification criteria. The photon identification efficiencies are measured to be above 90% (95%) for unconverted (converted) photon candidates with $E_{\mathrm{T}}^{\gamma} > 150\,\mathrm{GeV}$.

The measurement of the photon energy is based on the energy collected in calorimeter cells in an area of size $\Delta\eta \times \Delta\phi = 0.075 \times 0.175$ in the barrel and 0.125×0.125 in the endcaps. The photon energy calibration procedure is described in ref. [35]. The uncertainty in the photon energy scale at $E_{\mathrm{T}}^{\gamma} = 150\,\mathrm{GeV}$ is in the range 0.4%–3.1% (0.4%–2.8%) for unconverted (converted) candidates depending on $|\eta^{\gamma}|$, being largest in the region $1.81 < |\eta^{\gamma}| < 2.37$.

The selection of isolated photons is based on the amount of transverse energy inside a cone of size $\Delta R = 0.4$ in the η–ϕ plane around the photon candidate, excluding an area of size $\Delta\eta \times \Delta\phi = 0.125 \times 0.175$ centred on the photon. The isolation transverse energy ($E_{\mathrm{T}}^{\mathrm{iso}}$), which is computed from topological clusters of calorimeter cells [36], is corrected for the leakage of the photon energy into the isolation cone and the estimated contributions from the underlying event (UE) and additional inelastic pp interactions (pile-up) [37]. The combined correction to $E_{\mathrm{T}}^{\mathrm{iso}}$ for the last two effects is computed on an event-by-event basis using the jet-area method [38] and typically amounts to 3.5 GeV (1.3 GeV) for $|\eta^{\gamma}| < 1.37$ ($1.56 < |\eta^{\gamma}| < 2.37$). *In situ* corrections to $E_{\mathrm{T}}^{\mathrm{iso}}$ are applied in simulated events such that the peak position in the $E_{\mathrm{T}}^{\mathrm{iso}}$ distribution coincides with that in the data. After corrections, $E_{\mathrm{T}}^{\mathrm{iso}}$ is required to be less than $E_{\mathrm{T,cut}}^{\mathrm{iso}} \equiv 0.0042 \cdot E_{\mathrm{T}}^{\gamma} + 4.8$ GeV.

Events with at least one isolated photon candidate with $E_{\mathrm{T}}^{\gamma} > 150\,\mathrm{GeV}$ and $|\eta^{\gamma}| < 2.37$ are selected. Candidates in the region $1.37 < |\eta^{\gamma}| < 1.56$, which includes the transition region between the barrel and endcap calorimeters, are not considered. In events with more

JHEP03(2020)179

than one photon candidate satisfying the selection criteria, only the highest-E_{T}^{γ} (leading) photon is considered for further study.

3.3 Jet selection

The anti-k_t algorithm [39, 40] with radius parameter $R = 0.4$ is used to reconstruct jets. Topological clusters of calorimeter cells are used as input (jet constituents). The calorimeter cell energies are measured at the EM scale, which corresponds to the energy deposited by electromagnetically interacting particles. The jet four-momenta are computed from the sum of the jet-constituent four-momenta, treating each as a four-vector with zero mass. At this stage, the jet four-momentum values refer to the EM energy scale.

The calibration of the jets is performed following the methods described in ref. [41] and is discussed below. The four-momentum of jets is recalculated to point to the selected primary vertex of the event rather than the centre of the detector. The jet-area method is then used on a jet-by-jet basis [42] to subtract the contributions from the UE and pile-up. Subsequently, a calibration of the jet energy and direction is applied that corrects the reconstructed jet four-momentum to the particle level. For this purpose, simulated events are employed and the same jet algorithm used on data is applied to the generated stable particles. Stable particles are defined as those with a decay length $c\tau > 10\,\mathrm{mm}$. Muons, neutrinos and particles from pile-up interactions are excluded. The resulting jets are referred to as particle-level jets. Following the previous calibration, residual dependencies of the reconstructed jet energy on the longitudinal and transverse characteristics of the jet are observed. Corrections to reduce these dependencies are derived from simulated events, using global properties of the jet obtained from tracking information, calorimeter energy deposits and muon spectrometer information. These corrections are applied sequentially to the jet four-momentum while conserving the average jet response in the sample of dijet simulated events used to derive the corrections. These corrections improve the jet energy resolution and account for differences in energy response between quark- and gluon-initiated jets. Since the jet flavour composition of the final state $\gamma + \mathrm{jet} + \mathrm{jet}$ is, in principle, different from that used for the calibration (dijet events), the corrections help to reduce the dependence on the jet flavour composition assumed. In addition, systematic uncertainties due to the jet flavour response and composition are considered. A final correction is applied to account for differences in the jet response between data and simulations. The final correction is derived *in situ* from a combination of dijet, $\gamma + \mathrm{jet}$, $Z + \mathrm{jet}$ and multi-jet p_{T}-balance methods. Dijet events are used to correct the average response for forward jets to that for well-measured central jets. The other three *in situ* calibrations correct for differences between the average responses for central jets and well-measured reference objects. The uncertainty in the jet energy scale at $p_{\mathrm{T}}^{\mathrm{jet}} = 100\,\mathrm{GeV}$ varies in the range 1.5%–2% depending on the jet pseudorapidity.

Quality criteria are applied to reject events with jets reconstructed from calorimeter signals not originating from a pp collision [43]. These criteria suppress events with jets from beam-induced background due to proton losses upstream of the interaction point, cosmic-ray air showers overlapping with collision events and calorimeter noise from large-scale coherent noise or isolated pathological cells. Jets are required to have calibrated

JHEP03(2020)179

Requirements on photon	$E_{\mathrm{T}}^{\gamma} > 150\,\mathrm{GeV}$, $\lvert\eta^{\gamma}\rvert < 2.37$ (excluding $1.37 < \lvert\eta^{\gamma}\rvert < 1.56$) $E_{\mathrm{T}}^{\mathrm{iso}} < 0.0042 \cdot E_{\mathrm{T}}^{\gamma} + 4.8$ GeV (reconstruction level) $E_{\mathrm{T}}^{\mathrm{iso}} < 0.0042 \cdot E_{\mathrm{T}}^{\gamma} + 10$ GeV (particle level)		
Requirements on jets	at least two jets using anti-k_t algorithm with $R = 0.4$ $p_{\mathrm{T}}^{\mathrm{jet}} > 100\,\mathrm{GeV}$, $\lvert y^{\mathrm{jet}}\rvert < 2.5$, $\Delta R^{\gamma-\mathrm{jet}} > 0.8$		
Phase space	**total**	**fragmentation enriched** $E_{\mathrm{T}}^{\gamma} < p_{\mathrm{T}}^{\mathrm{jet2}}$	**direct enriched** $E_{\mathrm{T}}^{\gamma} > p_{\mathrm{T}}^{\mathrm{jet1}}$
Number of events	755 270	111 666	386 846

Table 1. Phase-space regions for the measurements and predictions. The number of data events selected in each phase space is also shown.

transverse momenta greater than 100 GeV and rapidity $|y^{\mathrm{jet}}| < 2.5$. Jets overlapping with the photon candidate are not considered if the jet axis lies within a cone of size $\Delta R = 0.8$ around the photon candidate; this requirement prevents any overlap between the photon isolation cone ($\Delta R = 0.4$) and the jet cone ($\Delta R = 0.4$). Finally, the event is selected if there are at least two jets (leading and sub-leading jets) satisfying the requirements above. The threshold $p_{\mathrm{T}}^{\mathrm{jet}} = 100\,\mathrm{GeV}$ is chosen to avoid the increasingly large uncertainties in the jet energy scale for lower values of $p_{\mathrm{T}}^{\mathrm{jet}}$.

3.4 Data samples

The number of data events selected by the requirements listed in the previous subsections is 755 270. Three samples of events are selected according to the following criteria: a 'total' sample in which no further requirement is applied; a 'fragmentation-enriched' sample in which the photon is required to have $E_{\mathrm{T}}^{\gamma} < p_{\mathrm{T}}^{\mathrm{jet2}}$, where $p_{\mathrm{T}}^{\mathrm{jet2}}$ is the p_{T} of the sub-leading jet; and a 'direct-enriched' sample in which the photon is required to have $E_{\mathrm{T}}^{\gamma} > p_{\mathrm{T}}^{\mathrm{jet1}}$, where $p_{\mathrm{T}}^{\mathrm{jet1}}$ is the p_{T} of the leading jet. A summary of the requirements on the photon and the jets is given in table 1, together with the number of selected events in each data sample.

4 Monte Carlo simulations and Standard Model theory predictions

4.1 Signal Monte Carlo simulations

Samples of events were generated to study the characteristics of the $pp \to \gamma + \mathrm{jet} + \mathrm{jet} + \mathrm{X}$ signal events. The programs Pythia 8.186 [17] and Sherpa 2.1.1 [18] were used for the predictions. In both cases, the event generation is performed using tree-level matrix elements, with the inclusion of initial- and final-state parton showers. The Lund string model [44] in the case of Pythia and a modified version of the cluster model [45] in Sherpa are used to describe the fragmentation into hadrons. The LO NNPDF2.3 [46] parton distribution functions (PDFs) were used by Pythia while the NLO CT10 [47] PDFs were used by Sherpa to parameterise the proton structure. Both samples include a simulation of the UE. The event-generator parameter values were set according to the A14 tune for Pythia [48] and the CT10 tune for Sherpa.

JHEP03(2020)179

The Pythia simulation of the signal includes LO photon-plus-jet events from both the direct processes (the subprocesses $qg \to q\gamma$ and $q\bar{q} \to g\gamma$, called the 'hard' component) and the photon bremsstrahlung in LO QCD dijet events (called the 'bremsstrahlung' component). The bremsstrahlung component was modelled by final-state QED radiation arising from calculations of all $2 \to 2$ QCD processes. The Sherpa samples were generated with LO matrix elements for photon-plus-jet final states with up to three additional partons ($2 \to n$ processes with n from 2 to 5); the matrix elements were merged with the Sherpa parton shower [49] using the ME+PS@LO prescription. The bremsstrahlung component is accounted for in Sherpa through the matrix elements of $2 \to n$ processes with $n \geq 3$. In the generation of the Sherpa samples, a requirement on the photon isolation at the matrix-element level was imposed using the criterion defined in ref. [50]. This criterion, commonly called Frixione's criterion, requires the total transverse energy inside a cone of size $\mathcal{V}$ around the generated final-state photon, excluding the photon itself, to be below a certain threshold, $E_{\mathrm{T}}^{\mathrm{max}}(\mathcal{V}) = \epsilon E_{\mathrm{T}}^{\gamma}((1-\cos\mathcal{V})/(1-\cos\mathcal{R}))^{n}$, for all $\mathcal{V} < \mathcal{R}$, and is applied to avoid singularities in the matrix-elements calculation. The parameter values for the threshold were chosen to be $\mathcal{R} = 0.3$, $n = 2$ and $\epsilon = 0.025$. These values guarantee a selection loose enough to minimise possible biases from the application of the photon isolation requirement at reconstruction and particle levels (see table 1).[4] A possible bias is accounted for by a systematic uncertainty (see section 7.1.5) estimated from a comparison with Pythia samples, for which no photon isolation requirement is applied during the event generation. The Sherpa predictions from this computation are referred to as LO Sherpa.

Pile-up from additional pp collisions in the same and neighbouring bunch crossings was simulated by overlaying each MC event with a variable number of simulated inelastic pp collisions generated using Pythia 8.186 with the ATLAS set of tuned parameters for minimum-bias events (A2 tune) [51] and the MSTW2008LO PDF set [52]. The MC events are weighted to reproduce the distribution of the average number of interactions per bunch crossing observed in the data, referred to as 'pile-up reweighting'.

All the samples of generated events were passed through the Geant4-based [53] ATLAS detector- and trigger-simulation programs [54]. They are reconstructed and analysed with the same program chain as the data.

4.2 Background Monte Carlo simulations

The main background to isolated-photon events arises from jets misidentified as photons. This background, which is typically below 5%, is subtracted using an *in situ* technique, as described in section 5. The background from electrons or positrons misidentified as photons is estimated using MC samples generated with the program Sherpa 2.2.1 [19–21]. The $Z^{(*)}/\gamma^{*} \to e^{+}e^{-}$ and $W^{(*)} \to e\nu$ processes were generated with matrix elements calculated for up to two additional partons at NLO and up to four partons at LO.

[4] Since Frixione's criterion requires the upper limit on the transverse energy isolation to be exactly zero at $\mathcal{V} = 0$, the criterion cannot be strictly looser than any non-zero photon isolation requirement at reconstruction or particle level for all $\mathcal{V} < \mathcal{R}$.

JHEP03(2020)179

4.3 Next-to-leading-order pQCD predictions

The NLO pQCD predictions presented in this paper are computed using the program Sherpa 2.2.2 [19]. This program consistently combines parton-level calculations of $\gamma +$ (1, 2)-jet events at NLO and $\gamma +$ (3, 4)-jet events at LO [20, 21] supplemented with a parton shower [22] while avoiding double-counting effects [23]. A requirement on the photon isolation at the matrix-element level is imposed using Frixione's criterion with $\mathcal{R} = 0.1$, $n = 2$ and $\epsilon = 0.1$; for the Sherpa NLO calculations the parameters are fixed to looser values than for the LO calculations to further minimise any possible bias from the application of the photon isolation requirement at particle level. The NNLO NNPDF3.0 PDFs [55] are used in conjunction with the corresponding Sherpa default tuning. Dynamic factorisation and renormalisation scales are adopted and set equal to E_{T}^{γ}, as well as a dynamical merging scale with $\bar{Q}_{\mathrm{cut}} = 20\,\mathrm{GeV}$ [56]. The strong coupling constant is set to $\alpha_{\mathrm{s}}(m_Z) = 0.118$. Fragmentation into hadrons and simulation of the UE are made using the same models as for the LO Sherpa samples of simulated events (see section 4.1). All the Sherpa NLO predictions are based on the particle-level observables from this computation after applying the requirements listed in table 1. In particular, the photon isolation requirement is applied at particle level using the procedure described in section 6.

5 Signal extraction

5.1 Multi-jet background subtraction

The main background to prompt-photon production consists of multi-jet events where one jet typically contains a π^0 or η meson that carries most of the jet energy and is misidentified as a photon because it decays into an almost collinear photon pair. The multi-jet background estimation relies on an *in situ* method based on signal-suppressed control regions. The method uses the same two-dimensional sideband technique as in previous analyses [7, 8, 37, 57–59] and it is described briefly in the following. The background subtraction procedure is performed bin by bin for each distribution. Two variables, the photon identification quality and $E_{\mathrm{T}}^{\mathrm{iso}}$, are used to define the control regions for the background estimation. The photon candidate is classified as 'isolated' if $E_{\mathrm{T}}^{\mathrm{iso}} < E_{\mathrm{T,cut}}^{\mathrm{iso}}$ and as 'non-isolated' if $E_{\mathrm{T,cut}}^{\mathrm{iso}} + 2\ \mathrm{GeV} < E_{\mathrm{T}}^{\mathrm{iso}} < 50\,\mathrm{GeV}$. The non-isolated region is separated by 2 GeV from the isolated region to reduce the contamination from signal events. The upper bound in $E_{\mathrm{T}}^{\mathrm{iso}}$ is applied to avoid highly non-isolated photons; in this way, the determination of the signal yield does not depend on the description by the MC generators of the distribution of $E_{\mathrm{T}}^{\mathrm{iso}}$ for prompt photons with high values of $E_{\mathrm{T}}^{\mathrm{iso}}$. A photon candidate is classified as 'tight' if tight identification criteria are satisfied. It is classified as 'non-tight' if it fails at least one of four tight requirements on the shower-shape variables computed from the energy deposits in the first layer of the electromagnetic calorimeter, but satisfies the tight requirements listed below: the tight requirement on the total lateral shower width in the first layer, all the other tight identification criteria in other layers and the tight requirement on the leakage into the hadronic calorimeter [34].

JHEP03(2020)179

The two-dimensional plane defined by $E_{\mathrm{T}}^{\mathrm{iso}}$ and the tight/non-tight photon-identification variable is divided into four non-overlapping regions: the 'signal' region of tight isolated candidates (region A) and three background control regions of tight non-isolated (region B), isolated non-tight (region C) and non-isolated non-tight (region D) photon candidates. The signal yield N_A^{sig} in region A is determined by using the relation

$$N_A^{\mathrm{sig}} = N_A - R_{\mathrm{bg}} \cdot (N_B - f_B N_A^{\mathrm{sig}}) \cdot \frac{(N_C - f_C N_A^{\mathrm{sig}})}{(N_D - f_D N_A^{\mathrm{sig}})}, \tag{5.1}$$

where N_K, with $K = A, B, C, D$, is the number of events in region K and $R_{\mathrm{bg}} = N_A^{\mathrm{bg}} \cdot N_D^{\mathrm{bg}}/(N_B^{\mathrm{bg}} \cdot N_C^{\mathrm{bg}})$ is the so-called background correlation and is taken as $R_{\mathrm{bg}} = 1$ for the nominal results; N_K^{bg} with $K = A, B, C, D$ is the unknown number of background events in each region. Equation (5.1) takes into account the expected number of signal events in the three background control regions (N_K^{sig}) via the signal leakage fractions, $f_K = N_K^{\mathrm{sig}}/N_A^{\mathrm{sig}}$ with $K = B, C, D$, which are estimated using the MC simulations of the signal.

The signal purity, defined as N_A^{sig}/N_A, is typically above 95%. The use of Pythia or LO Sherpa samples to extract the signal leakage fractions leads to similar signal purities; the difference in the signal purity is taken as a systematic uncertainty (see section 7.1.5). The photon isolation and identification variables are assumed to be uncorrelated ($R_{\mathrm{bg}} = 1$) for background events. The dependence of the signal yield on this assumption is investigated in validation regions, which are defined within the background-enriched regions B and D. A study of R_{bg} in the validation regions, accounting for signal leakage using either the Pythia or LO Sherpa simulations, shows deviations from unity, ranging from 10% to 50%, which are then propagated through eq. (5.1) and taken as systematic uncertainties (see section 7.1.7).

5.2 Other backgrounds

The background from electrons or positrons misidentified as photons, mainly produced in Drell-Yan $Z^{(*)}/\gamma^* \to e^+e^-$ and $W^{(*)} \to e\nu$ processes, is also studied. Such events are largely suppressed by the photon selection. The remaining background contribution is estimated using MC samples of fully simulated events and found to be sub-percent for most of the phase space considered. No subtraction is performed and a systematic uncertainty equal to the size of the estimated background is assigned (see section 7.1.8).

6 Unfolding kinematic distributions to particle level

Cross sections for isolated-photon production in association with at least two jets are measured in the fiducial phase-space regions outlined in table 1. The differential cross sections are obtained through the formula

$$\frac{\mathrm{d}\sigma}{\mathrm{d}O}(i) = \frac{N^{\mathrm{unf,sig}}(i)}{\mathcal{L}\ \Delta O(i)},$$

where $\mathrm{d}\sigma/\mathrm{d}O(i)$ is the cross section as a function of observable O in bin i, $N^{\mathrm{unf,sig}}(i)$ is the unfolded number of background-subtracted data events in bin i and is obtained as described below, $\mathcal{L}$ is the integrated luminosity and $\Delta O(i)$ is the width of bin i.

JHEP03(2020)179

The particle-level isolation transverse energy of the photon is calculated by summing the transverse energy of all stable particles, except for muons and neutrinos, in a cone of size $\Delta R = 0.4$ around the photon direction after the contribution from the underlying event is subtracted. The same subtraction procedure used on data is applied at the particle level; the particles associated with the overlaid pp collisions are not considered. The particle-level requirement on $E_{\mathrm{T}}^{\mathrm{iso}}$ is determined using the Pythia and LO Sherpa MC samples by comparing the calorimeter isolation transverse energy with the particle-level isolation on an event-by-event basis. The effect of the experimental isolation requirement used in the data is found to be close to a particle-level requirement of $E_{\mathrm{T}}^{\mathrm{iso}}(\text{particle}) < 0.0042 \cdot E_{\mathrm{T}}^{\gamma} + 10$ GeV; the same requirement is obtained whether Pythia or LO Sherpa is used. Particle-level jets are reconstructed with the anti-k_t algorithm with $R = 0.4$ using all stable final-state particles as input; muons, neutrinos and particles from pile-up activity are excluded.

The efficiency of the selection, defined as the fraction of the events generated in the fiducial region that are also reconstructed in that region, is evaluated using MC simulations. The selection efficiency using LO Sherpa (Pythia) samples is 76% (76%), 74% (77%), 71% (70%) for the total, fragmentation- and direct-enriched phase-space regions, respectively.

The data distributions, after background subtraction, are unfolded to the particle level using an unfolding method [60] based on the iterative application of Bayes' theorem, as implemented in RooUnfold [61]. In this method, an unfolding matrix is constructed using the samples of simulated events. The unfolding matrix encapsulates the migrations across bin boundaries of the observable when switching between particle and reconstruction levels. The binning of the distributions is chosen according to the resolution in those variables and in some cases, such as at high E_{T}^{γ} or $p_{\mathrm{T}}^{\mathrm{jet}}$, larger bin sizes are used to reduce the statistical uncertainties in the data. There are observables that are filled once per event, such as E_{T}^{γ}, $m^{\mathrm{jet\text{–}jet}}$, $\Delta\phi^{\mathrm{jet\text{–}jet}}$, $|\Delta y^{\mathrm{jet\text{–}jet}}|$ and $m^{\gamma\text{–}\mathrm{jet\text{–}jet}}$, and observables which are filled twice per event, such as $p_{\mathrm{T}}^{\mathrm{jet}}$, $|y^{\mathrm{jet}}|$, $\Delta\phi^{\gamma\text{–}\mathrm{jet}}$ and $|\Delta y^{\gamma\text{–}\mathrm{jet}}|$. The unfolding matrix is filled with those events that pass the selection requirements at both the reconstruction and particle levels. In addition, the reconstructed jet (photon) is required to be matched to a particle-level jet (photon) within $\Delta R = 0.4$ (0.2). Corrections are also applied to take into account the fractions of events for which there is no matching either at particle or reconstruction level; the fraction of unmatched particle-level (reconstruction-level) events is typically in the range 20%–40% (5%–25%). In the evaluation of the systematic uncertainties (see section 7.1), modifications of the unfolding matrix and of the corrections are applied simultaneously in a consistent way. Four iterations of the unfolding procedure are performed. The nominal cross sections are measured using the signal leakage fractions and unfolding matrices from LO Sherpa since these simulations describe the shape of the distributions of the signal yield better than those of Pythia. The results obtained by unfolding the data with Pythia are used to estimate the model dependence and their deviations from the nominal results are taken as systematic uncertainties, as explained in section 7.1.5. The results of the Bayesian unfolding procedure are checked with a bin-by-bin method based on LO Sherpa simulations, giving consistent results; the systematic uncertainty due to the unfolding procedure is negligible.

JHEP03(2020)179

7 Experimental and theoretical uncertainties

7.1 Uncertainties in the cross-section measurements

The sources of systematic uncertainty that affect the measurements are the photon energy scale and resolution, the photon-identification efficiency, the photon-isolation modelling, the jet energy scale and resolution, the parton-shower and hadronisation model dependence, the definition of the background control regions, the identification and isolation correlation in the background, the background from electrons or positrons faking photons, the modelling of pile-up, the trigger efficiency and the luminosity measurement. These sources of uncertainty and their effects are described below.

7.1.1 Photon energy scale and resolution

The uncertainties in the photon energy scale and resolution are described in ref. [35]. The sources of uncertainty include: the uncertainty in the overall energy scale adjustment using $Z \to e^+e^-$ decays; the uncertainty in the non-linearity of the energy measurement at the calorimeter cell level; the uncertainty in the relative calibration of the different calorimeter layers; the uncertainty in the amount of material in front of the calorimeter; the uncertainty in the modelling of the reconstruction of photon conversions; the uncertainty in the modelling of the lateral shower shape; the uncertainty in the modelling of the sampling term;[5] and the uncertainty in the measurement of the constant term in Z-boson decays. The uncertainties are split into independent components to account for correlations and their η dependence. The individual sources of uncertainty are varied by $\pm 1\sigma$ in the MC simulations and propagated through the analysis separately, to maintain the full information about the correlations. The uncertainties are propagated to the cross sections by modifying the unfolding matrix, the unmatched fractions and the signal yields. The impact of the photon energy resolution uncertainty is much smaller than that of the photon energy scale uncertainty except for high E_{T}^{γ} ($E_{\mathrm{T}}^{\gamma} > 500\,\mathrm{GeV}$), low $m^{\mathrm{jet\text{–}jet}}$ ($m^{\mathrm{jet\text{–}jet}} < 400\,\mathrm{GeV}$) and low $\Delta\phi^{\mathrm{jet\text{–}jet}}$ ($\Delta\phi^{\mathrm{jet\text{–}jet}} < 0.6\,\mathrm{rad}$) in the fragmentation-enriched region. The resulting uncertainty in the measured cross sections is obtained by adding in quadrature all the individual components. For $\mathrm{d}\sigma/\mathrm{d}E_{\mathrm{T}}^{\gamma}$ this uncertainty increases from 0.5% at $E_{\mathrm{T}}^{\gamma} = 150\,\mathrm{GeV}$ to 6% at $E_{\mathrm{T}}^{\gamma} = 2\,\mathrm{TeV}$.

7.1.2 Photon-identification efficiency

Scale factors are applied to simulated events to match the efficiency for tight photon identification measured in data [34]. The uncertainties in the scale factors are propagated to the measured cross sections by modifying the unfolding matrix, the unmatched fractions and the signal yields. The resulting uncertainty in the measured cross sections is in the range 1.5%–2%.

[5] The relative energy resolution is parameterised as $\sigma(E)/E = a/\sqrt{E} \oplus b/E \oplus c$, where a is the sampling term, b is the noise term and c is the constant term.

JHEP03(2020)179

7.1.3 Photon-isolation modelling

In situ corrections to $E_{\mathrm{T}}^{\mathrm{iso}}$ are applied in simulated events for the nominal results. The differences between the nominal results and those obtained without applying the aforementioned corrections are taken as systematic uncertainties due to the modelling of $E_{\mathrm{T}}^{\mathrm{iso}}$ in the MC simulation. The uncertainties are propagated to the cross sections by modifying the unfolding matrix, the unmatched fractions and the signal yields; the resulting uncertainties are not symmetrised. The resulting uncertainty in the measured cross sections is typically smaller than 1%.

7.1.4 Jet energy scale and resolution

The uncertainties in the jet energy scale and resolution are considered using the method reported in ref. [41]. The sources of uncertainty include: the uncertainty in the overall energy scale adjustment using $Z+\text{jet}$, $\gamma+\text{jet}$,[6] and multi-jet p_{T}-balance methods; the uncertainty due to modelling, statistics and calibration non-closure in the η intercalibration; the uncertainty from single-particle response studies of high-p_{T} jets; the uncertainty due to the modelling of the pile-up contribution; the uncertainty in the jet response and simulated jet composition of light-quark, b-quark, and gluon-initiated jets; and the uncertainty due to punch-through jets.[7] The individual sources of uncertainty are varied by $\pm1\sigma$ in the MC simulations and propagated through the analysis separately, to maintain the full information about the correlations. The uncertainties are propagated to the cross sections by modifying the unfolding matrix and the unmatched fractions. The resulting uncertainty in the measured cross sections is obtained by adding in quadrature all the individual components. For $\mathrm{d}\sigma/\mathrm{d}p_{\mathrm{T}}^{\mathrm{jet}}$ this uncertainty is in the range 3%–8%.

7.1.5 Parton-shower and hadronisation model dependence

The dependence of the signal purity and unfolding corrections on the parton-shower and hadronisation models used in the simulations are studied separately. The differences observed in the signal purity between the nominal results and those obtained using the Pythia MC samples for the determination of the signal leakage fractions are taken as systematic uncertainties. The uncertainties are propagated to the cross sections by modifying the signal yields. The resulting uncertainties in the measured cross sections are typically smaller than 1%. The differences between the nominal results and those obtained using the Pythia MC samples for the unfolding are taken as systematic uncertainties and are typically smaller than 2%. In both cases, for the signal leakage fractions and for the unfolding, the uncertainties also account for a possible bias due to the application of the Frixione's criterion at particle level in the LO Sherpa MC samples.

7.1.6 Definition of the background control regions

The signal yield depends on the definition of the background control regions. The dependence is investigated by (i) varying the lower limit on $E_{\mathrm{T}}^{\mathrm{iso}}$ of regions B and D by $\pm1\,\mathrm{GeV}$,

[6] The correlation between the uncertainty in the photon energy scale and the uncertainty in the jet energy scale arising from the *in situ* method based on $\gamma+\text{jet}$ events has negligible impact.

[7] High-p_{T} jets that are not fully contained in the calorimeter are referred to as punch-through jets.

JHEP03(2020)179

(ii) removing the upper limit on $E_{\mathrm{T}}^{\mathrm{iso}}$ of regions B and D, and (iii) changing the choice of inverted photon identification variables used in the selection of non-tight photons. The signal yields obtained after each variation are compared with the nominal results and the differences are taken as systematic uncertainties. The uncertainties are propagated to the cross sections by modifying the signal yields. The uncertainty in the measured cross sections is typically below 0.2%, 0.2%, and 1% for the (i), (ii) and (iii) variations, respectively.

7.1.7 Identification and isolation correlation in the background

In the *in situ* background subtraction (eq. (5.1)), R_{bg} is assumed to be unity. A range in R_{bg} is set to cover the deviations from unity observed in the validation regions after subtracting the signal leakage with either Pythia or LO Sherpa MC samples. The maximum deviations of R_{bg} from unity in the validation regions vary in the range 10%–50% depending on the observable. The uncertainties are propagated to the cross sections by modifying the signal yields. The resulting uncertainty in the measured cross sections is typically smaller than 1%.

7.1.8 Background from electrons or positrons faking photons

A systematic uncertainty is assigned by taking the full size of the estimated contribution; the W+jets and Z+jets contributions are added linearly. The uncertainties are propagated to the cross sections by modifying the signal yields. The resulting uncertainty in the measured cross sections is typically smaller than 1%.

7.1.9 Pile-up, trigger efficiency and integrated luminosity

The pile-up reweighting of simulated events is varied to cover the uncertainty in the ratio of the predicted and measured inelastic cross sections [62]. The uncertainties are propagated to the cross sections by modifying the unfolding matrix, the unmatched fractions and the signal yields. The resulting uncertainty in the measured cross sections is typically smaller than 1%. There might be double counting between this source of uncertainty and that in the modelling of the photon isolation. However, given the smallness of the uncertainties, the impact is limited. The uncertainty in the trigger efficiency is estimated using the same methodology as in ref. [31] and amounts to 0.22% for $150 < E_{\mathrm{T}}^{\gamma} < 175\,\mathrm{GeV}$, 0.08% for $175 < E_{\mathrm{T}}^{\gamma} < 200\,\mathrm{GeV}$, 0.04% for $200 < E_{\mathrm{T}}^{\gamma} < 470\,\mathrm{GeV}$, and 0.40% for $470 < E_{\mathrm{T}}^{\gamma} < 2500\,\mathrm{GeV}$. It is propagated linearly to the measured cross sections. The uncertainty in the integrated luminosity is 2.1% and is fully correlated between all bins of all the measured cross sections.

7.1.10 Total systematic uncertainty

The total systematic uncertainty is computed by adding in quadrature the uncertainties from the sources listed above and the statistical uncertainty from the MC samples. The latter is computed using the bootstrap resampling technique [63]. There are large correlations in the systematic uncertainties across bins of one observable, particularly in the uncertainties due to the photon and jet energy scales, which are dominant. The total systematic uncertainty in the measured cross sections, excluding the uncertainty of the

JHEP03(2020)179

Range of the relative uncertainty (in %) for each variable								
E_{T}^{γ}	$p_{\mathrm{T}}^{\mathrm{jet}}$	$\lvert y^{\mathrm{jet}}\rvert$	$\lvert\Delta y^{\gamma\text{–jet}}\rvert$	$\Delta\phi^{\gamma\text{–jet}}$	$\lvert\Delta y^{\mathrm{jet–jet}}\rvert$	$\Delta\phi^{\mathrm{jet–jet}}$	$m^{\mathrm{jet–jet}}$	$m^{\gamma\text{–jet–jet}}$
3.5%–6.5%	4%–15%	4%–6%	4%–9%	3.5%–6%	4%–8%	3%–7%	4%–9%	4%–11%

Table 2. The total systematic uncertainty in the measured cross sections, excluding the uncertainty of the luminosity determination, for the total phase space: the range for each variable is shown in percentage.

luminosity determination, for the total phase space varies in the range shown in table 2 depending on the variable.

Figures 2 and 3 show the total systematic uncertainty, excluding the uncertainty of the luminosity determination, for each measured cross section for the total phase space. The dominant components, namely the jet energy scale, the photon energy scale and the photon identification, are shown separately in these figures. There are variables such as $\Delta\phi^{\mathrm{jet–jet}}$ for which the systematic uncertainties due to the jet and photon energy scales depend on the variable itself. These dependencies arise from the event topology: at low $\Delta\phi^{\mathrm{jet–jet}}$ the two jets are close together and recoil against the photon whereas at high $\Delta\phi^{\mathrm{jet–jet}}$ the two jets recoil against each other and the photon has lower p_{T}. Thus, the populations in jet and photon p_{T} vary with $\Delta\phi^{\mathrm{jet–jet}}$. In the total phase space, the systematic uncertainty dominates the total experimental uncertainty for $E_{\mathrm{T}}^{\gamma} \lesssim 1\,\mathrm{TeV}$, $p_{\mathrm{T}}^{\mathrm{jet}} \lesssim 1.5\,\mathrm{TeV}$ and $m^{\gamma\text{–jet–jet}} \lesssim 4\,\mathrm{TeV}$. For higher E_{T}^{γ}, $p_{\mathrm{T}}^{\mathrm{jet}}$ and $m^{\gamma\text{–jet–jet}}$ values, the statistical uncertainty of the data limits the precision of the measurements. For other observables, the systematic uncertainty dominates in the whole measured range. In particular, in the tails of the distributions of $p_{\mathrm{T}}^{\mathrm{jet}}$, $\lvert\Delta y^{\gamma\text{–jet}}\rvert$ and $m^{\gamma\text{–jet–jet}}$ the contributions from the statistical uncertainties of the MC samples and the systematic uncertainty in the unfolding correction due to the parton-shower and hadronisation model dependence can be as large as the systematic uncertainty due to the jet energy scale.

7.2 Theoretical uncertainties in the predictions

The following sources of uncertainty in the theoretical predictions are considered. The uncertainty in the NLO pQCD predictions from Sherpa due to terms beyond NLO is estimated by repeating the calculations using values of the renormalisation (μ_{R}) and factorisation (μ_{F}) scales multiplied by the factors 0.5 or 2. The two scales are varied either simultaneously or individually. In all cases, the condition $0.5 \leq \mu_{\mathrm{R}}/\mu_{\mathrm{F}} \leq 2$ is imposed. The largest deviation from each nominal prediction among the six possible variations is taken as the uncertainty. The uncertainty in the predictions due to the proton PDFs is estimated by using 100 replicas from the NNPDF3.0 analysis [55]. The uncertainty in the predictions due to the uncertainty in α_{s} is estimated by repeating the calculations using two additional sets of proton PDFs from the NNPDF3.0 analysis, for which different values of $\alpha_{\mathrm{s}}(m_Z)$ were assumed in the fits, namely 0.117 and 0.119; in this way, the correlation between α_{s} and the PDFs is preserved.

The total theoretical uncertainty is obtained by adding in quadrature the individual uncertainties mentioned above. The dominant theoretical uncertainty is that arising from

JHEP03(2020)179

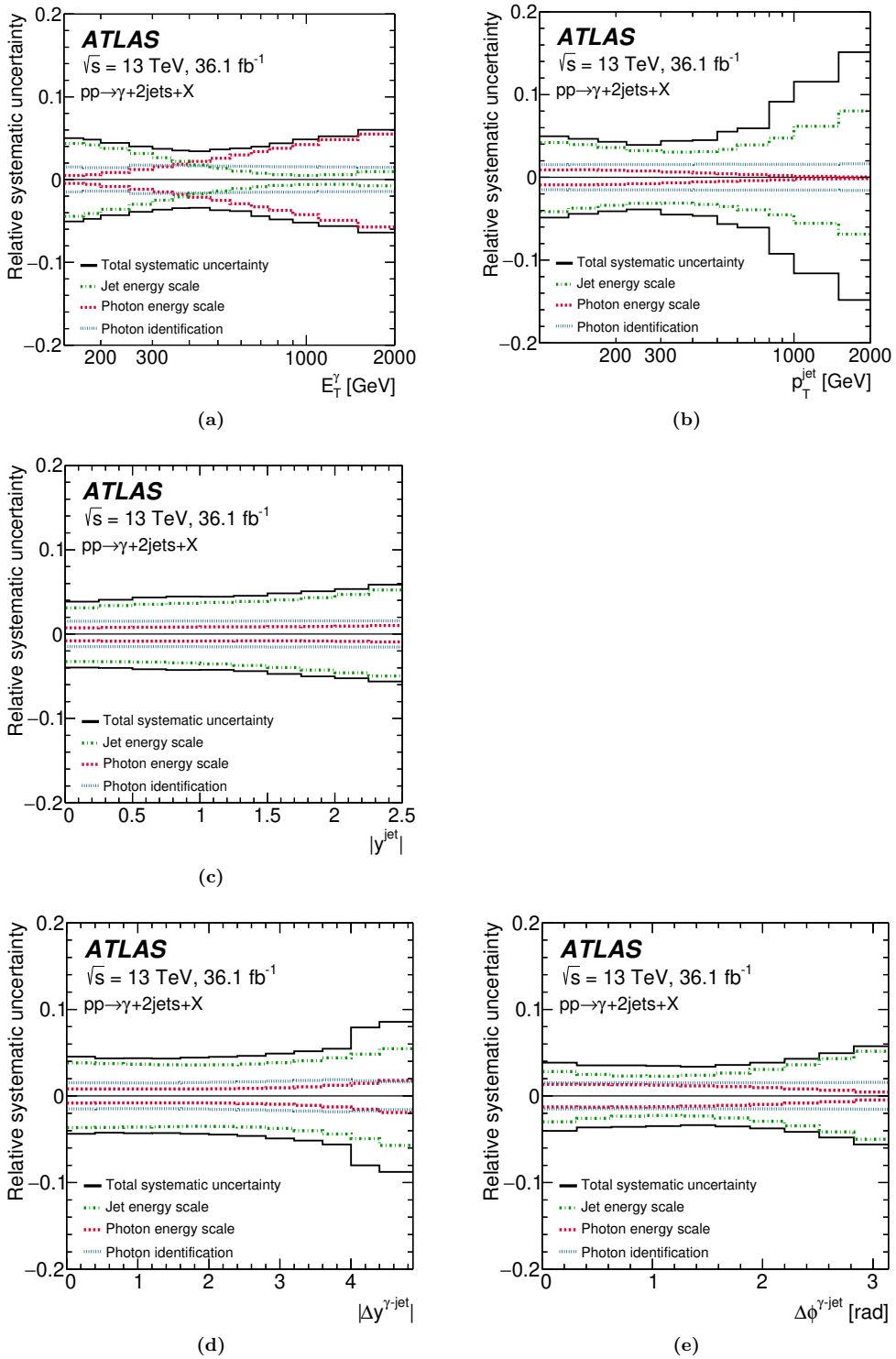

Figure 2. Total relative systematic uncertainty in the measured cross-sections (black lines), excluding the uncertainty of the luminosity determination, together with the three main contributions, namely jet energy scale (dot-dashed lines), photon energy scale (dashed lines) and photon identification (dotted lines), as a function of (a) E_{T}^{γ}, (b) $p_{\mathrm{T}}^{\mathrm{jet}}$, (c) $|y^{\mathrm{jet}}|$, (d) $|\Delta y^{\gamma-\mathrm{jet}}|$ and (e) $\Delta\phi^{\gamma-\mathrm{jet}}$ for the total phase space.

JHEP03(2020)179

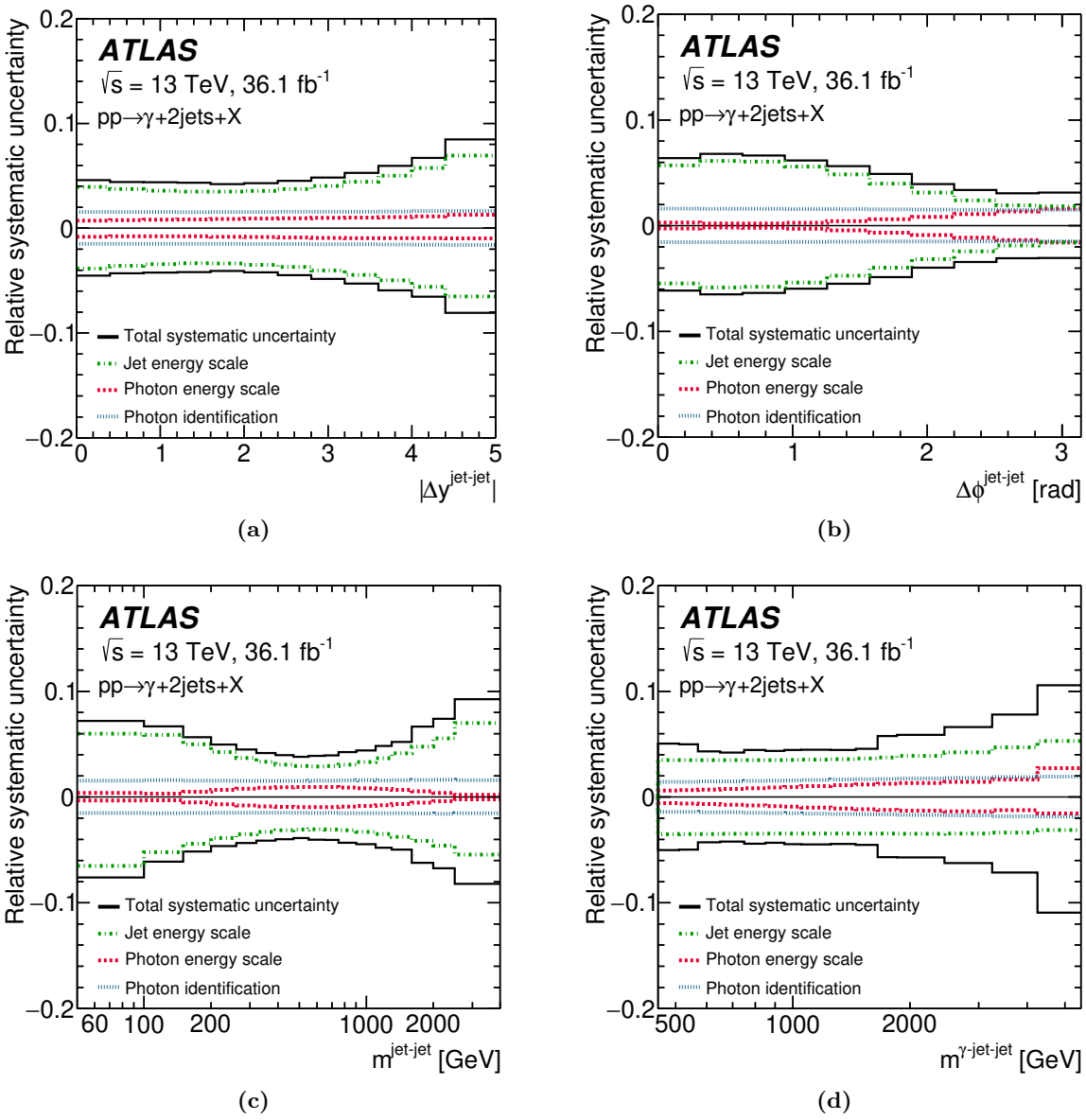

Figure 3. Total relative systematic uncertainty in the measured cross-sections (black lines), excluding the uncertainty of the luminosity determination, together with the three main contributions, namely jet energy scale (dot-dashed lines), photon energy scale (dashed lines) and photon identification (dotted lines), as a function of (a) $|\Delta y^{\text{jet–jet}}|$, (b) $\Delta\phi^{\text{jet–jet}}$, (c) $m^{\text{jet–jet}}$ and (d) $m^{\gamma\text{–jet–jet}}$ for the total phase space.

JHEP03(2020)179

terms beyond NLO and typically varies between about 20% and about 40%, depending on the observable and region of phase space. The uncertainty in the predictions arising from those in the PDFs is below 6% and that arising from the value of $\alpha_s(m_Z)$ is below 6% for all observables and phase-space regions.

8 Results

The measured isolated-photon plus two-jets cross sections in the three phase-space regions are shown in figures 4 to 9.

The measured $d\sigma/dE_T^\gamma$ is shown in figure 4a for the total phase space. The cross section decreases by approximately five orders of magnitude in the 150–2000 GeV range. The measured $d\sigma/dE_T^\gamma$ for the fragmentation- and direct-enriched phase-space regions are shown in figures 6a and 8a, respectively; it is observed that the E_T^γ spectrum for the direct-enriched phase space is harder than that for the fragmentation-enriched one.

The measured $d\sigma/dp_T^{jet}$ for the total phase space, shown in figure 4b, decreases by approximately five orders of magnitude in the measured range. Values of p_T^{jet} up to 2 TeV are measured. The measured $d\sigma/dp_T^{jet}$ for the fragmentation-enriched phase space (see figure 6b) has a harder spectrum than that for the direct-enriched one (see figure 8b).

Figure 4c shows the measured $d\sigma/d|y^{jet}|$ for the total phase space. The measured cross section decreases as $|y^{jet}|$ increases. The measured $d\sigma/d|y^{jet}|$ for the fragmentation- and direct-enriched phase-space regions are shown in figures 6c and 8c, respectively, and are similar for $|y^{jet}| < 1$, but for $1 < |y^{jet}| < 2.5$ the spectrum for the fragmentation-enriched phase space decreases faster as $|y^{jet}|$ increases.

The measured $d\sigma/d|\Delta y^{\gamma-jet}|$ for the total, fragmentation-enriched and direct-enriched phase-space regions are shown in figures 4d, 6d and 8d, respectively. The measured cross sections decrease as $|\Delta y^{\gamma-jet}|$ increases in all three phase-space regions.

The measured $d\sigma/d\Delta\phi^{\gamma-jet}$ for the total phase space is shown in figure 4e. The measured cross sections for the total and direct-enriched (see figure 8e) phase-space regions increase as $\Delta\phi^{\gamma-jet}$ increases and display a maximum at $\Delta\phi^{\gamma-jet} \sim 2.8$ rad. In contrast, $d\sigma/d\Delta\phi^{\gamma-jet}$ for the fragmentation-enriched phase space (see figure 6e) exhibits a peak at lower $\Delta\phi^{\gamma-jet}$ values, $\Delta\phi^{\gamma-jet} \sim 2.2$ rad. The difference between the distributions of $\Delta\phi^{\gamma-jet}$ for the direct- and fragmentation-enriched phase-space regions is partly due to the kinematical constraints that define those regions, namely $E_T^\gamma > p_T^{jet1}$ and $E_T^\gamma < p_T^{jet2}$, respectively.

Figures 5a, 7a and 9a show the measured $d\sigma/d|\Delta y^{jet-jet}|$ for the total, fragmentation- and direct-enriched phase-space regions, respectively. The measured cross sections have similar shapes in the three phase-space regions. However, the measured $d\sigma/d\Delta\phi^{jet-jet}$ (see figures 5b, 7b and 9b) have very different shapes in the three phase-space regions. For the fragmentation-enriched phase space, the two jets primarily populate the range $\Delta\phi^{jet-jet} > 2.2$ rad whereas for the direct-enriched one they mostly populate the range $0 < \Delta\phi^{jet-jet} < 2.2$ rad. The jet radius parameter of $R = 0.4$ has an effect for $\Delta\phi^{jet-jet} < 0.4$ as can be seen in figures 5b and 9b. The kinematical constraints that define the direct- and fragmentation-enriched phase-space regions have also an effect on the distributions of

JHEP03(2020)179

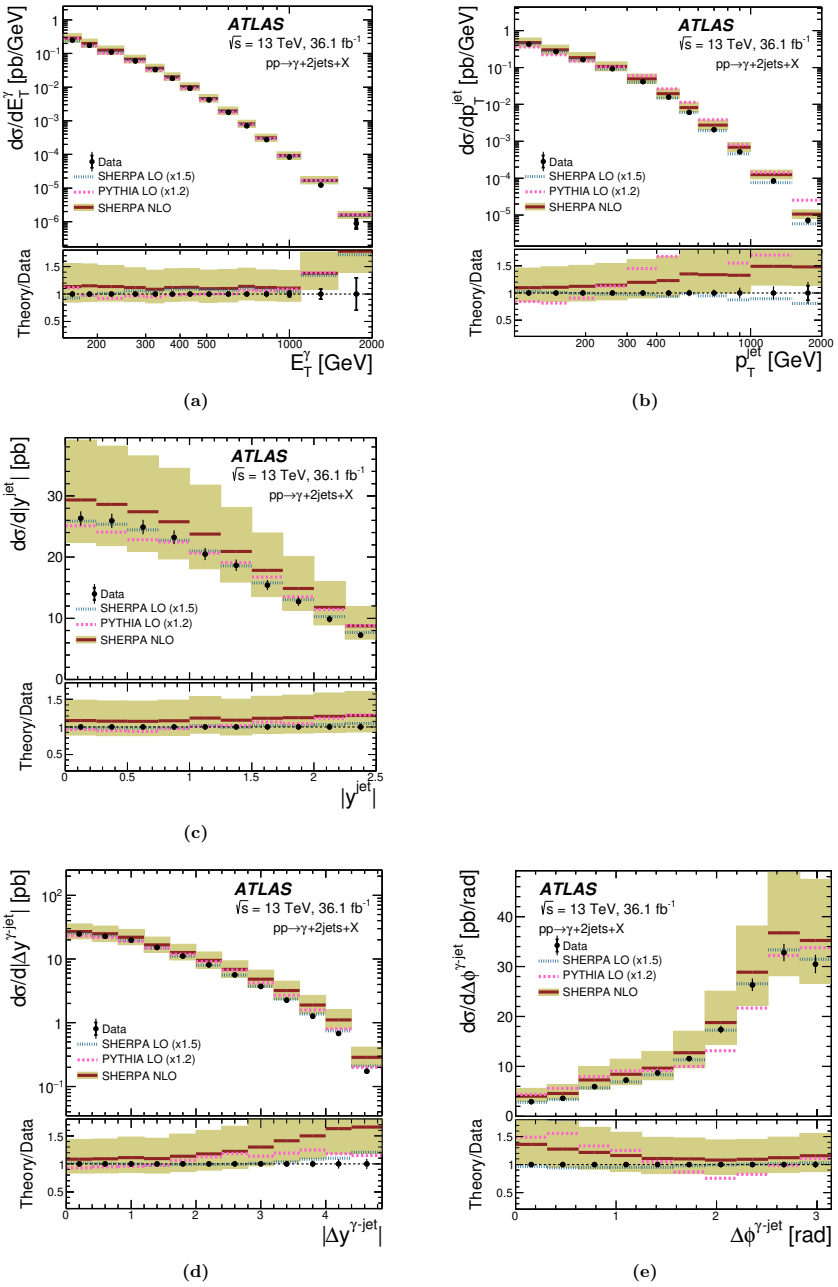

Figure 4. Measured cross sections for isolated-photon plus two-jet production (dots) as functions of (a) E_{T}^{γ}, (b) $p_{\mathrm{T}}^{\mathrm{jet}}$, (c) $|y^{\mathrm{jet}}|$, (d) $|\Delta y^{\gamma-\mathrm{jet}}|$ and (e) $\Delta\phi^{\gamma-\mathrm{jet}}$ for the total phase space. The NLO QCD predictions from Sherpa (solid lines) based on the NNPDF3.0 PDFs are also shown. The tree-level plus parton-shower predictions from LO Sherpa (dotted lines) and Pythia (dashed lines) normalised to the integrated measured cross section (using the factors indicated in parentheses) are also shown. The bottom part of each figure shows the ratio of the predictions to the measured cross section. The inner (outer) error bars represent the statistical uncertainties (the statistical and systematic uncertainties added in quadrature) and the filled bands represent the theoretical uncertainty of the NLO QCD predictions. For most of the points, the inner and outer error bars are smaller than the marker size and, thus, not visible. The visible thin error bars represent the outer error bars.

JHEP03(2020)179

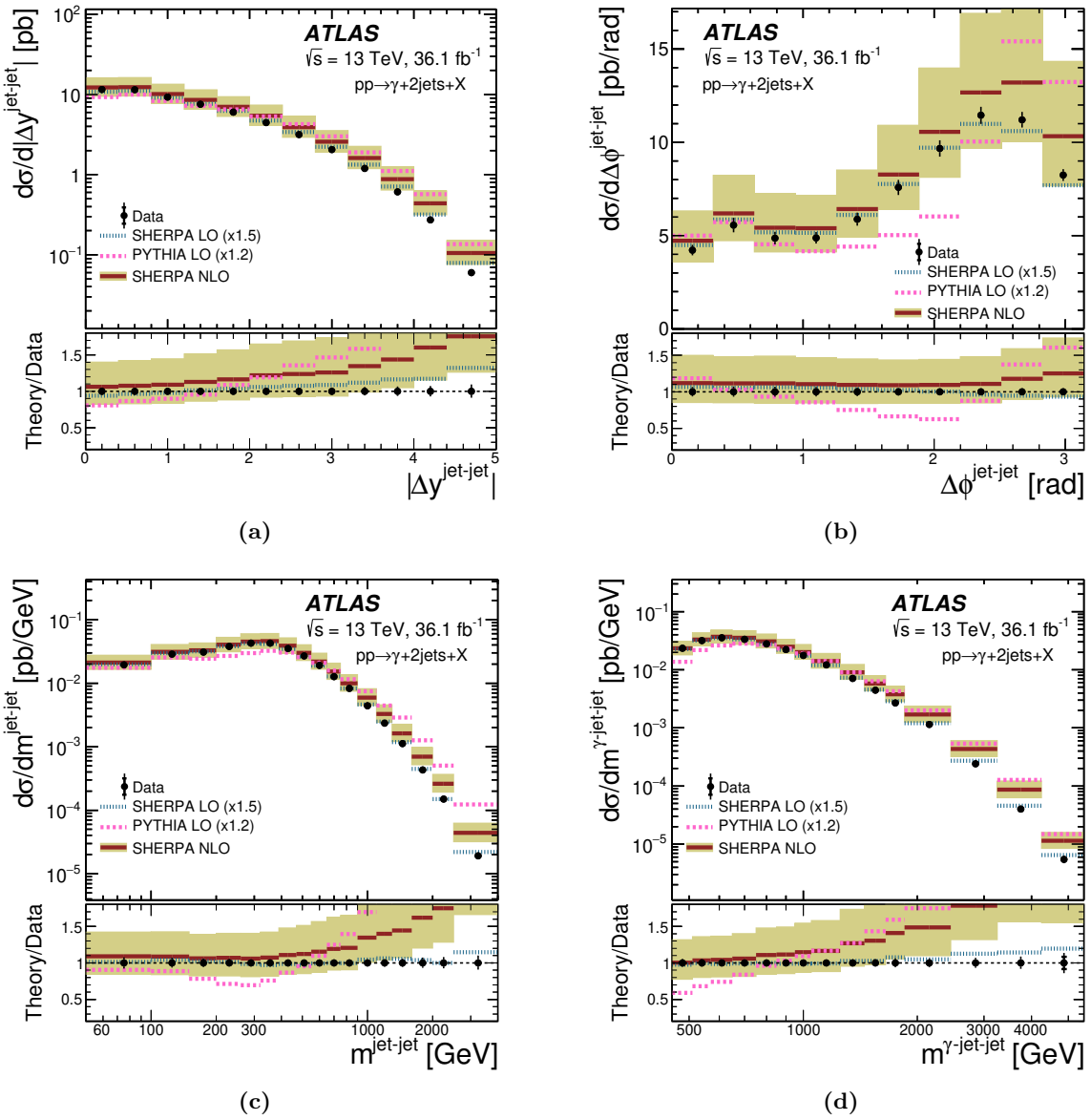

Figure 5. Measured cross sections for isolated-photon plus two-jet production (dots) as functions of (a) $|\Delta y^{\text{jet–jet}}|$, (b) $\Delta\phi^{\text{jet–jet}}$, (c) $m^{\text{jet–jet}}$ and (d) $m^{\gamma\text{–jet–jet}}$ for the total phase space. The NLO QCD predictions from SHERPA (solid lines) based on the NNPDF3.0 PDFs are also shown. The tree-level plus parton-shower predictions from LO SHERPA (dotted lines) and PYTHIA (dashed lines) normalised to the integrated measured cross section (using the factors indicated in parentheses) are also shown. The bottom part of each figure shows the ratio of the predictions to the measured cross section. The inner (outer) error bars represent the statistical uncertainties (the statistical and systematic uncertainties added in quadrature) and the filled bands represent the theoretical uncertainty of the NLO QCD predictions. For most of the points, the inner and outer error bars are smaller than the marker size and, thus, not visible. The visible thin error bars represent the outer error bars.

JHEP03(2020)179

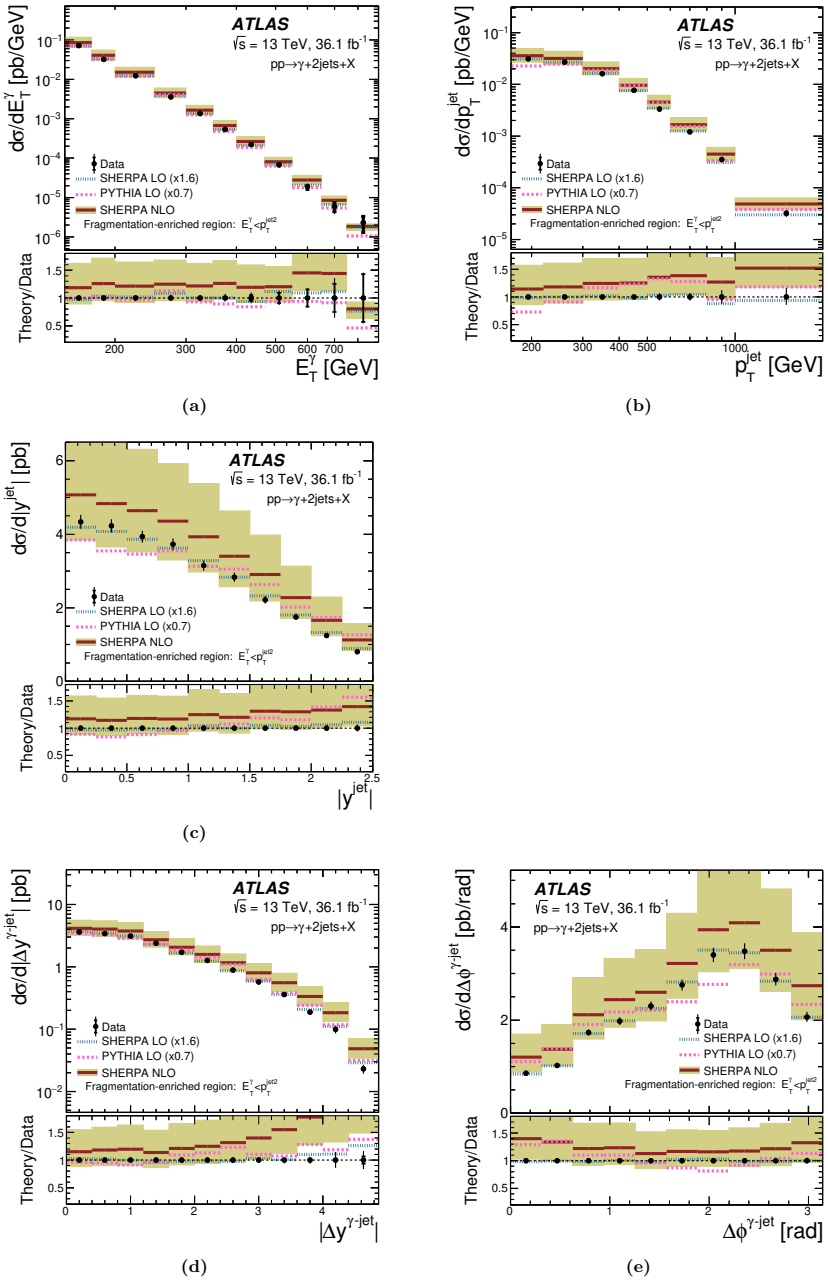

Figure 6. Measured cross sections for isolated-photon plus two-jet production (dots) as functions of (a) E_{T}^{γ}, (b) $p_{\mathrm{T}}^{\mathrm{jet}}$, (c) $|y^{\mathrm{jet}}|$, (d) $|\Delta y^{\gamma-\mathrm{jet}}|$ and (e) $\Delta\phi^{\gamma-\mathrm{jet}}$ for the fragmentation-enriched phase space. The NLO QCD predictions from SHERPA (solid lines) based on the NNPDF3.0 PDFs are also shown. The tree-level plus parton-shower predictions from LO SHERPA (dotted lines) and PYTHIA (dashed lines) normalised to the integrated measured cross section (using the factors indicated in parentheses) are also shown. The bottom part of each figure shows the ratio of the predictions to the measured cross section. The inner (outer) error bars represent the statistical uncertainties (the statistical and systematic uncertainties added in quadrature) and the filled bands represent the theoretical uncertainty of the NLO QCD predictions. For most of the points, the inner and outer error bars are smaller than the marker size and, thus, not visible. The visible thin error bars represent the outer error bars.

JHEP03(2020)179

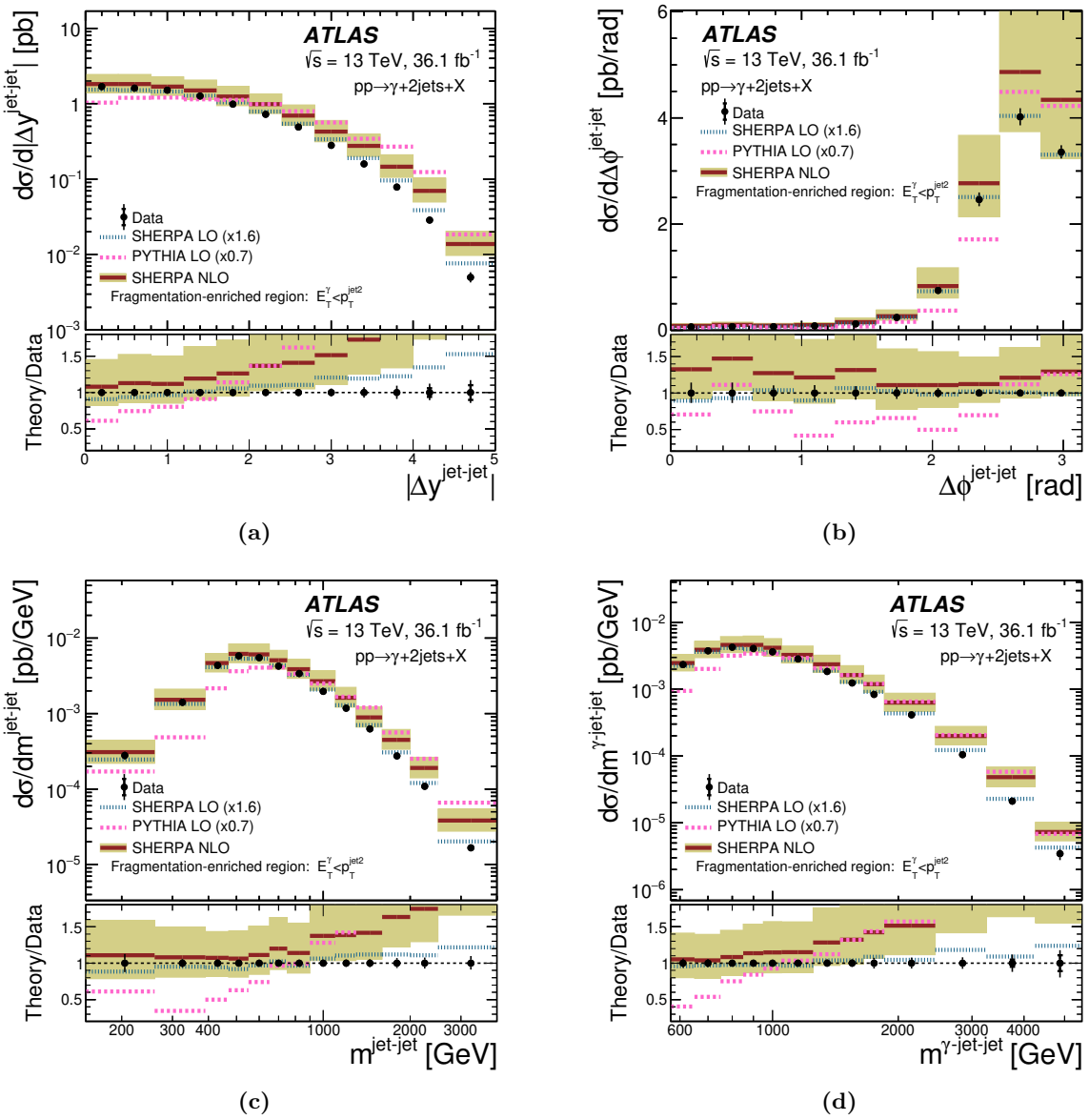

Figure 7. Measured cross sections for isolated-photon plus two-jet production (dots) as functions of (a) $|\Delta y^{\text{jet–jet}}|$, (b) $\Delta\phi^{\text{jet–jet}}$, (c) $m^{\text{jet–jet}}$ and (d) $m^{\gamma\text{–jet–jet}}$ for the fragmentation-enriched phase space. The NLO QCD predictions from SHERPA (solid lines) based on the NNPDF3.0 PDFs are also shown. The tree-level plus parton-shower predictions from LO SHERPA (dotted lines) and PYTHIA (dashed lines) normalised to the integrated measured cross section (using the factors indicated in parentheses) are also shown. The bottom part of each figure shows the ratio of the predictions to the measured cross section. The inner (outer) error bars represent the statistical uncertainties (the statistical and systematic uncertainties added in quadrature) and the filled bands represent the theoretical uncertainty of the NLO QCD predictions. For most of the points, the inner and outer error bars are smaller than the marker size and, thus, not visible. The visible thin error bars represent the outer error bars.

JHEP03(2020)179

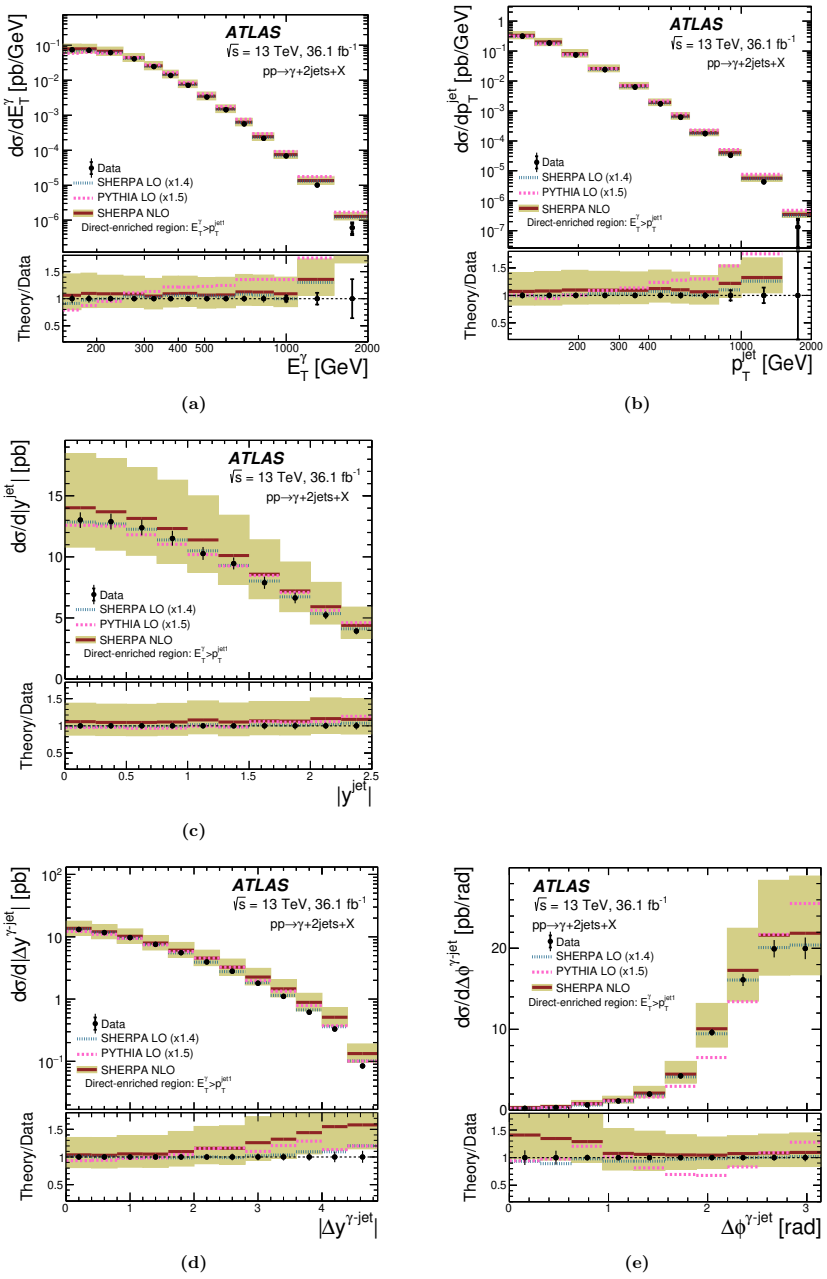

Figure 8. Measured cross sections for isolated-photon plus two-jet production (dots) as functions of (a) E_{T}^{γ}, (b) $p_{\mathrm{T}}^{\mathrm{jet}}$, (c) $|y^{\mathrm{jet}}|$, (d) $|\Delta y^{\gamma-\mathrm{jet}}|$ and (e) $\Delta\phi^{\gamma-\mathrm{jet}}$ for the direct-enriched phase space. The NLO QCD predictions from Sherpa (solid lines) based on the NNPDF3.0 PDFs are also shown. The tree-level plus parton-shower predictions from LO Sherpa (dotted lines) and Pythia (dashed lines) normalised to the integrated measured cross section (using the factors indicated in parentheses) are also shown. The bottom part of each figure shows the ratio of the predictions to the measured cross section. The inner (outer) error bars represent the statistical uncertainties (the statistical and systematic uncertainties added in quadrature) and the filled bands represent the theoretical uncertainty of the NLO QCD predictions. For most of the points, the inner and outer error bars are smaller than the marker size and, thus, not visible. The visible thin error bars represent the outer error bars.

JHEP03(2020)179

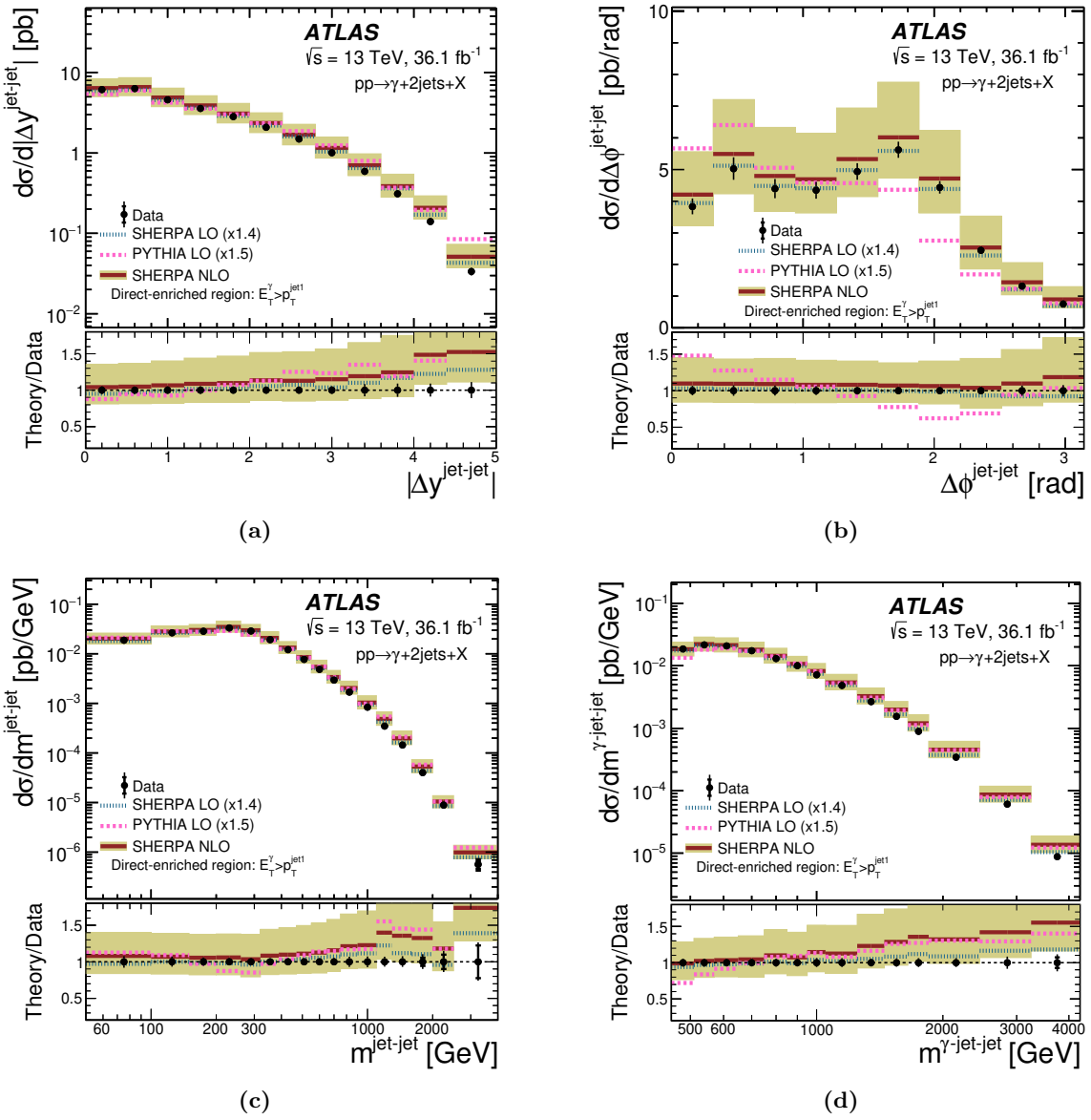

Figure 9. Measured cross sections for isolated-photon plus two-jet production (dots) as functions of (a) $|\Delta y^{\text{jet–jet}}|$, (b) $\Delta\phi^{\text{jet–jet}}$, (c) $m^{\text{jet–jet}}$ and (d) $m^{\gamma\text{–jet–jet}}$ for the direct-enriched phase space. The NLO QCD predictions from SHERPA (solid lines) based on the NNPDF3.0 PDFs are also shown. The tree-level plus parton-shower predictions from LO SHERPA (dotted lines) and PYTHIA (dashed lines) normalised to the integrated measured cross section (using the factors indicated in parentheses) are also shown. The bottom part of each figure shows the ratio of the predictions to the measured cross section. The inner (outer) error bars represent the statistical uncertainties (the statistical and systematic uncertainties added in quadrature) and the filled bands represent the theoretical uncertainty of the NLO QCD predictions. For most of the points, the inner and outer error bars are smaller than the marker size and, thus, not visible. The visible thin error bars represent the outer error bars.

JHEP03(2020)179

$\Delta\phi^{\text{jet–jet}}$; for instance, $\mathrm{d}\sigma/\mathrm{d}\Delta\phi^{\text{jet–jet}}$ for the fragmentation-enriched phase-space region is suppressed at low $\Delta\phi^{\text{jet–jet}}$.

The dependence of the cross sections on $m^{\text{jet–jet}}$ and $m^{\gamma\text{–jet–jet}}$ is measured up to values of 4 TeV and 5.5 TeV, respectively. For $\mathrm{d}\sigma/\mathrm{d}m^{\text{jet–jet}}$ (see figures 5c, 7c and 9c), the measured spectra have different shapes in the three phase-space regions. The cross section for the fragmentation-enriched phase space is suppressed at low $m^{\text{jet–jet}}$ values, but it is harder than that for the direct-enriched one at high $m^{\text{jet–jet}}$ values. The kinematical constraints have some effect on the differences between the distributions of $m^{\text{jet–jet}}$ for the direct- and fragmentation-enriched phase-space regions. For $\mathrm{d}\sigma/\mathrm{d}m^{\gamma\text{–jet–jet}}$ (see figures 5d, 7d and 9d), the shapes of the spectra are more similar, but the distribution for the fragmentation-enriched phase space is harder than for the direct-enriched one.

8.1 Comparison with tree-level plus parton-shower Monte Carlo models

The predictions of the tree-level plus parton-shower MC models of Pythia and Sherpa are compared with the data in figures 4 to 9. These predictions are normalised to the measured integrated cross section in each phase space to compare the shapes of the predictions with the data. The normalisation factors relative to the cross-section predictions of the generators are indicated in figures 4 to 9. Being tree-level predictions, the theoretical uncertainties in these models can be as large as 50% and are not included in the figures.

The predictions of LO Sherpa provide a good description of the shape of the data, except at high E_{T}^{γ}, $|\Delta y^{\text{jet–jet}}|$ and $m^{\gamma\text{–jet–jet}}$. The predictions of Pythia, in general, fail to describe the shape of the data. There are two reasons for this disagreement. First, since Pythia uses $2 \to 2$ matrix elements, the second jet necessarily originates from the parton shower; Sherpa incorporates matrix elements for the processes $2 \to n$ with $n = 2$ to 5 and thus the second jet is better simulated. Second, the fragmentation component in Pythia is overestimated for the parameter settings used here. This is particularly visible in the cross section for the total phase space as a function of $p_{\mathrm{T}}^{\text{jet}}$ in the region $p_{\mathrm{T}}^{\text{jet}} > 300\,\text{GeV}$, where the prediction overestimates the data by 50% or more. It is also visible in the cross section for the total phase space as a function of $m^{\text{jet–jet}}$ and $m^{\gamma\text{–jet–jet}}$, where the predictions of Pythia overestimate the data by up to an order of magnitude. The overestimation of the fragmentation component is also supported by the fact that the normalisation factor for the predictions from Pythia is 1.2 (0.7) for the total (fragmentation-enriched) phase space. The inclusion of higher-order tree-level matrix elements for the processes $2 \to n$ with $n = 3$ to 5 in Sherpa significantly improves the description of the data for all observables and phase-space regions.

8.2 Comparison with next-to-leading-order plus parton-shower QCD predictions

The predictions of the NLO calculations of Sherpa are compared with the data in figures 4 to 9. The uncertainties in the predictions include those due to missing higher-order terms in the perturbative expansion, those due to the uncertainties in the PDFs and those due to the uncertainty in $\alpha_{\mathrm{s}}(m_Z)$, as explained in section 7.2. The predictions are shown with the theory normalisation, so the comparison between data and theory is done in terms of both

JHEP03(2020)179

normalisation and shape, except for the LO Sherpa predictions (see section 8.1) which are normalised to the data. The NLO Sherpa predictions describe the data adequately in shape and normalisation within the experimental and theoretical uncertainties except for ranges at high values of $|\Delta y^{\gamma\text{–jet}}|$, $|\Delta y^{\text{jet–jet}}|$, $m^{\text{jet–jet}}$ and $m^{\gamma\text{–jet–jet}}$, where the predictions overestimate the data in the total and fragmentation-enriched phase-space regions. In those ranges, the overestimation of the predictions relative to the data is larger in the fragmentation-enriched phase space than when considering the total phase space. These discrepancies might be attributable to unaccounted higher-order corrections given the fact that the variation of the renormalisation and factorisation scales leads to relatively large uncertainties in the predictions. In particular, the use of E_{T}^{γ} as the scale might not be optimal in the ranges where $p_{\text{T}}^{\text{jet}}$ is much larger than E_{T}^{γ}. A mismodelling of the high tail in $m^{\text{jet–jet}}$ is also observed for the measurements of the final state $V+\text{jet}+\text{jet}$ with $V = W^{\pm}$ or Z boson [64–66]. In addition, decorrelation effects from multiple parton emission might be present at large values of $|\Delta y^{\gamma\text{–jet}}|$ and $|\Delta y^{\text{jet–jet}}|$. The comparison of the predictions based on different parameterisations of the proton PDFs shows that the description of the data does not depend significantly on the specific PDF used. The theoretical uncertainties are much larger than the experimental ones and, therefore, more precise calculations are needed, either in the form of resummed calculations or through the inclusion of higher-order terms. Once the size of the uncertainties of the predictions is reduced significantly, a meaningful comparison with predictions including electroweak effects will be possible.

9 Summary

Measurements of the cross sections for the production of an isolated photon in association with two jets in pp collisions at $\sqrt{s} = 13\,\text{TeV}$, $pp \to \gamma + \text{jet} + \text{jet} + \text{X}$, are presented. These measurements are based on an integrated luminosity of 36.1 fb^{-1} of ATLAS data recorded at the LHC. The photon is required to have $E_{\text{T}}^{\gamma} > 150\,\text{GeV}$ and $|\eta^{\gamma}| < 2.37$, excluding the region $1.37 < |\eta^{\gamma}| < 1.56$. The jets are reconstructed using the anti-k_t algorithm with radius parameter $R = 0.4$. The cross sections are measured as functions of E_{T}^{γ}, $p_{\text{T}}^{\text{jet}}$, $|y^{\text{jet}}|$, $\Delta\phi^{\gamma\text{–jet}}$, $|\Delta y^{\gamma\text{–jet}}|$, $m^{\text{jet–jet}}$, $\Delta\phi^{\text{jet–jet}}$, $|\Delta y^{\text{jet–jet}}|$ and $m^{\gamma\text{–jet–jet}}$ in three different regions of phase space, namely the total phase space, the fragmentation-photon enriched phase space where $E_{\text{T}}^{\gamma} < p_{\text{T}}^{\text{jet2}}$ and the direct-photon enriched phase space where $E_{\text{T}}^{\gamma} > p_{\text{T}}^{\text{jet1}}$. The measurements extend up to values of 2 TeV in E_{T}^{γ} and $p_{\text{T}}^{\text{jet}}$. The dependence of the cross sections on $m^{\text{jet–jet}}$ and $m^{\gamma\text{–jet–jet}}$ is measured up to values of 4 TeV and 5.5 TeV, respectively. The measured cross sections in the fragmentation-photon and direct-photon enriched phase-space regions exhibit the features expected from the two underlying production mechanisms, each of which dominates in one of the two regions, and for some observables, from the effects of the kinematical constraints that define the two phase-space regions.

The predictions of the tree-level plus parton-shower MC model in LO Sherpa give a good description of the shape of the data distributions, except at high E_{T}^{γ}, $|\Delta y^{\text{jet–jet}}|$ and $m^{\gamma\text{–jet–jet}}$. In contrast, the predictions from Pythia, for which the sub-leading jet must necessarily originate from the parton shower, generally fail to describe the shape of the distributions in the data. The improved description of the data by the predictions

JHEP03(2020)179

from LO Sherpa is attributed to the inclusion of tree-level higher-order matrix elements. The precision of the measurements is significantly better than the differences between the predictions. The NLO predictions from Sherpa describe the data adequately in shape and normalisation within the experimental and theoretical uncertainties except for the regions at high values of $|\Delta y^{\gamma\text{–jet}}|$, $|\Delta y^{\text{jet–jet}}|$, $m^{\text{jet–jet}}$ and $m^{\gamma\text{–jet–jet}}$, where the predictions overestimate the data for the total and fragmentation-photon enriched phase-space regions. There are regions in which the NLO predictions exhibit trends that differ from those in the data, such as at high E_{T}^{γ} and $p_{\text{T}}^{\text{jet}}$, and at low $\Delta\phi^{\gamma\text{–jet}}$. The theoretical uncertainties are much larger than those of experimental nature, preventing a more precise test of the theory. The measurements provide tests of pQCD at energy scales as high as 2 TeV for the photon and jet transverse momenta and scrutinise the NLO QCD description of the dynamics of isolated-photon plus two-jet production in pp collisions.

Acknowledgments

We thank CERN for the very successful operation of the LHC, as well as the support staff from our institutions without whom ATLAS could not be operated efficiently.

We acknowledge the support of ANPCyT, Argentina; YerPhI, Armenia; ARC, Australia; FWF, BMWFW, Austria; ANAS, Azerbaijan; SSTC, Belarus; CNPq, FAPESP, Brazil; NSERC, CFI, NRC, Canada; CERN, CERN; CONICYT, Chile; CAS, NSFC, MOST, China; COLCIENCIAS, Colombia; VSC CR, MSMT CR, MPO CR, Czech Republic; DNSRC, DNRF, Denmark; IN2P3-CNRS, CEA-DRF/IRFU, France; SRNSFG, Georgia; MPG, HGF, BMBF, Germany; GSRT, Greece; RGC, Hong Kong SAR, Hong Kong China; Benoziyo Center, ISF, Israel; INFN, Italy; JSPS, MEXT, Japan; JINR, JINR; CNRST, Morocco; NWO, Netherlands; RCN, Norway; MNiSW, NCN, Poland; FCT, Portugal; MNE/IFA, Romania; NRC KI, MES of Russia, Russia Federation; MESTD, Serbia; MSSR, Slovakia; ARRS, MIZŠ, Slovenia; DST/NRF, South Africa; MINECO, Spain; SRC, Wallenberg Foundation, Sweden; Cantons of Bern and Geneva, SNSF, SERI, Switzerland; MOST, Taiwan; TAEK, Turkey; STFC, United Kingdom; DOE, NSF, United states of America. In addition, individual groups and members have received support from CRC, Compute Canada, Canarie, BCKDF, Canada; Marie Skłodowska-Curie, COST, ERDF, ERC, Horizon 2020, European Union; ANR, Investissements d'Avenir Labex and Idex, France; AvH, DFG, Germany; Herakleitos, Thales and Aristeia programmes co-financed by EU-ESF and the Greek NSRF, Greece; BSF-NSF, GIF, Israel; PROMETEO Programme Generalitat Valenciana, CERCA Generalitat de Catalunya, Spain; Leverhulme Trust, The Royal Society, United Kingdom.

The crucial computing support from all WLCG partners is acknowledged gratefully, in particular from CERN, the ATLAS Tier-1 facilities at TRIUMF (Canada), NDGF (Denmark, Norway, Sweden), CC-IN2P3 (France), KIT/GridKA (Germany), INFN-CNAF (Italy), NL-T1 (Netherlands), PIC (Spain), ASGC (Taiwan), RAL (U.K.) and BNL (U.S.A.), the Tier-2 facilities worldwide and large non-WLCG resource providers. Major contributors of computing resources are listed in ref. [67].

JHEP03(2020)179

References

[1] T. Pietrycki and A. Szczurek, *Photon-jet correlations in pp and $p\bar{p}$ collisions*, *Phys. Rev.* **D 76** (2007) 034003 [arXiv:0704.2158] [INSPIRE].

[2] Z. Belghobsi, M. Fontannaz, J.P. Guillet, G. Heinrich, E. Pilon and M. Werlen, *Photon-Jet Correlations and Constraints on Fragmentation Functions*, *Phys. Rev.* **D 79** (2009) 114024 [arXiv:0903.4834] [INSPIRE].

[3] J.H. Kühn, A. Kulesza, S. Pozzorini and M. Schulze, *Electroweak corrections to hadronic photon production at large transverse momenta*, *JHEP* **03** (2006) 059 [hep-ph/0508253] [INSPIRE].

[4] U. Baur, *Weak Boson Emission in Hadron Collider Processes*, *Phys. Rev.* **D 75** (2007) 013005 [hep-ph/0611241] [INSPIRE].

[5] T. Becher and X. Garcia i Tormo, *Electroweak Sudakov effects in W, Z and γ production at large transverse momentum*, *Phys. Rev.* **D 88** (2013) 013009 [arXiv:1305.4202] [INSPIRE].

[6] T. Becher and X. Garcia i Tormo, *Addendum: Electroweak Sudakov effects in W, Z and γ production at large transverse momentum*, *Phys. Rev.* **D 92** (2015) 073011 [arXiv:1509.01961] [INSPIRE].

[7] ATLAS collaboration, *Measurement of the production cross section of an isolated photon associated with jets in proton-proton collisions at $\sqrt{s} = 7$ TeV with the ATLAS detector*, *Phys. Rev.* **D 85** (2012) 092014 [arXiv:1203.3161] [INSPIRE].

[8] ATLAS collaboration, *Dynamics of isolated-photon plus jet production in pp collisions at $\sqrt{s} = 7$ TeV with the ATLAS detector*, *Nucl. Phys.* **B 875** (2013) 483 [arXiv:1307.6795] [INSPIRE].

[9] ATLAS collaboration, *High-E_{T} isolated-photon plus jets production in pp collisions at $\sqrt{s} = 8$ TeV with the ATLAS detector*, *Nucl. Phys.* **B 918** (2017) 257 [arXiv:1611.06586] [INSPIRE].

[10] ATLAS collaboration, *Measurement of the cross section for isolated-photon plus jet production in pp collisions at $\sqrt{s} = 13$ TeV using the ATLAS detector*, *Phys. Lett.* **B 780** (2018) 578 [arXiv:1801.00112] [INSPIRE].

[11] CMS collaboration, *Rapidity Distributions in Exclusive $Z+$ Jet and $\gamma+$ Jet Events in pp Collisions at $\sqrt{s} = 7$ TeV*, *Phys. Rev.* **D 88** (2013) 112009 [arXiv:1310.3082] [INSPIRE].

[12] CMS collaboration, *Measurement of the Triple-Differential Cross Section for Photon+Jets Production in Proton-Proton Collisions at $\sqrt{s} = 7$ TeV*, *JHEP* **06** (2014) 009 [arXiv:1311.6141] [INSPIRE].

[13] CMS collaboration, *Comparison of the $Z/\gamma^* +$ jets to $\gamma +$ jets cross sections in pp collisions at $\sqrt{s} = 8$ TeV*, *JHEP* **10** (2015) 128 [*Erratum JHEP* **04** (2016) 010] [arXiv:1505.06520] [INSPIRE].

[14] CMS collaboration, *Measurement of differential cross sections for inclusive isolated-photon and photon+jets production in proton-proton collisions at $\sqrt{s} = 13$ TeV*, *Eur. Phys. J.* **C 79** (2019) 20 [arXiv:1807.00782] [INSPIRE].

JHEP03(2020)179

[15] CMS collaboration, *Measurements of triple-differential cross sections for inclusive isolated-photon + jet events in pp collisions at $\sqrt{s} = 8$ TeV*, *Eur. Phys. J.* **C 79** (2019) 969 [arXiv:1907.08155] [INSPIRE].

[16] S. Keller and J.F. Owens, *Event structure in photon plus two jet final states*, *Phys. Lett.* **B 269** (1991) 445 [INSPIRE].

[17] T. Sjöstrand, S. Mrenna and P.Z. Skands, *A Brief Introduction to PYTHIA 8.1*, *Comput. Phys. Commun.* **178** (2008) 852 [arXiv:0710.3820] [INSPIRE].

[18] T. Gleisberg et al., *Event generation with SHERPA 1.1*, *JHEP* **02** (2009) 007 [arXiv:0811.4622] [INSPIRE].

[19] SHERPA collaboration, *Event Generation with Sherpa 2.2*, *SciPost Phys.* **7** (2019) 034 [arXiv:1905.09127] [INSPIRE].

[20] F. Krauss, R. Kühn and G. Soff, *AMEGIC++ 1.0: A Matrix element generator in C++*, *JHEP* **02** (2002) 044 [hep-ph/0109036] [INSPIRE].

[21] F. Cascioli, P. Maierhöfer and S. Pozzorini, *Scattering Amplitudes with Open Loops*, *Phys. Rev. Lett.* **108** (2012) 111601 [arXiv:1111.5206] [INSPIRE].

[22] S. Schumann and F. Krauss, *A Parton shower algorithm based on Catani-Seymour dipole factorisation*, *JHEP* **03** (2008) 038 [arXiv:0709.1027] [INSPIRE].

[23] S. Höche, F. Krauss, M. Schönherr and F. Siegert, *QCD matrix elements + parton showers: The NLO case*, *JHEP* **04** (2013) 027 [arXiv:1207.5030] [INSPIRE].

[24] ATLAS collaboration, *The ATLAS Experiment at the CERN Large Hadron Collider*, 2008 *JINST* **3** S08003 [INSPIRE].

[25] ATLAS collaboration, *ATLAS Insertable B-Layer Technical Design Report*, CERN-LHCC-2010-013 (2010) [ATLAS-TDR-19] [INSPIRE].

[26] ATLAS IBL collaboration, *Production and Integration of the ATLAS Insertable B-Layer*, 2018 *JINST* **13** T05008 [arXiv:1803.00844] [INSPIRE].

[27] ATLAS collaboration, *Performance of the ATLAS Trigger System in 2015*, *Eur. Phys. J.* **C 77** (2017) 317 [arXiv:1611.09661] [INSPIRE].

[28] ATLAS collaboration, *ATLAS data quality operations and performance for 2015–2018 data-taking*, arXiv:1911.04632 [INSPIRE].

[29] ATLAS collaboration, *Luminosity determination in pp collisions at $\sqrt{s} = 13$ TeV using the ATLAS detector at the LHC*, ATLAS-CONF-2019-021 (2019) [INSPIRE].

[30] G. Avoni et al., *The new LUCID-2 detector for luminosity measurement and monitoring in ATLAS*, 2018 *JINST* **13** P07017 [INSPIRE].

[31] ATLAS collaboration, *Performance of electron and photon triggers in ATLAS during LHC Run 2*, *Eur. Phys. J.* **C 80** (2020) 47 [arXiv:1909.00761] [INSPIRE].

[32] ATLAS collaboration, *Vertex Reconstruction Performance of the ATLAS Detector at $\sqrt{s} = 13$ TeV*, ATL-PHYS-PUB-2015-026 (2015).

[33] ATLAS collaboration, *Measurement of the inclusive isolated-photon cross section in pp collisions at $\sqrt{s} = 13$ TeV using 36 fb^{-1} of ATLAS data*, *JHEP* **10** (2019) 203 [arXiv:1908.02746] [INSPIRE].

JHEP03(2020)179

[34] ATLAS collaboration, *Measurement of the photon identification efficiencies with the ATLAS detector using LHC Run 2 data collected in 2015 and 2016*, *Eur. Phys. J.* **C 79** (2019) 205 [arXiv:1810.05087] [INSPIRE].

[35] ATLAS collaboration, *Electron and photon energy calibration with the ATLAS detector using 2015–2016 LHC proton-proton collision data*, 2019 *JINST* **14** P03017 [arXiv:1812.03848] [INSPIRE].

[36] ATLAS collaboration, *Topological cell clustering in the ATLAS calorimeters and its performance in LHC Run 1*, *Eur. Phys. J.* **C 77** (2017) 490 [arXiv:1603.02934] [INSPIRE].

[37] ATLAS collaboration, *Measurement of the inclusive isolated prompt photon cross section in pp collisions at $\sqrt{s} = 7$ TeV with the ATLAS detector*, *Phys. Rev.* **D 83** (2011) 052005 [arXiv:1012.4389] [INSPIRE].

[38] M. Cacciari, G.P. Salam and G. Soyez, *The Catchment Area of Jets*, *JHEP* **04** (2008) 005 [arXiv:0802.1188] [INSPIRE].

[39] M. Cacciari, G.P. Salam and G. Soyez, *The anti-k_t jet clustering algorithm*, *JHEP* **04** (2008) 063 [arXiv:0802.1189] [INSPIRE].

[40] M. Cacciari, G.P. Salam and G. Soyez, *FastJet User Manual*, *Eur. Phys. J.* **C 72** (2012) 1896 [arXiv:1111.6097] [INSPIRE].

[41] ATLAS collaboration, *Jet energy scale measurements and their systematic uncertainties in proton-proton collisions at $\sqrt{s} = 13$ TeV with the ATLAS detector*, *Phys. Rev.* **D 96** (2017) 072002 [arXiv:1703.09665] [INSPIRE].

[42] ATLAS collaboration, *Performance of pile-up mitigation techniques for jets in pp collisions at $\sqrt{s} = 8$ TeV using the ATLAS detector*, *Eur. Phys. J.* **C 76** (2016) 581 [arXiv:1510.03823] [INSPIRE].

[43] ATLAS collaboration, *Selection of jets produced in 13 TeV proton-proton collisions with the ATLAS detector*, ATLAS-CONF-2015-029 (2015) [INSPIRE].

[44] B. Andersson, G. Gustafson, G. Ingelman and T. Sjöstrand, *Parton Fragmentation and String Dynamics*, *Phys. Rept.* **97** (1983) 31 [INSPIRE].

[45] J.-C. Winter, F. Krauss and G. Soff, *A Modified cluster hadronization model*, *Eur. Phys. J.* **C 36** (2004) 381 [hep-ph/0311085] [INSPIRE].

[46] R.D. Ball et al., *Parton distributions with LHC data*, *Nucl. Phys.* **B 867** (2013) 244 [arXiv:1207.1303] [INSPIRE].

[47] H.-L. Lai et al., *New parton distributions for collider physics*, *Phys. Rev.* **D 82** (2010) 074024 [arXiv:1007.2241] [INSPIRE].

[48] ATLAS collaboration, *ATLAS PYTHIA 8 tunes to 7 TeV datas*, ATL-PHYS-PUB-2014-021 (2014).

[49] S. Höche, F. Krauss, S. Schumann and F. Siegert, *QCD matrix elements and truncated showers*, *JHEP* **05** (2009) 053 [arXiv:0903.1219] [INSPIRE].

[50] S. Frixione, *Isolated photons in perturbative QCD*, *Phys. Lett.* **B 429** (1998) 369 [hep-ph/9801442] [INSPIRE].

[51] ATLAS collaboration, *Summary of ATLAS PYTHIA 8 tunes*, ATL-PHYS-PUB-2012-003 (2012) [INSPIRE].

JHEP03(2020)179

[52] A.D. Martin, W.J. Stirling, R.S. Thorne and G. Watt, *Parton distributions for the LHC*, *Eur. Phys. J.* **C 63** (2009) 189 [arXiv:0901.0002] [INSPIRE].

[53] GEANT4 collaboration, *GEANT4: A Simulation toolkit*, *Nucl. Instrum. Meth.* **A 506** (2003) 250 [INSPIRE].

[54] ATLAS collaboration, *The ATLAS Simulation Infrastructure*, *Eur. Phys. J.* **C 70** (2010) 823 [arXiv:1005.4568] [INSPIRE].

[55] NNPDF collaboration, *Parton distributions for the LHC Run II*, *JHEP* **04** (2015) 040 [arXiv:1410.8849] [INSPIRE].

[56] F. Siegert, *A practical guide to event generation for prompt photon production with Sherpa*, *J. Phys.* **G 44** (2017) 044007 [arXiv:1611.07226] [INSPIRE].

[57] ATLAS collaboration, *Measurement of the inclusive isolated prompt photon cross-section in pp collisions at $\sqrt{s} = 7$ TeV using 35 pb^{-1} of ATLAS data*, *Phys. Lett.* **B 706** (2011) 150 [arXiv:1108.0253] [INSPIRE].

[58] ATLAS collaboration, *Measurement of the inclusive isolated prompt photon cross section in pp collisions at $\sqrt{s} = 8$ TeV with the ATLAS detector*, *JHEP* **08** (2016) 005 [arXiv:1605.03495] [INSPIRE].

[59] ATLAS collaboration, *Measurement of the cross section for inclusive isolated-photon production in pp collisions at $\sqrt{s} = 13$ TeV using the ATLAS detector*, *Phys. Lett.* **B 770** (2017) 473 [arXiv:1701.06882] [INSPIRE].

[60] G. D'Agostini, *A Multidimensional unfolding method based on Bayes' theorem*, *Nucl. Instrum. Meth.* **A 362** (1995) 487 [INSPIRE].

[61] T. Adye, *Unfolding algorithms and tests using RooUnfold*, in proceedings of the *PHYSTAT 2011 Workshop on Statistical Issues Related to Discovery Claims in Search Experiments and Unfolding*, CERN, Geneva, Switzerland, 17–20 January 2011, pp. 313–318 [arXiv:1105.1160] [INSPIRE].

[62] ATLAS collaboration, *Measurement of the Inelastic Proton-Proton Cross Section at $\sqrt{s} = 13$ TeV with the ATLAS Detector at the LHC*, *Phys. Rev. Lett.* **117** (2016) 182002 [arXiv:1606.02625] [INSPIRE].

[63] G. Bohm and G. Zech, *Introduction to statistics and data analysis for physicists*, Deutsches Elektronen-Synchrotron, Hamburg Germany (2014) [ISBN: 978–3–935702–41–6] and online pdf version at https://doi.org/10.3204/DESY-BOOK/statistics.

[64] ATLAS collaboration, *Measurement of the cross-section for electroweak production of dijets in association with a Z boson in pp collisions at $\sqrt{s} = 13$ TeV with the ATLAS detector*, *Phys. Lett.* **B 775** (2017) 206 [arXiv:1709.10264] [INSPIRE].

[65] ATLAS collaboration, *Measurements of electroweak Wjj production and constraints on anomalous gauge couplings with the ATLAS detector*, *Eur. Phys. J.* **C 77** (2017) 474 [arXiv:1703.04362] [INSPIRE].

[66] ATLAS collaboration, *Measurement of differential cross sections and W^+/W^- cross-section ratios for W boson production in association with jets at $\sqrt{s} = 8$ TeV with the ATLAS detector*, *JHEP* **05** (2018) 077 [arXiv:1711.03296] [INSPIRE].

[67] ATLAS collaboration, *ATLAS Computing Acknowledgements*, ATL-GEN-PUB-2016-002 (2016).

JHEP03(2020)179

The ATLAS collaboration

G. Aad[102], B. Abbott[129], D.C. Abbott[103], A. Abed Abud[71a,71b], K. Abeling[53], D.K. Abhayasinghe[94], S.H. Abidi[167], O.S. AbouZeid[40], N.L. Abraham[156], H. Abramowicz[161], H. Abreu[160], Y. Abulaiti[6], B.S. Acharya[67a,67b,o], B. Achkar[53], S. Adachi[163], L. Adam[100], C. Adam Bourdarios[5], L. Adamczyk[84a], L. Adamek[167], J. Adelman[121], M. Adersberger[114], A. Adiguzel[12c], S. Adorni[54], T. Adye[144], A.A. Affolder[146], Y. Afik[160], C. Agapopoulou[65], M.N. Agaras[38], A. Aggarwal[119], C. Agheorghiesei[27c], J.A. Aguilar-Saavedra[140f,140a,aj], F. Ahmadov[80], W.S. Ahmed[104], X. Ai[18], G. Aielli[74a,74b], S. Akatsuka[86], T.P.A. Åkesson[97], E. Akilli[54], A.V. Akimov[111], K. Al Khoury[65], G.L. Alberghi[23b,23a], J. Albert[176], M.J. Alconada Verzini[161], S. Alderweireldt[36], M. Aleksa[36], I.N. Aleksandrov[80], C. Alexa[27b], D. Alexandre[19], T. Alexopoulos[10], A. Alfonsi[120], F. Alfonsi[23b,23a], M. Alhroob[129], B. Ali[142], G. Alimonti[69a], J. Alison[37], S.P. Alkire[148], C. Allaire[65], B.M.M. Allbrooke[156], B.W. Allen[132], P.P. Allport[21], A. Aloisio[70a,70b], A. Alonso[40], F. Alonso[89], C. Alpigiani[148], A.A. Alshehri[57], M. Alvarez Estevez[99], D. Álvarez Piqueras[174], M.G. Alviggi[70a,70b], Y. Amaral Coutinho[81b], A. Ambler[104], L. Ambroz[135], C. Amelung[26], D. Amidei[106], S.P. Amor Dos Santos[140a], S. Amoroso[46], C.S. Amrouche[54], F. An[79], C. Anastopoulos[149], N. Andari[145], T. Andeen[11], C.F. Anders[61b], J.K. Anders[20], A. Andreazza[69a,69b], V. Andrei[61a], C.R. Anelli[176], S. Angelidakis[38], A. Angerami[39], A.V. Anisenkov[122b,122a], A. Annovi[72a], C. Antel[61a], M.T. Anthony[149], E. Antipov[130], M. Antonelli[51], D.J.A. Antrim[171], F. Anulli[73a], M. Aoki[82], J.A. Aparisi Pozo[174], L. Aperio Bella[15a], G. Arabidze[107], J.P. Araque[140a], V. Araujo Ferraz[81b], R. Araujo Pereira[81b], C. Arcangeletti[51], A.T.H. Arce[49], F.A. Arduh[89], J-F. Arguin[110], S. Argyropoulos[78], J.-H. Arling[46], A.J. Armbruster[36], A. Armstrong[171], O. Arnaez[167], H. Arnold[120], Z.P. Arrubarrena Tame[114], A. Artamonov[124,*], G. Artoni[135], S. Artz[100], S. Asai[163], N. Asbah[59], E.M. Asimakopoulou[172], L. Asquith[156], J. Assahsah[35d], K. Assamagan[29], R. Astalos[28a], R.J. Atkin[33a], M. Atkinson[173], N.B. Atlay[19], H. Atmani[65], K. Augsten[142], G. Avolio[36], R. Avramidou[60a], M.K. Ayoub[15a], A.M. Azoulay[168b], G. Azuelos[110,ax], H. Bachacou[145], K. Bachas[68a,68b], M. Backes[135], F. Backman[45a,45b], P. Bagnaia[73a,73b], M. Bahmani[85], H. Bahrasemani[152], A.J. Bailey[174], V.R. Bailey[173], J.T. Baines[144], M. Bajic[40], C. Bakalis[10], O.K. Baker[183], P.J. Bakker[120], D. Bakshi Gupta[8], S. Balaji[157], E.M. Baldin[122b,122a], P. Balek[180], F. Balli[145], W.K. Balunas[135], J. Balz[100], E. Banas[85], A. Bandyopadhyay[24], Sw. Banerjee[181,j], A.A.E. Bannoura[182], L. Barak[161], W.M. Barbe[38], E.L. Barberio[105], D. Barberis[55b,55a], M. Barbero[102], G. Barbour[95], T. Barillari[115], M-S. Barisits[36], J. Barkeloo[132], T. Barklow[153], R. Barnea[160], S.L. Barnes[60c], B.M. Barnett[144], R.M. Barnett[18], Z. Barnovska-Blenessy[60a], A. Baroncelli[60a], G. Barone[29], A.J. Barr[135], L. Barranco Navarro[45a,45b], F. Barreiro[99], J. Barreiro Guimarães da Costa[15a], S. Barsov[138], R. Bartoldus[153], G. Bartolini[102], A.E. Barton[90], P. Bartos[28a], A. Basalaev[46], A. Bassalat[65,aq], M.J. Basso[167], R.L. Bates[57], S. Batlamous[35e], J.R. Batley[32], B. Batool[151], M. Battaglia[146], M. Bauce[73a,73b], F. Bauer[145], K.T. Bauer[171], H.S. Bawa[31,m], J.B. Beacham[49], T. Beau[136], P.H. Beauchemin[170], F. Becherer[52], P. Bechtle[24], H.C. Beck[53], H.P. Beck[20,s], K. Becker[52], M. Becker[100], C. Becot[46], A. Beddall[12d], A.J. Beddall[12a], V.A. Bednyakov[80], M. Bedognetti[120], C.P. Bee[155], T.A. Beermann[182], M. Begalli[81b], M. Begel[29], A. Behera[155], J.K. Behr[46], F. Beisiegel[24], A.S. Bell[95], G. Bella[161], L. Bellagamba[23b], A. Bellerive[34], P. Bellos[9], K. Beloborodov[122b,122a], K. Belotskiy[112], N.L. Belyaev[112], D. Benchekroun[35a], N. Benekos[10], Y. Benhammou[161], D.P. Benjamin[6], M. Benoit[54], J.R. Bensinger[26], S. Bentvelsen[120], L. Beresford[135], M. Beretta[51], D. Berge[46], E. Bergeaas Kuutmann[172], N. Berger[5], B. Bergmann[142], L.J. Bergsten[26], J. Beringer[18], S. Berlendis[7], G. Bernardi[136], C. Bernius[153], F.U. Bernlochner[24], T. Berry[94], P. Berta[100], C. Bertella[15a], I.A. Bertram[90], O. Bessidskaia Bylund[182], N. Besson[145], A. Bethani[101],

JHEP03(2020)179

S. Bethke[115], A. Betti[42], A.J. Bevan[93], J. Beyer[115], D.S. Bhattacharya[177], P. Bhattarai[26], R. Bi[139], R.M. Bianchi[139], O. Biebel[114], D. Biedermann[19], R. Bielski[36], K. Bierwagen[100], N.V. Biesuz[72a,72b], M. Biglietti[75a], T.R.V. Billoud[110], M. Bindi[53], A. Bingul[12d], C. Bini[73a,73b], S. Biondi[23b,23a], M. Birman[180], T. Bisanz[53], J.P. Biswal[161], D. Biswas[181,j], A. Bitadze[101], C. Bittrich[48], K. Bjørke[134], K.M. Black[25], T. Blazek[28a], I. Bloch[46], C. Blocker[26], A. Blue[57], U. Blumenschein[93], G.J. Bobbink[120], V.S. Bobrovnikov[122b,122a], S.S. Bocchetta[97], A. Bocci[49], D. Boerner[46], D. Bogavac[14], A.G. Bogdanchikov[122b,122a], C. Bohm[45a], V. Boisvert[94], P. Bokan[53,172], T. Bold[84a], A.S. Boldyrev[113], A.E. Bolz[61b], M. Bomben[136], M. Bona[93], J.S. Bonilla[132], M. Boonekamp[145], C.D. Booth[94], H.M. Borecka-Bielska[91], A. Borisov[123], G. Borissov[90], J. Bortfeldt[36], D. Bortoletto[135], D. Boscherini[23b], M. Bosman[14], J.D. Bossio Sola[104], K. Bouaouda[35a], J. Boudreau[139], E.V. Bouhova-Thacker[90], D. Boumediene[38], S.K. Boutle[57], A. Boveia[127], J. Boyd[36], D. Boye[33c,ar], I.R. Boyko[80], A.J. Bozson[94], J. Bracinik[21], N. Brahimi[102], G. Brandt[182], O. Brandt[32], F. Braren[46], B. Brau[103], J.E. Brau[132], W.D. Breaden Madden[57], K. Brendlinger[46], L. Brenner[46], R. Brenner[172], S. Bressler[180], B. Brickwedde[100], D.L. Briglin[21], D. Britton[57], D. Britzger[115], I. Brock[24], R. Brock[107], G. Brooijmans[39], W.K. Brooks[147c], E. Brost[121], J.H Broughton[21], P.A. Bruckman de Renstrom[85], D. Bruncko[28b], A. Bruni[23b], G. Bruni[23b], L.S. Bruni[120], S. Bruno[74a,74b], M. Bruschi[23b], N. Bruscino[139], P. Bryant[37], L. Bryngemark[97], T. Buanes[17], Q. Buat[36], P. Buchholz[151], A.G. Buckley[57], I.A. Budagov[80], M.K. Bugge[134], F. Bührer[52], O. Bulekov[112], T.J. Burch[121], S. Burdin[91], C.D. Burgard[120], A.M. Burger[130], B. Burghgrave[8], J.T.P. Burr[46], C.D. Burton[11], J.C. Burzynski[103], V. Büscher[100], E. Buschmann[53], P.J. Bussey[57], J.M. Butler[25], C.M. Buttar[57], J.M. Butterworth[95], P. Butti[36], W. Buttinger[36], C.J. Buxo Vazquez[107], A. Buzatu[158], A.R. Buzykaev[122b,122a], G. Cabras[23b,23a], S. Cabrera Urbán[174], D. Caforio[56], H. Cai[173], V.M.M. Cairo[153], O. Cakir[4a], N. Calace[36], P. Calafiura[18], A. Calandri[102], G. Calderini[136], P. Calfayan[66], G. Callea[57], L.P. Caloba[81b], S. Calvente Lopez[99], D. Calvet[38], S. Calvet[38], T.P. Calvet[155], M. Calvetti[72a,72b], R. Camacho Toro[136], S. Camarda[36], D. Camarero Munoz[99], P. Camarri[74a,74b], D. Cameron[134], R. Caminal Armadans[103], C. Camincher[36], S. Campana[36], M. Campanelli[95], A. Camplani[40], A. Campoverde[151], V. Canale[70a,70b], A. Canesse[104], M. Cano Bret[60c], J. Cantero[130], T. Cao[161], Y. Cao[173], M.D.M. Capeans Garrido[36], M. Capua[41b,41a], R. Cardarelli[74a], F. Cardillo[149], G. Carducci[41b,41a], I. Carli[143], T. Carli[36], G. Carlino[70a], B.T. Carlson[139], L. Carminati[69a,69b], R.M.D. Carney[45a,45b], S. Caron[119], E. Carquin[147c], S. Carrá[46], J.W.S. Carter[167], M.P. Casado[14,e], A.F. Casha[167], D.W. Casper[171], R. Castelijn[120], F.L. Castillo[174], V. Castillo Gimenez[174], N.F. Castro[140a,140e], A. Catinaccio[36], J.R. Catmore[134], A. Cattai[36], J. Caudron[24], V. Cavaliere[29], E. Cavallaro[14], M. Cavalli-Sforza[14], V. Cavasinni[72a,72b], E. Celebi[12b], F. Ceradini[75a,75b], L. Cerda Alberich[174], K. Cerny[131], A.S. Cerqueira[81a], A. Cerri[156], L. Cerrito[74a,74b], F. Cerutti[18], A. Cervelli[23b,23a], S.A. Cetin[12b], Z. Chadi[35a], D. Chakraborty[121], S.K. Chan[59], W.S. Chan[120], W.Y. Chan[91], J.D. Chapman[32], B. Chargeishvili[159b], D.G. Charlton[21], T.P. Charman[93], C.C. Chau[34], S. Che[127], S. Chekanov[6], S.V. Chekulaev[168a], G.A. Chelkov[80,aw], M.A. Chelstowska[36], B. Chen[79], C. Chen[60a], C.H. Chen[79], H. Chen[29], J. Chen[60a], J. Chen[39], S. Chen[137], S.J. Chen[15c], X. Chen[15b,av], Y. Chen[83], Y-H. Chen[46], H.C. Cheng[63a], H.J. Cheng[15a], A. Cheplakov[80], E. Cheremushkina[123], R. Cherkaoui El Moursli[35e], E. Cheu[7], K. Cheung[64], T.J.A. Chevalérias[145], L. Chevalier[145], V. Chiarella[51], G. Chiarelli[72a], G. Chiodini[68a], A.S. Chisholm[21], A. Chitan[27b], I. Chiu[163], Y.H. Chiu[176], M.V. Chizhov[80], K. Choi[66], A.R. Chomont[73a,73b], S. Chouridou[162], Y.S. Chow[120], M.C. Chu[63a], X. Chu[15a,15d], J. Chudoba[141], A.J. Chuinard[104], J.J. Chwastowski[85], L. Chytka[131], D. Cieri[115], K.M. Ciesla[85], D. Cinca[47], V. Cindro[92], I.A. Cioară[27b], A. Ciocio[18], F. Cirotto[70a,70b], Z.H. Citron[180,k], M. Citterio[69a], D.A. Ciubotaru[27b], B.M. Ciungu[167], A. Clark[54], M.R. Clark[39], P.J. Clark[50], C. Clement[45a,45b], Y. Coadou[102], M. Cobal[67a,67c], A. Coccaro[55b], J. Cochran[79],

JHEP03(2020)179

H. Cohen[161], A.E.C. Coimbra[36], L. Colasurdo[119], B. Cole[39], A.P. Colijn[120], J. Collot[58], P. Conde Muiño[140a,f], E. Coniavitis[52], S.H. Connell[33c], I.A. Connelly[57], S. Constantinescu[27b], F. Conventi[70a,ay], A.M. Cooper-Sarkar[135], F. Cormier[175], K.J.R. Cormier[167], L.D. Corpe[95], M. Corradi[73a,73b], E.E. Corrigan[97], F. Corriveau[104,af], A. Cortes-Gonzalez[36], M.J. Costa[174], F. Costanza[5], D. Costanzo[149], G. Cowan[94], J.W. Cowley[32], J. Crane[101], K. Cranmer[125], S.J. Crawley[57], R.A. Creager[137], S. Crépé-Renaudin[58], F. Crescioli[136], M. Cristinziani[24], V. Croft[120], G. Crosetti[41b,41a], A. Cueto[5], T. Cuhadar Donszelmann[149], A.R. Cukierman[153], W.R. Cunningham[57], S. Czekierda[85], P. Czodrowski[36], M.J. Da Cunha Sargedas De Sousa[60b], J.V. Da Fonseca Pinto[81b], C. Da Via[101], W. Dabrowski[84a], T. Dado[28a], S. Dahbi[35e], T. Dai[106], C. Dallapiccola[103], M. Dam[40], G. D'amen[29], V. D'Amico[75a,75b], J. Damp[100], J.R. Dandoy[137], M.F. Daneri[30], N.P. Dang[181,j], N.S. Dann[101], M. Danninger[175], V. Dao[36], G. Darbo[55b], O. Dartsi[5], A. Dattagupta[132], T. Daubney[46], S. D'Auria[69a,69b], W. Davey[24], C. David[46], T. Davidek[143], D.R. Davis[49], I. Dawson[149], K. De[8], R. De Asmundis[70a], M. De Beurs[120], S. De Castro[23b,23a], S. De Cecco[73a,73b], N. De Groot[119], P. de Jong[120], H. De la Torre[107], A. De Maria[15c], D. De Pedis[73a], A. De Salvo[73a], U. De Sanctis[74a,74b], M. De Santis[74a,74b], A. De Santo[156], K. De Vasconcelos Corga[102], J.B. De Vivie De Regie[65], C. Debenedetti[146], D.V. Dedovich[80], A.M. Deiana[42], M. Del Gaudio[41b,41a], J. Del Peso[99], Y. Delabat Diaz[46], D. Delgove[65], F. Deliot[145,r], C.M. Delitzsch[7], M. Della Pietra[70a,70b], D. Della Volpe[54], A. Dell'Acqua[36], L. Dell'Asta[74a,74b], M. Delmastro[5], C. Delporte[65], P.A. Delsart[58], D.A. DeMarco[167], S. Demers[183], M. Demichev[80], G. Demontigny[110], S.P. Denisov[123], D. Denysiuk[120], L. D'Eramo[136], D. Derendarz[85], J.E. Derkaoui[35d], F. Derue[136], P. Dervan[91], K. Desch[24], C. Deterre[46], K. Dette[167], C. Deutsch[24], M.R. Devesa[30], P.O. Deviveiros[36], A. Dewhurst[144], F.A. Di Bello[54], A. Di Ciaccio[74a,74b], L. Di Ciaccio[5], W.K. Di Clemente[137], C. Di Donato[70a,70b], A. Di Girolamo[36], G. Di Gregorio[72a,72b], B. Di Micco[75a,75b], R. Di Nardo[103], K.F. Di Petrillo[59], R. Di Sipio[167], D. Di Valentino[34], C. Diaconu[102], F.A. Dias[40], T. Dias Do Vale[140a], M.A. Diaz[147a], J. Dickinson[18], E.B. Diehl[106], J. Dietrich[19], S. Díez Cornell[46], A. Dimitrievska[18], W. Ding[15b], J. Dingfelder[24], F. Dittus[36], F. Djama[102], T. Djobava[159b], J.I. Djuvsland[17], M.A.B. Do Vale[81c], M. Dobre[27b], D. Dodsworth[26], C. Doglioni[97], J. Dolejsi[143], Z. Dolezal[143], M. Donadelli[81d], B. Dong[60c], J. Donini[38], A. D'onofrio[93], M. D'Onofrio[91], J. Dopke[144], A. Doria[70a], M.T. Dova[89], A.T. Doyle[57], E. Drechsler[152], E. Dreyer[152], T. Dreyer[53], A.S. Drobac[170], D. Du[60b], Y. Duan[60b], F. Dubinin[111], M. Dubovsky[28a], A. Dubreuil[54], E. Duchovni[180], G. Duckeck[114], A. Ducourthial[136], O.A. Ducu[110], D. Duda[115], A. Dudarev[36], A.C. Dudder[100], E.M. Duffield[18], L. Duflot[65], M. Dührssen[36], C. Dülsen[182], M. Dumancic[180], A.E. Dumitriu[27b], A.K. Duncan[57], M. Dunford[61a], A. Duperrin[102], H. Duran Yildiz[4a], M. Düren[56], A. Durglishvili[159b], D. Duschinger[48], B. Dutta[46], D. Duvnjak[1], G.I. Dyckes[137], M. Dyndal[36], S. Dysch[101], B.S. Dziedzic[85], K.M. Ecker[115], R.C. Edgar[106], M.G. Eggleston[49], T. Eifert[36], G. Eigen[17], K. Einsweiler[18], T. Ekelof[172], H. El Jarrari[35e], M. El Kacimi[35c], R. El Kosseifi[102], V. Ellajosyula[172], M. Ellert[172], F. Ellinghaus[182], A.A. Elliot[93], N. Ellis[36], J. Elmsheuser[29], M. Elsing[36], D. Emeliyanov[144], A. Emerman[39], Y. Enari[163], M.B. Epland[49], J. Erdmann[47], A. Ereditato[20], M. Errenst[36], M. Escalier[65], C. Escobar[174], O. Estrada Pastor[174], E. Etzion[161], H. Evans[66], A. Ezhilov[138], F. Fabbri[57], L. Fabbri[23b,23a], V. Fabiani[119], G. Facini[95], R.M. Faisca Rodrigues Pereira[140a], R.M. Fakhrutdinov[123], S. Falciano[73a], P.J. Falke[5], S. Falke[5], J. Faltova[143], Y. Fang[15a], Y. Fang[15a], G. Fanourakis[44], M. Fanti[69a,69b], M. Faraj[67a,67c,u], A. Farbin[8], A. Farilla[75a], E.M. Farina[71a,71b], T. Farooque[107], S. Farrell[18], S.M. Farrington[50], P. Farthouat[36], F. Fassi[35e], P. Fassnacht[36], D. Fassouliotis[9], M. Faucci Giannelli[50], W.J. Fawcett[32], L. Fayard[65], O.L. Fedin[138,p], W. Fedorko[175], M. Feickert[42], L. Feligioni[102], A. Fell[149], C. Feng[60b], E.J. Feng[36], M. Feng[49], M.J. Fenton[57], A.B. Fenyuk[123], J. Ferrando[46], A. Ferrante[173], A. Ferrari[172],

JHEP03(2020)179

P. Ferrari[120], R. Ferrari[71a], D.E. Ferreira de Lima[61b], A. Ferrer[174], D. Ferrere[54], C. Ferretti[106], F. Fiedler[100], A. Filipčič[92], F. Filthaut[119], K.D. Finelli[25], M.C.N. Fiolhais[140a,140c,a], L. Fiorini[174], F. Fischer[114], W.C. Fisher[107], I. Fleck[151], P. Fleischmann[106], R.R.M. Fletcher[137], T. Flick[182], B.M. Flierl[114], L. Flores[137], L.R. Flores Castillo[63a], F.M. Follega[76a,76b], N. Fomin[17], J.H. Foo[167], G.T. Forcolin[76a,76b], A. Formica[145], F.A. Förster[14], A.C. Forti[101], A.G. Foster[21], M.G. Foti[135], D. Fournier[65], H. Fox[90], P. Francavilla[72a,72b], S. Francescato[73a,73b], M. Franchini[23b,23a], S. Franchino[61a], D. Francis[36], L. Franconi[20], M. Franklin[59], A.N. Fray[93], P.M. Freeman[21], B. Freund[110], W.S. Freund[81b], E.M. Freundlich[47], D.C. Frizzell[129], D. Froidevaux[36], J.A. Frost[135], C. Fukunaga[164], E. Fullana Torregrosa[174], E. Fumagalli[55b,55a], T. Fusayasu[116], J. Fuster[174], A. Gabrielli[23b,23a], A. Gabrielli[18], G.P. Gach[84a], S. Gadatsch[54], P. Gadow[115], G. Gagliardi[55b,55a], L.G. Gagnon[110], C. Galea[27b], B. Galhardo[140a], G.E. Gallardo[135], E.J. Gallas[135], B.J. Gallop[144], G. Galster[40], R. Gamboa Goni[93], K.K. Gan[127], S. Ganguly[180], J. Gao[60a], Y. Gao[50], Y.S. Gao[31,m], C. García[174], J.E. García Navarro[174], J.A. García Pascual[15a], C. Garcia-Argos[52], M. Garcia-Sciveres[18], R.W. Gardner[37], N. Garelli[153], S. Gargiulo[52], V. Garonne[134], A. Gaudiello[55b,55a], G. Gaudio[71a], I.L. Gavrilenko[111], A. Gavrilyuk[124], C. Gay[175], G. Gaycken[46], E.N. Gazis[10], A.A. Geanta[27b], C.M. Gee[146], C.N.P. Gee[144], J. Geisen[53], M. Geisen[100], C. Gemme[55b], M.H. Genest[58], C. Geng[106], S. Gentile[73a,73b], S. George[94], T. Geralis[44], L.O. Gerlach[53], P. Gessinger-Befurt[100], G. Gessner[47], S. Ghasemi[151], M. Ghasemi Bostanabad[176], A. Ghosh[65], A. Ghosh[78], B. Giacobbe[23b], S. Giagu[73a,73b], N. Giangiacomi[23b,23a], P. Giannetti[72a], A. Giannini[70a,70b], G. Giannini[14], S.M. Gibson[94], M. Gignac[146], D. Gillberg[34], G. Gilles[182], D.M. Gingrich[3,ax], M.P. Giordani[67a,67c], F.M. Giorgi[23b], P.F. Giraud[145], G. Giugliarelli[67a,67c], D. Giugni[69a], F. Giuli[74a,74b], S. Gkaitatzis[162], I. Gkialas[9,h], E.L. Gkougkousis[14], P. Gkountoumis[10], L.K. Gladilin[113], C. Glasman[99], J. Glatzer[14], P.C.F. Glaysher[46], A. Glazov[46], G.R. Gledhill[132], M. Goblirsch-Kolb[26], D. Godin[110], S. Goldfarb[105], T. Golling[54], D. Golubkov[123], A. Gomes[140a,140b], R. Goncalves Gama[53], R. Gonçalo[140a], G. Gonella[52], L. Gonella[21], A. Gongadze[80], F. Gonnella[21], J.L. Gonski[59], S. González de la Hoz[174], S. Gonzalez-Sevilla[54], G.R. Gonzalvo Rodriguez[174], L. Goossens[36], P.A. Gorbounov[124], H.A. Gordon[29], B. Gorini[36], E. Gorini[68a,68b], A. Gorišek[92], A.T. Goshaw[49], M.I. Gostkin[80], C.A. Gottardo[119], M. Gouighri[35b], D. Goujdami[35c], A.G. Goussiou[148], N. Govender[33c], C. Goy[5], E. Gozani[160], I. Grabowska-Bold[84a], E.C. Graham[91], J. Gramling[171], E. Gramstad[134], S. Grancagnolo[19], M. Grandi[156], V. Gratchev[138], P.M. Gravila[27f], F.G. Gravili[68a,68b], C. Gray[57], H.M. Gray[18], C. Grefe[24], K. Gregersen[97], I.M. Gregor[46], P. Grenier[153], K. Grevtsov[46], C. Grieco[14], N.A. Grieser[129], A.A. Grillo[146], K. Grimm[31,l], S. Grinstein[14,aa], J.-F. Grivaz[65], S. Groh[100], E. Gross[180], J. Grosse-Knetter[53], Z.J. Grout[95], C. Grud[106], A. Grummer[118], L. Guan[106], W. Guan[181], J. Guenther[36], A. Guerguichon[65], J.G.R. Guerrero Rojas[174], F. Guescini[115], D. Guest[171], R. Gugel[52], T. Guillemin[5], S. Guindon[36], U. Gul[57], J. Guo[60c], W. Guo[106], Y. Guo[60a,t], Z. Guo[102], R. Gupta[46], S. Gurbuz[12c], G. Gustavino[129], M. Guth[52], P. Gutierrez[129], C. Gutschow[95], C. Guyot[145], C. Gwenlan[135], C.B. Gwilliam[91], A. Haas[125], C. Haber[18], H.K. Hadavand[8], N. Haddad[35e], A. Hadef[60a], S. Hageböck[36], M. Haleem[177], J. Haley[130], G. Halladjian[107], G.D. Hallewell[102], K. Hamacher[182], P. Hamal[131], K. Hamano[176], H. Hamdaoui[35e], G.N. Hamity[149], K. Han[60a,z], L. Han[60a], S. Han[15a], Y.F. Han[167], K. Hanagaki[82,x], M. Hance[146], D.M. Handl[114], B. Haney[137], R. Hankache[136], E. Hansen[97], J.B. Hansen[40], J.D. Hansen[40], M.C. Hansen[24], P.H. Hansen[40], E.C. Hanson[101], K. Hara[169], T. Harenberg[182], S. Harkusha[108], P.F. Harrison[178], N.M. Hartmann[114], Y. Hasegawa[150], A. Hasib[50], S. Hassani[145], S. Haug[20], R. Hauser[107], L.B. Havener[39], M. Havranek[142], C.M. Hawkes[21], R.J. Hawkings[36], D. Hayden[107], C. Hayes[155], R.L. Hayes[175], C.P. Hays[135], J.M. Hays[93], H.S. Hayward[91], S.J. Haywood[144], F. He[60a], M.P. Heath[50], V. Hedberg[97], L. Heelan[8], S. Heer[24], K.K. Heidegger[52], W.D. Heidorn[79], J. Heilman[34], S. Heim[46], T. Heim[18], B. Heinemann[46,as], J.J. Heinrich[132], L. Heinrich[36],

JHEP03(2020)179

C. Heinz[56], J. Hejbal[141], L. Helary[61b], A. Held[175], S. Hellesund[134], C.M. Helling[146], S. Hellman[45a,45b], C. Helsens[36], R.C.W. Henderson[90], Y. Heng[181], S. Henkelmann[175], A.M. Henriques Correia[36], G.H. Herbert[19], H. Herde[26], V. Herget[177], Y. Hernández Jiménez[33e], H. Herr[100], M.G. Herrmann[114], T. Herrmann[48], G. Herten[52], R. Hertenberger[114], L. Hervas[36], T.C. Herwig[137], G.G. Hesketh[95], N.P. Hessey[168a], A. Higashida[163], S. Higashino[82], E. Higón-Rodriguez[174], K. Hildebrand[37], E. Hill[176], J.C. Hill[32], K.K. Hill[29], K.H. Hiller[46], S.J. Hillier[21], M. Hils[48], I. Hinchliffe[18], F. Hinterkeuser[24], M. Hirose[133], S. Hirose[52], D. Hirschbuehl[182], B. Hiti[92], O. Hladik[141], D.R. Hlaluku[33e], X. Hoad[50], J. Hobbs[155], N. Hod[180], M.C. Hodgkinson[149], A. Hoecker[36], F. Hoenig[114], D. Hohn[52], D. Hohov[65], T.R. Holmes[37], M. Holzbock[114], L.B.A.H. Hommels[32], S. Honda[169], T.M. Hong[139], J.C. Honig[52], A. Hönle[115], B.H. Hooberman[173], W.H. Hopkins[6], Y. Horii[117], P. Horn[48], L.A. Horyn[37], S. Hou[158], A. Hoummada[35a], J. Howarth[101], J. Hoya[89], M. Hrabovsky[131], J. Hrdinka[77], I. Hristova[19], J. Hrivnac[65], A. Hrynevich[109], T. Hryn'ova[5], P.J. Hsu[64], S.-C. Hsu[148], Q. Hu[29], S. Hu[60c], Y.F. Hu[15a,15d], D.P. Huang[95], Y. Huang[60a], Y. Huang[15a], Z. Hubacek[142], F. Hubaut[102], M. Huebner[24], F. Huegging[24], T.B. Huffman[135], M. Huhtinen[36], R.F.H. Hunter[34], P. Huo[155], A.M. Hupe[34], N. Huseynov[80,ah], J. Huston[107], J. Huth[59], R. Hyneman[106], S. Hyrych[28a], G. Iacobucci[54], G. Iakovidis[29], I. Ibragimov[151], L. Iconomidou-Fayard[65], Z. Idrissi[35e], P. Iengo[36], R. Ignazzi[40], O. Igonkina[120,ac,*], R. Iguchi[163], T. Iizawa[54], Y. Ikegami[82], M. Ikeno[82], D. Iliadis[162], N. Ilic[119,167,af], F. Iltzsche[48], G. Introzzi[71a,71b], M. Iodice[75a], K. Iordanidou[168a], V. Ippolito[73a,73b], M.F. Isacson[172], M. Ishino[163], W. Islam[130], C. Issever[19,46], S. Istin[160], F. Ito[169], J.M. Iturbe Ponce[63a], R. Iuppa[76a,76b], A. Ivina[180], H. Iwasaki[82], J.M. Izen[43], V. Izzo[70a], P. Jacka[141], P. Jackson[1], R.M. Jacobs[24], B.P. Jaeger[152], V. Jain[2], G. Jäkel[182], K.B. Jakobi[100], K. Jakobs[52], T. Jakoubek[141], J. Jamieson[57], K.W. Janas[84a], R. Jansky[54], J. Janssen[24], M. Janus[53], P.A. Janus[84a], G. Jarlskog[97], N. Javadov[80,ah], T. Javůrek[36], M. Javurkova[52], F. Jeanneau[145], L. Jeanty[132], J. Jejelava[159a,ai], A. Jelinskas[178], P. Jenni[52,b], J. Jeong[46], N. Jeong[46], S. Jézéquel[5], H. Ji[181], J. Jia[155], H. Jiang[79], Y. Jiang[60a], Z. Jiang[153,q], S. Jiggins[52], F.A. Jimenez Morales[38], J. Jimenez Pena[115], S. Jin[15c], A. Jinaru[27b], O. Jinnouchi[165], H. Jivan[33e], P. Johansson[149], K.A. Johns[7], C.A. Johnson[66], K. Jon-And[45a,45b], R.W.L. Jones[90], S.D. Jones[156], S. Jones[7], T.J. Jones[91], J. Jongmanns[61a], P.M. Jorge[140a], J. Jovicevic[36], X. Ju[18], J.J. Junggeburth[115], A. Juste Rozas[14,aa], A. Kaczmarska[85], M. Kado[73a,73b], H. Kagan[127], M. Kagan[153], A. Kahn[39], C. Kahra[100], T. Kaji[179], E. Kajomovitz[160], C.W. Kalderon[97], A. Kaluza[100], A. Kamenshchikov[123], M. Kaneda[163], L. Kanjir[92], Y. Kano[117], V.A. Kantserov[112], J. Kanzaki[82], L.S. Kaplan[181], D. Kar[33e], K. Karava[135], M.J. Kareem[168b], S.N. Karpov[80], Z.M. Karpova[80], V. Kartvelishvili[90], A.N. Karyukhin[123], L. Kashif[181], R.D. Kass[127], A. Kastanas[45a,45b], C. Kato[60d,60c], J. Katzy[46], K. Kawade[150], K. Kawagoe[88], T. Kawaguchi[117], T. Kawamoto[163], G. Kawamura[53], E.F. Kay[176], V.F. Kazanin[122b,122a], R. Keeler[176], R. Kehoe[42], J.S. Keller[34], E. Kellermann[97], D. Kelsey[156], J.J. Kempster[21], J. Kendrick[21], K.E. Kennedy[39], O. Kepka[141], S. Kersten[182], B.P. Kerševan[92], S. Ketabchi Haghighat[167], M. Khader[173], F. Khalil-Zada[13], M. Khandoga[145], A. Khanov[130], A.G. Kharlamov[122b,122a], T. Kharlamova[122b,122a], E.E. Khoda[175], A. Khodinov[166], T.J. Khoo[54], E. Khramov[80], J. Khubua[159b], S. Kido[83], M. Kiehn[54], C.R. Kilby[94], Y.K. Kim[37], N. Kimura[95], O.M. Kind[19], B.T. King[91,*], D. Kirchmeier[48], J. Kirk[144], A.E. Kiryunin[115], T. Kishimoto[163], D.P. Kisliuk[167], V. Kitali[46], O. Kivernyk[5], T. Klapdor-Kleingrothaus[52], M. Klassen[61a], M.H. Klein[106], M. Klein[91], U. Klein[91], K. Kleinknecht[100], P. Klimek[121], A. Klimentov[29], T. Klingl[24], T. Klioutchnikova[36], F.F. Klitzner[114], P. Kluit[120], S. Kluth[115], E. Kneringer[77], E.B.F.G. Knoops[102], A. Knue[52], D. Kobayashi[88], T. Kobayashi[163], M. Kobel[48], M. Kocian[153], P. Kodys[143], P.T. Koenig[24], T. Koffas[34], N.M. Köhler[36], T. Koi[153], M. Kolb[61b], I. Koletsou[5], T. Komarek[131], T. Kondo[82], N. Kondrashova[60c], K. Köneke[52], A.C. König[119], T. Kono[126], R. Konoplich[125,an],

JHEP03(2020)179

V. Konstantinides[95], N. Konstantinidis[95], B. Konya[97], R. Kopeliansky[66], S. Koperny[84a], K. Korcyl[85], K. Kordas[162], G. Koren[161], A. Korn[95], I. Korolkov[14], E.V. Korolkova[149], N. Korotkova[113], O. Kortner[115], S. Kortner[115], T. Kosek[143], V.V. Kostyukhin[166,166], A. Kotsokechagia[65], A. Kotwal[49], A. Koulouris[10], A. Kourkoumeli-Charalampidi[71a,71b], C. Kourkoumelis[9], E. Kourlitis[149], V. Kouskoura[29], A.B. Kowalewska[85], R. Kowalewski[176], C. Kozakai[163], W. Kozanecki[145], A.S. Kozhin[123], V.A. Kramarenko[113], G. Kramberger[92], D. Krasnopevtsev[60a], M.W. Krasny[136], A. Krasznahorkay[36], D. Krauss[115], J.A. Kremer[84a], J. Kretzschmar[91], P. Krieger[167], F. Krieter[114], A. Krishnan[61b], K. Krizka[18], K. Kroeninger[47], H. Kroha[115], J. Kroll[141], J. Kroll[137], K.S. Krowpman[107], J. Krstic[16], U. Kruchonak[80], H. Krüger[24], N. Krumnack[79], M.C. Kruse[49], J.A. Krzysiak[85], T. Kubota[105], O. Kuchinskaia[166], S. Kuday[4b], J.T. Kuechler[46], S. Kuehn[36], A. Kugel[61a], T. Kuhl[46], V. Kukhtin[80], R. Kukla[102], Y. Kulchitsky[108,ak], S. Kuleshov[147c], Y.P. Kulinich[173], M. Kuna[58], T. Kunigo[86], A. Kupco[141], T. Kupfer[47], O. Kuprash[52], H. Kurashige[83], L.L. Kurchaninov[168a], Y.A. Kurochkin[108], A. Kurova[112], M.G. Kurth[15a,15d], E.S. Kuwertz[36], M. Kuze[165], A.K. Kvam[148], J. Kvita[131], T. Kwan[104], A. La Rosa[115], L. La Rotonda[41b,41a], F. La Ruffa[41b,41a], C. Lacasta[174], F. Lacava[73a,73b], D.P.J. Lack[101], H. Lacker[19], D. Lacour[136], E. Ladygin[80], R. Lafaye[5], B. Laforge[136], T. Lagouri[33e], S. Lai[53], S. Lammers[66], W. Lampl[7], C. Lampoudis[162], E. Lançon[29], U. Landgraf[52], M.P.J. Landon[93], M.C. Lanfermann[54], V.S. Lang[46], J.C. Lange[53], R.J. Langenberg[36], A.J. Lankford[171], F. Lanni[29], K. Lantzsch[24], A. Lanza[71a], A. Lapertosa[55b,55a], S. Laplace[136], J.F. Laporte[145], T. Lari[69a], F. Lasagni Manghi[23b,23a], M. Lassnig[36], T.S. Lau[63a], A. Laudrain[65], A. Laurier[34], M. Lavorgna[70a,70b], S.D. Lawlor[94], M. Lazzaroni[69a,69b], B. Le[105], E. Le Guirriec[102], M. LeBlanc[7], T. LeCompte[6], F. Ledroit-Guillon[58], A.C.A. Lee[95], C.A. Lee[29], G.R. Lee[17], L. Lee[59], S.C. Lee[158], S.J. Lee[34], S. Lee[79], B. Lefebvre[168a], H.P. Lefebvre[94], M. Lefebvre[176], F. Legger[114], C. Leggett[18], K. Lehmann[152], N. Lehmann[182], G. Lehmann Miotto[36], W.A. Leight[46], A. Leisos[162,y], M.A.L. Leite[81d], C.E. Leitgeb[114], R. Leitner[143], D. Lellouch[180,*], K.J.C. Leney[42], T. Lenz[24], B. Lenzi[36], R. Leone[7], S. Leone[72a], C. Leonidopoulos[50], A. Leopold[136], G. Lerner[156], C. Leroy[110], R. Les[167], C.G. Lester[32], M. Levchenko[138], J. Levêque[5], D. Levin[106], L.J. Levinson[180], D.J. Lewis[21], B. Li[15b], B. Li[106], C-Q. Li[60a], F. Li[60c], H. Li[60a], H. Li[60b], J. Li[60c], K. Li[153], L. Li[60c], M. Li[15a,15d], Q. Li[15a,15d], Q.Y. Li[60a], S. Li[60d,60c], X. Li[46], Y. Li[46], Z. Li[60b], Z. Liang[15a], B. Liberti[74a], A. Liblong[167], K. Lie[63c], C.Y. Lin[32], K. Lin[107], T.H. Lin[100], R.A. Linck[66], J.H. Lindon[21], A.L. Lionti[54], E. Lipeles[137], A. Lipniacka[17], M. Lisovyi[61b], T.M. Liss[173,au], A. Lister[175], A.M. Litke[146], J.D. Little[8], B. Liu[79], B.L. Liu[6], H.B. Liu[29], H. Liu[106], J.B. Liu[60a], J.K.K. Liu[135], K. Liu[136], M. Liu[60a], P. Liu[18], Y. Liu[15a,15d], Y.L. Liu[106], Y.W. Liu[60a], M. Livan[71a,71b], A. Lleres[58], J. Llorente Merino[152], S.L. Lloyd[93], C.Y. Lo[63b], F. Lo Sterzo[42], E.M. Lobodzinska[46], P. Loch[7], S. Loffredo[74a,74b], T. Lohse[19], K. Lohwasser[149], M. Lokajicek[141], J.D. Long[173], R.E. Long[90], L. Longo[36], K.A. Looper[127], J.A. Lopez[147c], I. Lopez Paz[101], A. Lopez Solis[149], J. Lorenz[114], N. Lorenzo Martinez[5], M. Losada[22], P.J. Lösel[114], A. Lösle[52], X. Lou[46], X. Lou[15a], A. Lounis[65], J. Love[6], P.A. Love[90], J.J. Lozano Bahilo[174], M. Lu[60a], Y.J. Lu[64], H.J. Lubatti[148], C. Luci[73a,73b], A. Lucotte[58], C. Luedtke[52], F. Luehring[66], I. Luise[136], L. Luminari[73a], B. Lund-Jensen[154], M.S. Lutz[103], D. Lynn[29], R. Lysak[141], E. Lytken[97], F. Lyu[15a], V. Lyubushkin[80], T. Lyubushkina[80], H. Ma[29], L.L. Ma[60b], Y. Ma[60b], G. Maccarrone[51], A. Macchiolo[115], C.M. Macdonald[149], J. Machado Miguens[137], D. Madaffari[174], R. Madar[38], W.F. Mader[48], N. Madysa[48], J. Maeda[83], T. Maeno[29], M. Maerker[48], A.S. Maevskiy[113], V. Magerl[52], N. Magini[79], D.J. Mahon[39], C. Maidantchik[81b], T. Maier[114], A. Maio[140a,140b,140d], K. Maj[84a], O. Majersky[28a], S. Majewski[132], Y. Makida[82], N. Makovec[65], B. Malaescu[136], Pa. Malecki[85], V.P. Maleev[138], F. Malek[58], U. Mallik[78], D. Malon[6], C. Malone[32], S. Maltezos[10], S. Malyukov[80], J. Mamuzic[174], G. Mancini[51], I. Mandić[92], L. Manhaes de Andrade Filho[81a], I.M. Maniatis[162],

JHEP03(2020)179

J. Manjarres Ramos[48], K.H. Mankinen[97], A. Mann[114], A. Manousos[77], B. Mansoulie[145], I. Manthos[162], S. Manzoni[120], A. Marantis[162], G. Marceca[30], L. Marchese[135], G. Marchiori[136], M. Marcisovsky[141], L. Marcoccia[74a,74b], C. Marcon[97], C.A. Marin Tobon[36], M. Marjanovic[129], Z. Marshall[18], M.U.F. Martensson[172], S. Marti-Garcia[174], C.B. Martin[127], T.A. Martin[178], V.J. Martin[50], B. Martin dit Latour[17], L. Martinelli[75a,75b], M. Martinez[14,aa], V.I. Martinez Outschoorn[103], S. Martin-Haugh[144], V.S. Martoiu[27b], A.C. Martyniuk[95], A. Marzin[36], S.R. Maschek[115], L. Masetti[100], T. Mashimo[163], R. Mashinistov[111], J. Masik[101], A.L. Maslennikov[122b,122a], L. Massa[74a,74b], P. Massarotti[70a,70b], P. Mastrandrea[72a,72b], A. Mastroberardino[41b,41a], T. Masubuchi[163], D. Matakias[10], A. Matic[114], P. Mättig[24], J. Maurer[27b], B. Maček[92], D.A. Maximov[122b,122a], R. Mazini[158], I. Maznas[162], S.M. Mazza[146], S.P. Mc Kee[106], T.G. McCarthy[115], W.P. McCormack[18], E.F. McDonald[105], J.A. Mcfayden[36], G. Mchedlidze[159b], M.A. McKay[42], K.D. McLean[176], S.J. McMahon[144], P.C. McNamara[105], C.J. McNicol[178], R.A. McPherson[176,af], J.E. Mdhluli[33e], Z.A. Meadows[103], S. Meehan[36], T. Megy[52], S. Mehlhase[114], A. Mehta[91], T. Meideck[58], B. Meirose[43], D. Melini[174], B.R. Mellado Garcia[33e], J.D. Mellenthin[53], M. Melo[28a], F. Meloni[46], A. Melzer[24], S.B. Menary[101], E.D. Mendes Gouveia[140a,140e], L. Meng[36], X.T. Meng[106], S. Menke[115], E. Meoni[41b,41a], S. Mergelmeyer[19], S.A.M. Merkt[139], C. Merlassino[20], P. Mermod[54], L. Merola[70a,70b], C. Meroni[69a], O. Meshkov[113,111], J.K.R. Meshreki[151], A. Messina[73a,73b], J. Metcalfe[6], A.S. Mete[171], C. Meyer[66], J. Meyer[160], J-P. Meyer[145], H. Meyer Zu Theenhausen[61a], F. Miano[156], M. Michetti[19], R.P. Middleton[144], L. Mijović[50], G. Mikenberg[180], M. Mikestikova[141], M. Mikuž[92], H. Mildner[149], M. Milesi[105], A. Milic[167], D.A. Millar[93], D.W. Miller[37], A. Milov[180], D.A. Milstead[45a,45b], R.A. Mina[153,q], A.A. Minaenko[123], M. Miñano Moya[174], I.A. Minashvili[159b], A.I. Mincer[125], B. Mindur[84a], M. Mineev[80], Y. Minegishi[163], L.M. Mir[14], A. Mirto[68a,68b], K.P. Mistry[137], T. Mitani[179], J. Mitrevski[114], V.A. Mitsou[174], M. Mittal[60c], O. Miu[167], A. Miucci[20], P.S. Miyagawa[149], A. Mizukami[82], J.U. Mjörnmark[97], T. Mkrtchyan[184], M. Mlynarikova[143], T. Moa[45a,45b], K. Mochizuki[110], P. Mogg[52], S. Mohapatra[39], R. Moles-Valls[24], M.C. Mondragon[107], K. Mönig[46], J. Monk[40], E. Monnier[102], A. Montalbano[152], J. Montejo Berlingen[36], M. Montella[95], F. Monticelli[89], S. Monzani[69a], N. Morange[65], D. Moreno[22], M. Moreno Llácer[174], C. Moreno Martinez[14], P. Morettini[55b], M. Morgenstern[120], S. Morgenstern[48], D. Mori[152], M. Morii[59], M. Morinaga[179], V. Morisbak[134], A.K. Morley[36], G. Mornacchi[36], A.P. Morris[95], L. Morvaj[155], P. Moschovakos[36], B. Moser[120], M. Mosidze[159b], T. Moskalets[145], H.J. Moss[149], J. Moss[31,n], E.J.W. Moyse[103], S. Muanza[102], J. Mueller[139], R.S.P. Mueller[114], D. Muenstermann[90], G.A. Mullier[97], D.P. Mungo[69a,69b], J.L. Munoz Martinez[14], F.J. Munoz Sanchez[101], P. Murin[28b], W.J. Murray[178,144], A. Murrone[69a,69b], M. Muškinja[18], C. Mwewa[33a], A.G. Myagkov[123,ao], J. Myers[132], M. Myska[142], B.P. Nachman[18], O. Nackenhorst[47], A.Nag Nag[48], K. Nagai[135], K. Nagano[82], Y. Nagasaka[62], M. Nagel[52], J.L. Nagle[29], E. Nagy[102], A.M. Nairz[36], Y. Nakahama[117], K. Nakamura[82], T. Nakamura[163], I. Nakano[128], H. Nanjo[133], F. Napolitano[61a], R.F. Naranjo Garcia[46], R. Narayan[42], I. Naryshkin[138], T. Naumann[46], G. Navarro[22], P.Y. Nechaeva[111], F. Nechansky[46], T.J. Neep[21], A. Negri[71a,71b], M. Negrini[23b], C. Nellist[53], M.E. Nelson[135], S. Nemecek[141], P. Nemethy[125], M. Nessi[36,d], M.S. Neubauer[173], M. Neumann[182], P.R. Newman[21], Y.S. Ng[19], Y.W.Y. Ng[171], B. Ngair[35e], H.D.N. Nguyen[102], T. Nguyen Manh[110], E. Nibigira[38], R.B. Nickerson[135], R. Nicolaidou[145], D.S. Nielsen[40], J. Nielsen[146], N. Nikiforou[11], V. Nikolaenko[123,ao], I. Nikolic-Audit[136], K. Nikolopoulos[21], P. Nilsson[29], H.R. Nindhito[54], Y. Ninomiya[82], A. Nisati[73a], N. Nishu[60c], R. Nisius[115], I. Nitsche[47], T. Nitta[179], T. Nobe[163], Y. Noguchi[86], I. Nomidis[136], M.A. Nomura[29], M. Nordberg[36], N. Norjoharuddeen[135], T. Novak[92], O. Novgorodova[48], R. Novotny[142], L. Nozka[131], K. Ntekas[171], E. Nurse[95], F.G. Oakham[34,ax], H. Oberlack[115], J. Ocariz[136], A. Ochi[83], I. Ochoa[39], J.P. Ochoa-Ricoux[147a], K. O'Connor[26],

JHEP03(2020)179

S. Oda[88], S. Odaka[82], S. Oerdek[53], A. Ogrodnik[84a], A. Oh[101], S.H. Oh[49], C.C. Ohm[154], H. Oide[165], M.L. Ojeda[167], H. Okawa[169], Y. Okazaki[86], Y. Okumura[163], T. Okuyama[82], A. Olariu[27b], L.F. Oleiro Seabra[140a], S.A. Olivares Pino[147a], D. Oliveira Damazio[29], J.L. Oliver[1], M.J.R. Olsson[171], A. Olszewski[85], J. Olszowska[85], D.C. O'Neil[152], A.P. O'neill[135], A. Onofre[140a,140e], P.U.E. Onyisi[11], H. Oppen[134], M.J. Oreglia[37], G.E. Orellana[89], D. Orestano[75a,75b], N. Orlando[14], R.S. Orr[167], V. O'Shea[57], R. Ospanov[60a], G. Otero y Garzon[30], H. Otono[88], P.S. Ott[61a], M. Ouchrif[35d], J. Ouellette[29], F. Ould-Saada[134], A. Ouraou[145], Q. Ouyang[15a], M. Owen[57], R.E. Owen[21], V.E. Ozcan[12c], N. Ozturk[8], J. Pacalt[131], H.A. Pacey[32], K. Pachal[49], A. Pacheco Pages[14], C. Padilla Aranda[14], S. Pagan Griso[18], M. Paganini[183], G. Palacino[66], S. Palazzo[50], S. Palestini[36], M. Palka[84b], D. Pallin[38], I. Panagoulias[10], C.E. Pandini[36], J.G. Panduro Vazquez[94], P. Pani[46], G. Panizzo[67a,67c], L. Paolozzi[54], C. Papadatos[110], K. Papageorgiou[9,h], S. Parajuli[43], A. Paramonov[6], D. Paredes Hernandez[63b], S.R. Paredes Saenz[135], B. Parida[166], T.H. Park[167], A.J. Parker[31], M.A. Parker[32], F. Parodi[55b,55a], E.W. Parrish[121], J.A. Parsons[39], U. Parzefall[52], L. Pascual Dominguez[136], V.R. Pascuzzi[167], J.M.P. Pasner[146], F. Pasquali[120], E. Pasqualucci[73a], S. Passaggio[55b], F. Pastore[94], P. Pasuwan[45a,45b], S. Pataraia[100], J.R. Pater[101], A. Pathak[181,j], T. Pauly[36], B. Pearson[115], M. Pedersen[134], L. Pedraza Diaz[119], R. Pedro[140a], T. Peiffer[53], S.V. Peleganchuk[122b,122a], O. Penc[141], H. Peng[60a], B.S. Peralva[81a], M.M. Perego[65], A.P. Pereira Peixoto[140a], D.V. Perepelitsa[29], F. Peri[19], L. Perini[69a,69b], H. Pernegger[36], S. Perrella[70a,70b], K. Peters[46], R.F.Y. Peters[101], B.A. Petersen[36], T.C. Petersen[40], E. Petit[102], A. Petridis[1], C. Petridou[162], P. Petroff[65], M. Petrov[135], F. Petrucci[75a,75b], M. Pettee[183], N.E. Pettersson[103], K. Petukhova[143], A. Peyaud[145], R. Pezoa[147c], L. Pezzotti[71a,71b], T. Pham[105], F.H. Phillips[107], P.W. Phillips[144], M.W. Phipps[173], G. Piacquadio[155], E. Pianori[18], A. Picazio[103], R.H. Pickles[101], R. Piegaia[30], D. Pietreanu[27b], J.E. Pilcher[37], A.D. Pilkington[101], M. Pinamonti[74a,74b], J.L. Pinfold[3], M. Pitt[161], L. Pizzimento[74a,74b], M.-A. Pleier[29], V. Pleskot[143], E. Plotnikova[80], P. Podberezko[122b,122a], R. Poettgen[97], R. Poggi[54], L. Poggioli[65], I. Pogrebnyak[107], D. Pohl[24], I. Pokharel[53], G. Polesello[71a], A. Poley[18], A. Policicchio[73a,73b], R. Polifka[143], A. Polini[23b], C.S. Pollard[46], V. Polychronakos[29], D. Ponomarenko[112], L. Pontecorvo[36], S. Popa[27a], G.A. Popeneciu[27d], L. Portales[5], D.M. Portillo Quintero[58], S. Pospisil[142], K. Potamianos[46], I.N. Potrap[80], C.J. Potter[32], H. Potti[11], T. Poulsen[97], J. Poveda[36], T.D. Powell[149], G. Pownall[46], M.E. Pozo Astigarraga[36], P. Pralavorio[102], S. Prell[79], D. Price[101], M. Primavera[68a], S. Prince[104], M.L. Proffitt[148], N. Proklova[112], K. Prokofiev[63c], F. Prokoshin[80], S. Protopopescu[29], J. Proudfoot[6], M. Przybycien[84a], D. Pudzha[138], A. Puri[173], P. Puzo[65], J. Qian[106], Y. Qin[101], A. Quadt[53], M. Queitsch-Maitland[46], A. Qureshi[1], M. Racko[28a], P. Rados[105], F. Ragusa[69a,69b], G. Rahal[98], J.A. Raine[54], S. Rajagopalan[29], A. Ramirez Morales[93], K. Ran[15a,15d], T. Rashid[65], S. Raspopov[5], D.M. Rauch[46], F. Rauscher[114], S. Rave[100], B. Ravina[149], I. Ravinovich[180], J.H. Rawling[101], M. Raymond[36], A.L. Read[134], N.P. Readioff[58], M. Reale[68a,68b], D.M. Rebuzzi[71a,71b], A. Redelbach[177], G. Redlinger[29], K. Reeves[43], L. Rehnisch[19], J. Reichert[137], D. Reikher[161], A. Reiss[100], A. Rej[151], C. Rembser[36], M. Renda[27b], M. Rescigno[73a], S. Resconi[69a], E.D. Resseguie[137], S. Rettie[175], E. Reynolds[21], O.L. Rezanova[122b,122a], P. Reznicek[143], E. Ricci[76a,76b], R. Richter[115], S. Richter[46], E. Richter-Was[84b], O. Ricken[24], M. Ridel[136], P. Rieck[115], O. Rifki[46], M. Rijssenbeek[155], A. Rimoldi[71a,71b], M. Rimoldi[46], L. Rinaldi[23b], G. Ripellino[154], I. Riu[14], J.C. Rivera Vergara[176], F. Rizatdinova[130], E. Rizvi[93], C. Rizzi[36], R.T. Roberts[101], S.H. Robertson[104,af], M. Robin[46], D. Robinson[32], J.E.M. Robinson[46], C.M. Robles Gajardo[147c], A. Robson[57], A. Rocchi[74a,74b], E. Rocco[100], C. Roda[72a,72b], S. Rodriguez Bosca[174], A. Rodriguez Perez[14], D. Rodriguez Rodriguez[174], A.M. Rodríguez Vera[168b], S. Roe[36], O. Røhne[134], R. Röhrig[115], R.A. Rojas[147c], C.P.A. Roland[66], J. Roloff[29], A. Romaniouk[112], M. Romano[23b,23a], N. Rompotis[91], M. Ronzani[125], L. Roos[136],

JHEP03(2020)179

S. Rosati[73a], K. Rosbach[52], G. Rosin[103], B.J. Rosser[137], E. Rossi[46], E. Rossi[75a,75b], E. Rossi[70a,70b], L.P. Rossi[55b], L. Rossini[69a,69b], R. Rosten[14], M. Rotaru[27b], J. Rothberg[148], D. Rousseau[65], G. Rovelli[71a,71b], A. Roy[11], D. Roy[33e], A. Rozanov[102], Y. Rozen[160], X. Ruan[33e], F. Rühr[52], A. Ruiz-Martinez[174], A. Rummler[36], Z. Rurikova[52], N.A. Rusakovich[80], H.L. Russell[104], L. Rustige[38,47], J.P. Rutherfoord[7], E.M. Rüttinger[149], M. Rybar[39], G. Rybkin[65], E.B. Rye[134], A. Ryzhov[123], J.A. Sabater Iglesias[46], P. Sabatini[53], G. Sabato[120], S. Sacerdoti[65], H.F-W. Sadrozinski[146], R. Sadykov[80], F. Safai Tehrani[73a], B. Safarzadeh Samani[156], P. Saha[121], S. Saha[104], M. Sahinsoy[61a], A. Sahu[182], M. Saimpert[46], M. Saito[163], T. Saito[163], H. Sakamoto[163], A. Sakharov[125,an], D. Salamani[54], G. Salamanna[75a,75b], J.E. Salazar Loyola[147c], A. Salnikov[153], J. Salt[174], D. Salvatore[41b,41a], F. Salvatore[156], A. Salvucci[63a,63b,63c], A. Salzburger[36], J. Samarati[36], D. Sammel[52], D. Sampsonidis[162], D. Sampsonidou[162], J. Sánchez[174], A. Sanchez Pineda[67a,36,67c], H. Sandaker[134], C.O. Sander[46], I.G. Sanderswood[90], M. Sandhoff[182], C. Sandoval[22], D.P.C. Sankey[144], M. Sannino[55b,55a], Y. Sano[117], A. Sansoni[51], C. Santoni[38], H. Santos[140a,140b], S.N. Santpur[18], A. Santra[174], A. Sapronov[80], J.G. Saraiva[140a,140d], O. Sasaki[82], K. Sato[169], F. Sauerburger[52], E. Sauvan[5], P. Savard[167,ax], N. Savic[115], R. Sawada[163], C. Sawyer[144], L. Sawyer[96,al], C. Sbarra[23b], A. Sbrizzi[23a], T. Scanlon[95], J. Schaarschmidt[148], P. Schacht[115], B.M. Schachtner[114], D. Schaefer[37], L. Schaefer[137], J. Schaeffer[100], S. Schaepe[36], U. Schäfer[100], A.C. Schaffer[65], D. Schaile[114], R.D. Schamberger[155], N. Scharmberg[101], V.A. Schegelsky[138], D. Scheirich[143], F. Schenck[19], M. Schernau[171], C. Schiavi[55b,55a], S. Schier[146], L.K. Schildgen[24], Z.M. Schillaci[26], E.J. Schioppa[36], M. Schioppa[41b,41a], K.E. Schleicher[52], S. Schlenker[36], K.R. Schmidt-Sommerfeld[115], K. Schmieden[36], C. Schmitt[100], S. Schmitt[46], S. Schmitz[100], J.C. Schmoeckel[46], U. Schnoor[52], L. Schoeffel[145], A. Schoening[61b], P.G. Scholer[52], E. Schopf[135], M. Schott[100], J.F.P. Schouwenberg[119], J. Schovancova[36], S. Schramm[54], F. Schroeder[182], A. Schulte[100], H-C. Schultz-Coulon[61a], M. Schumacher[52], B.A. Schumm[146], Ph. Schune[145], A. Schwartzman[153], T.A. Schwarz[106], Ph. Schwemling[145], R. Schwienhorst[107], A. Sciandra[146], G. Sciolla[26], M. Scodeggio[46], M. Scornajenghi[41b,41a], F. Scuri[72a], F. Scutti[105], L.M. Scyboz[115], C.D. Sebastiani[73a,73b], P. Seema[19], S.C. Seidel[118], A. Seiden[146], B.D. Seidlitz[29], T. Seiss[37], J.M. Seixas[81b], G. Sekhniaidze[70a], K. Sekhon[106], S.J. Sekula[42], N. Semprini-Cesari[23b,23a], S. Sen[49], C. Serfon[77], L. Serin[65], L. Serkin[67a,67b], M. Sessa[60a], H. Severini[129], T. Šfiligoj[92], F. Sforza[55b,55a], A. Sfyrla[54], E. Shabalina[53], J.D. Shahinian[146], N.W. Shaikh[45a,45b], D. Shaked Renous[180], L.Y. Shan[15a], J.T. Shank[25], M. Shapiro[18], A. Sharma[135], A.S. Sharma[1], P.B. Shatalov[124], K. Shaw[156], S.M. Shaw[101], A. Shcherbakova[138], M. Shehade[180], Y. Shen[129], N. Sherafati[34], A.D. Sherman[25], P. Sherwood[95], L. Shi[158,at], S. Shimizu[82], C.O. Shimmin[183], Y. Shimogama[179], M. Shimojima[116], I.P.J. Shipsey[135], S. Shirabe[88], M. Shiyakova[80,ad], J. Shlomi[180], A. Shmeleva[111], M.J. Shochet[37], J. Shojaii[105], D.R. Shope[129], S. Shrestha[127], E.M. Shrif[33e], E. Shulga[180], P. Sicho[141], A.M. Sickles[173], P.E. Sidebo[154], E. Sideras Haddad[33e], O. Sidiropoulou[36], A. Sidoti[23b,23a], F. Siegert[48], Dj. Sijacki[16], M.Jr. Silva[181], M.V. Silva Oliveira[81a], S.B. Silverstein[45a], S. Simion[65], E. Simioni[100], R. Simoniello[100], S. Simsek[12b], P. Sinervo[167], V. Sinetckii[113,111], N.B. Sinev[132], M. Sioli[23b,23a], I. Siral[106], S.Yu. Sivoklokov[113], J. Sjölin[45a,45b], E. Skorda[97], P. Skubic[129], M. Slawinska[85], K. Sliwa[170], R. Slovak[143], V. Smakhtin[180], B.H. Smart[144], J. Smiesko[28a], N. Smirnov[112], S.Yu. Smirnov[112], Y. Smirnov[112], L.N. Smirnova[113,v], O. Smirnova[97], J.W. Smith[53], M. Smizanska[90], K. Smolek[142], A. Smykiewicz[85], A.A. Snesarev[111], H.L. Snoek[120], I.M. Snyder[132], S. Snyder[29], R. Sobie[176,af], A. Soffer[161], A. Søgaard[50], F. Sohns[53], C.A. Solans Sanchez[36], E.Yu. Soldatov[112], U. Soldevila[174], A.A. Solodkov[123], A. Soloshenko[80], O.V. Solovyanov[123], V. Solovyev[138], P. Sommer[149], H. Son[170], W. Song[144], W.Y. Song[168b], A. Sopczak[142], F. Sopkova[28b], C.L. Sotiropoulou[72a,72b], S. Sottocornola[71a,71b], R. Soualah[67a,67c,g], A.M. Soukharev[122b,122a], D. South[46], S. Spagnolo[68a,68b], M. Spalla[115], M. Spangenberg[178],

JHEP03(2020)179

F. Spanò[94], D. Sperlich[52], T.M. Spieker[61a], R. Spighi[23b], G. Spigo[36], M. Spina[156], D.P. Spiteri[57], M. Spousta[143], A. Stabile[69a,69b], B.L. Stamas[121], R. Stamen[61a], M. Stamenkovic[120], E. Stanecka[85], B. Stanislaus[135], M.M. Stanitzki[46], M. Stankaityte[135], B. Stapf[120], E.A. Starchenko[123], G.H. Stark[146], J. Stark[58], S.H. Stark[40], P. Staroba[141], P. Starovoitov[61a], S. Stärz[104], R. Staszewski[85], G. Stavropoulos[44], M. Stegler[46], P. Steinberg[29], A.L. Steinhebel[132], B. Stelzer[152], H.J. Stelzer[139], O. Stelzer-Chilton[168a], H. Stenzel[56], T.J. Stevenson[156], G.A. Stewart[36], M.C. Stockton[36], G. Stoicea[27b], M. Stolarski[140a], S. Stonjek[115], A. Straessner[48], J. Strandberg[154], S. Strandberg[45a,45b], M. Strauss[129], P. Strizenec[28b], R. Ströhmer[177], D.M. Strom[132], R. Stroynowski[42], A. Strubig[50], S.A. Stucci[29], B. Stugu[17], J. Stupak[129], N.A. Styles[46], D. Su[153], S. Suchek[61a], V.V. Sulin[111], M.J. Sullivan[91], D.M.S. Sultan[54], S. Sultansoy[4c], T. Sumida[86], S. Sun[106], X. Sun[3], K. Suruliz[156], C.J.E. Suster[157], M.R. Sutton[156], S. Suzuki[82], M. Svatos[141], M. Swiatlowski[37], S.P. Swift[2], T. Swirski[177], A. Sydorenko[100], I. Sykora[28a], M. Sykora[143], T. Sykora[143], D. Ta[100], K. Tackmann[46,ab], J. Taenzer[161], A. Taffard[171], R. Tafirout[168a], H. Takai[29], R. Takashima[87], K. Takeda[83], T. Takeshita[150], E.P. Takeva[50], Y. Takubo[82], M. Talby[102], A.A. Talyshev[122b,122a], N.M. Tamir[161], J. Tanaka[163], M. Tanaka[165], R. Tanaka[65], S. Tapia Araya[173], S. Tapprogge[100], A. Tarek Abouelfadl Mohamed[136], S. Tarem[160], K. Tariq[60b], G. Tarna[27b,c], G.F. Tartarelli[69a], P. Tas[143], M. Tasevsky[141], T. Tashiro[86], E. Tassi[41b,41a], A. Tavares Delgado[140a,140b], Y. Tayalati[35e], A.J. Taylor[50], G.N. Taylor[105], W. Taylor[168b], A.S. Tee[90], R. Teixeira De Lima[153], P. Teixeira-Dias[94], H. Ten Kate[36], J.J. Teoh[120], S. Terada[82], K. Terashi[163], J. Terron[99], S. Terzo[14], M. Testa[51], R.J. Teuscher[167,af], S.J. Thais[183], T. Theveneaux-Pelzer[46], F. Thiele[40], D.W. Thomas[94], J.O. Thomas[42], J.P. Thomas[21], A.S. Thompson[57], P.D. Thompson[21], L.A. Thomsen[183], E. Thomson[137], E.J. Thorpe[93], R.E. Ticse Torres[53], V.O. Tikhomirov[111,ap], Yu.A. Tikhonov[122b,122a], S. Timoshenko[112], P. Tipton[183], S. Tisserant[102], K. Todome[23b,23a], S. Todorova-Nova[5], S. Todt[48], J. Tojo[88], S. Tokár[28a], K. Tokushuku[82], E. Tolley[127], K.G. Tomiwa[33e], M. Tomoto[117], L. Tompkins[153,q], B. Tong[59], P. Tornambe[103], E. Torrence[132], H. Torres[48], E. Torró Pastor[148], C. Tosciri[135], J. Toth[102,ae], D.R. Tovey[149], A. Traeet[17], C.J. Treado[125], T. Trefzger[177], F. Tresoldi[156], A. Tricoli[29], I.M. Trigger[168a], S. Trincaz-Duvoid[136], W. Trischuk[167], B. Trocmé[58], A. Trofymov[145], C. Troncon[69a], M. Trovatelli[176], F. Trovato[156], L. Truong[33c], M. Trzebinski[85], A. Trzupek[85], F. Tsai[46], J.C-L. Tseng[135], P.V. Tsiareshka[108,ak], A. Tsirigotis[162], V. Tsiskaridze[155], E.G. Tskhadadze[159a], M. Tsopoulou[162], I.I. Tsukerman[124], V. Tsulaia[18], S. Tsuno[82], D. Tsybychev[155], Y. Tu[63b], A. Tudorache[27b], V. Tudorache[27b], T.T. Tulbure[27a], A.N. Tuna[59], S. Turchikhin[80], D. Turgeman[180], I. Turk Cakir[4b,w], R.J. Turner[21], R.T. Turra[69a], P.M. Tuts[39], S. Tzamarias[162], E. Tzovara[100], G. Ucchielli[47], K. Uchida[163], I. Ueda[82], M. Ughetto[45a,45b], F. Ukegawa[169], G. Unal[36], A. Undrus[29], G. Unel[171], F.C. Ungaro[105], Y. Unno[82], K. Uno[163], J. Urban[28b], P. Urquijo[105], G. Usai[8], Z. Uysal[12d], V. Vacek[142], B. Vachon[104], K.O.H. Vadla[134], A. Vaidya[95], C. Valderanis[114], E. Valdes Santurio[45a,45b], M. Valente[54], S. Valentinetti[23b,23a], A. Valero[174], L. Valéry[46], R.A. Vallance[21], A. Vallier[36], J.A. Valls Ferrer[174], T.R. Van Daalen[14], P. Van Gemmeren[6], I. Van Vulpen[120], M. Vanadia[74a,74b], W. Vandelli[36], E.R. Vandewall[130], A. Vaniachine[166], D. Vannicola[73a,73b], R. Vari[73a], E.W. Varnes[7], C. Varni[55b,55a], T. Varol[158], D. Varouchas[65], K.E. Varvell[157], M.E. Vasile[27b], G.A. Vasquez[176], J.G. Vasquez[183], F. Vazeille[38], D. Vazquez Furelos[14], T. Vazquez Schroeder[36], J. Veatch[53], V. Vecchio[75a,75b], M.J. Veen[120], L.M. Veloce[167], F. Veloso[140a,140c], S. Veneziano[73a], A. Ventura[68a,68b], N. Venturi[36], A. Verbytskyi[115], V. Vercesi[71a], M. Verducci[72a,72b], C.M. Vergel Infante[79], C. Vergis[24], W. Verkerke[120], A.T. Vermeulen[120], J.C. Vermeulen[120], M.C. Vetterli[152,ax], N. Viaux Maira[147c], M. Vicente Barreto Pinto[54], T. Vickey[149], O.E. Vickey Boeriu[149], G.H.A. Viehhauser[135], L. Vigani[61b], M. Villa[23b,23a], M. Villaplana Perez[69a,69b], E. Vilucchi[51], M.G. Vincter[34], G.S. Virdee[21], A. Vishwakarma[46],

JHEP03(2020)179

C. Vittori[23b,23a], I. Vivarelli[156], M. Vogel[182], P. Vokac[142], S.E. von Buddenbrock[33e], E. Von Toerne[24], V. Vorobel[143], K. Vorobev[112], M. Vos[174], J.H. Vossebeld[91], M. Vozak[101], N. Vranjes[16], M. Vranjes Milosavljevic[16], V. Vrba[142], M. Vreeswijk[120], R. Vuillermet[36], I. Vukotic[37], P. Wagner[24], W. Wagner[182], J. Wagner-Kuhr[114], S. Wahdan[182], H. Wahlberg[89], V.M. Walbrecht[115], J. Walder[90], R. Walker[114], S.D. Walker[94], W. Walkowiak[151], V. Wallangen[45a,45b], A.M. Wang[59], C. Wang[60c], C. Wang[60b], F. Wang[181], H. Wang[18], H. Wang[3], J. Wang[63a], J. Wang[157], J. Wang[61b], P. Wang[42], Q. Wang[129], R.-J. Wang[100], R. Wang[60a], R. Wang[6], S.M. Wang[158], W.T. Wang[60a], W. Wang[15c,ag], W.X. Wang[60a,ag], Y. Wang[60a,am], Z. Wang[60c], C. Wanotayaroj[46], A. Warburton[104], C.P. Ward[32], D.R. Wardrope[95], N. Warrack[57], A. Washbrook[50], A.T. Watson[21], M.F. Watson[21], G. Watts[148], B.M. Waugh[95], A.F. Webb[11], S. Webb[100], C. Weber[183], M.S. Weber[20], S.A. Weber[34], S.M. Weber[61a], A.R. Weidberg[135], J. Weingarten[47], M. Weirich[100], C. Weiser[52], P.S. Wells[36], T. Wenaus[29], T. Wengler[36], S. Wenig[36], N. Wermes[24], M.D. Werner[79], M. Wessels[61a], T.D. Weston[20], K. Whalen[132], N.L. Whallon[148], A.M. Wharton[90], A.S. White[106], A. White[8], M.J. White[1], D. Whiteson[171], B.W. Whitmore[90], W. Wiedenmann[181], M. Wielers[144], N. Wieseotte[100], C. Wiglesworth[40], L.A.M. Wiik-Fuchs[52], F. Wilk[101], H.G. Wilkens[36], L.J. Wilkins[94], H.H. Williams[137], S. Williams[32], C. Willis[107], S. Willocq[103], J.A. Wilson[21], I. Wingerter-Seez[5], E. Winkels[156], F. Winklmeier[132], O.J. Winston[156], B.T. Winter[52], M. Wittgen[153], M. Wobisch[96], A. Wolf[100], T.M.H. Wolf[120], R. Wolff[102], R. Wölker[135], J. Wollrath[52], M.W. Wolter[85], H. Wolters[140a,140c], V.W.S. Wong[175], N.L. Woods[146], S.D. Worm[21], B.K. Wosiek[85], K.W. Woźniak[85], K. Wraight[57], S.L. Wu[181], X. Wu[54], Y. Wu[60a], T.R. Wyatt[101], B.M. Wynne[50], S. Xella[40], Z. Xi[106], L. Xia[178], X. Xiao[106], I. Xiotidis[156], D. Xu[15a], H. Xu[60a,c], L. Xu[29], T. Xu[145], W. Xu[106], Z. Xu[60b], Z. Xu[153], B. Yabsley[157], S. Yacoob[33a], K. Yajima[133], D.P. Yallup[95], D. Yamaguchi[165], Y. Yamaguchi[165], A. Yamamoto[82], M. Yamatani[163], T. Yamazaki[163], Y. Yamazaki[83], Z. Yan[25], H.J. Yang[60c,60d], H.T. Yang[18], S. Yang[78], X. Yang[60b,58], Y. Yang[163], W-M. Yao[18], Y.C. Yap[46], Y. Yasu[82], E. Yatsenko[60c,60d], J. Ye[42], S. Ye[29], I. Yeletskikh[80], M.R. Yexley[90], E. Yigitbasi[25], K. Yorita[179], K. Yoshihara[137], C.J.S. Young[36], C. Young[153], J. Yu[79], R. Yuan[60b,i], X. Yue[61a], S.P.Y. Yuen[24], M. Zaazoua[35e], B. Zabinski[85], G. Zacharis[10], E. Zaffaroni[54], J. Zahreddine[136], A.M. Zaitsev[123,ao], T. Zakareishvili[159b], N. Zakharchuk[34], S. Zambito[59], D. Zanzi[36], D.R. Zaripovas[57], S.V. Zeißner[47], C. Zeitnitz[182], G. Zemaityte[135], J.C. Zeng[173], O. Zenin[123], T. Ženiš[28a], D. Zerwas[65], M. Zgubič[135], B. Zhang[15c], D.F. Zhang[15b], G. Zhang[15b], H. Zhang[15c], J. Zhang[6], L. Zhang[15c], L. Zhang[60a], M. Zhang[173], R. Zhang[24], X. Zhang[60b], Y. Zhang[15a,15d], Z. Zhang[63a], Z. Zhang[65], P. Zhao[49], Y. Zhao[60b], Z. Zhao[60a], A. Zhemchugov[80], Z. Zheng[106], D. Zhong[173], B. Zhou[106], C. Zhou[181], M.S. Zhou[15a,15d], M. Zhou[155], N. Zhou[60c], Y. Zhou[7], C.G. Zhu[60b], C. Zhu[15a,15d], H.L. Zhu[60a], H. Zhu[15a], J. Zhu[106], Y. Zhu[60a], X. Zhuang[15a], K. Zhukov[111], V. Zhulanov[122b,122a], D. Zieminska[66], N.I. Zimine[80], S. Zimmermann[52], Z. Zinonos[115], M. Ziolkowski[151], L. Živković[16], G. Zobernig[181], A. Zoccoli[23b,23a], K. Zoch[53], T.G. Zorbas[149], R. Zou[37], L. Zwalinski[36]

[1] *Department of Physics, University of Adelaide, Adelaide, Australia*
[2] *Physics Department, SUNY Albany, Albany NY, United States of America*
[3] *Department of Physics, University of Alberta, Edmonton AB, Canada*
[4] [(a)] *Department of Physics, Ankara University, Ankara;* [(b)] *Istanbul Aydin University, Istanbul;* [(c)] *Division of Physics, TOBB University of Economics and Technology, Ankara, Turkey*
[5] *LAPP, Université Grenoble Alpes, Université Savoie Mont Blanc, CNRS/IN2P3, Annecy, France*
[6] *High Energy Physics Division, Argonne National Laboratory, Argonne IL, United States of America*
[7] *Department of Physics, University of Arizona, Tucson AZ, United States of America*
[8] *Department of Physics, University of Texas at Arlington, Arlington TX, United States of America*
[9] *Physics Department, National and Kapodistrian University of Athens, Athens, Greece*
[10] *Physics Department, National Technical University of Athens, Zografou, Greece*

JHEP03(2020)179

[11] Department of Physics, University of Texas at Austin, Austin TX, United States of America
[12] [(a)] Bahcesehir University, Faculty of Engineering and Natural Sciences, Istanbul; [(b)] Istanbul Bilgi University, Faculty of Engineering and Natural Sciences, Istanbul; [(c)] Department of Physics, Bogazici University, Istanbul; [(d)] Department of Physics Engineering, Gaziantep University, Gaziantep, Turkey
[13] Institute of Physics, Azerbaijan Academy of Sciences, Baku, Azerbaijan
[14] Institut de Física d'Altes Energies (IFAE), Barcelona Institute of Science and Technology, Barcelona, Spain
[15] [(a)] Institute of High Energy Physics, Chinese Academy of Sciences, Beijing; [(b)] Physics Department, Tsinghua University, Beijing; [(c)] Department of Physics, Nanjing University, Nanjing; [(d)] University of Chinese Academy of Science (UCAS), Beijing, China
[16] Institute of Physics, University of Belgrade, Belgrade, Serbia
[17] Department for Physics and Technology, University of Bergen, Bergen, Norway
[18] Physics Division, Lawrence Berkeley National Laboratory and University of California, Berkeley CA, United States of America
[19] Institut für Physik, Humboldt Universität zu Berlin, Berlin, Germany
[20] Albert Einstein Center for Fundamental Physics and Laboratory for High Energy Physics, University of Bern, Bern, Switzerland
[21] School of Physics and Astronomy, University of Birmingham, Birmingham, United Kingdom
[22] Facultad de Ciencias y Centro de Investigaciónes, Universidad Antonio Nariño, Bogota, Colombia
[23] [(a)] INFN Bologna and Universita' di Bologna, Dipartimento di Fisica; [(b)] INFN Sezione di Bologna, Italy
[24] Physikalisches Institut, Universität Bonn, Bonn, Germany
[25] Department of Physics, Boston University, Boston MA, United States of America
[26] Department of Physics, Brandeis University, Waltham MA, United States of America
[27] [(a)] Transilvania University of Brasov, Brasov; [(b)] Horia Hulubei National Institute of Physics and Nuclear Engineering, Bucharest; [(c)] Department of Physics, Alexandru Ioan Cuza University of Iasi, Iasi; [(d)] National Institute for Research and Development of Isotopic and Molecular Technologies, Physics Department, Cluj-Napoca; [(e)] University Politehnica Bucharest, Bucharest; [(f)] West University in Timisoara, Timisoara, Romania
[28] [(a)] Faculty of Mathematics, Physics and Informatics, Comenius University, Bratislava; [(b)] Department of Subnuclear Physics, Institute of Experimental Physics of the Slovak Academy of Sciences, Kosice, Slovak Republic
[29] Physics Department, Brookhaven National Laboratory, Upton NY, United States of America
[30] Departamento de Física, Universidad de Buenos Aires, Buenos Aires, Argentina
[31] California State University, CA, United States of America
[32] Cavendish Laboratory, University of Cambridge, Cambridge, United Kingdom
[33] [(a)] Department of Physics, University of Cape Town, Cape Town; [(b)] iThemba Labs, Western Cape; [(c)] Department of Mechanical Engineering Science, University of Johannesburg, Johannesburg; [(d)] University of South Africa, Department of Physics, Pretoria; [(e)] School of Physics, University of the Witwatersrand, Johannesburg, South Africa
[34] Department of Physics, Carleton University, Ottawa ON, Canada
[35] [(a)] Faculté des Sciences Ain Chock, Réseau Universitaire de Physique des Hautes Energies — Université Hassan II, Casablanca; [(b)] Faculté des Sciences, Université Ibn-Tofail, Kénitra; [(c)] Faculté des Sciences Semlalia, Université Cadi Ayyad, LPHEA-Marrakech; [(d)] Faculté des Sciences, Université Mohamed Premier and LPTPM, Oujda; [(e)] Faculté des sciences, Université Mohammed V, Rabat, Morocco
[36] CERN, Geneva, Switzerland
[37] Enrico Fermi Institute, University of Chicago, Chicago IL, United States of America
[38] LPC, Université Clermont Auvergne, CNRS/IN2P3, Clermont-Ferrand, France
[39] Nevis Laboratory, Columbia University, Irvington NY, United States of America
[40] Niels Bohr Institute, University of Copenhagen, Copenhagen, Denmark

JHEP03(2020)179

[41] [(a)] Dipartimento di Fisica, Università della Calabria, Rende; [(b)] INFN Gruppo Collegato di Cosenza, Laboratori Nazionali di Frascati, Italy
[42] Physics Department, Southern Methodist University, Dallas TX, United States of America
[43] Physics Department, University of Texas at Dallas, Richardson TX, United States of America
[44] National Centre for Scientific Research "Demokritos", Agia Paraskevi, Greece
[45] [(a)] Department of Physics, Stockholm University; [(b)] Oskar Klein Centre, Stockholm, Sweden
[46] Deutsches Elektronen-Synchrotron DESY, Hamburg and Zeuthen, Germany
[47] Lehrstuhl für Experimentelle Physik IV, Technische Universität Dortmund, Dortmund, Germany
[48] Institut für Kern und Teilchenphysik, Technische Universität Dresden, Dresden, Germany
[49] Department of Physics, Duke University, Durham NC, United States of America
[50] SUPA — School of Physics and Astronomy, University of Edinburgh, Edinburgh, United Kingdom
[51] INFN e Laboratori Nazionali di Frascati, Frascati, Italy
[52] Physikalisches Institut, Albert-Ludwigs-Universität Freiburg, Freiburg, Germany
[53] II. Physikalisches Institut, Georg-August-Universität Göttingen, Göttingen, Germany
[54] Département de Physique Nucléaire et Corpusculaire, Université de Genève, Genève, Switzerland
[55] [(a)] Dipartimento di Fisica, Università di Genova, Genova; [(b)] INFN Sezione di Genova, Italy
[56] II. Physikalisches Institut, Justus-Liebig-Universität Giessen, Giessen, Germany
[57] SUPA — School of Physics and Astronomy, University of Glasgow, Glasgow, United Kingdom
[58] LPSC, Université Grenoble Alpes, CNRS/IN2P3, Grenoble INP, Grenoble, France
[59] Laboratory for Particle Physics and Cosmology, Harvard University, Cambridge MA, United States of America
[60] [(a)] Department of Modern Physics and State Key Laboratory of Particle Detection and Electronics, University of Science and Technology of China, Hefei; [(b)] Institute of Frontier and Interdisciplinary Science and Key Laboratory of Particle Physics and Particle Irradiation (MOE), Shandong University, Qingdao; [(c)] School of Physics and Astronomy, Shanghai Jiao Tong University, KLPPAC-MoE, SKLPPC, Shanghai; [(d)] Tsung-Dao Lee Institute, Shanghai, China
[61] [(a)] Kirchhoff-Institut für Physik, Ruprecht-Karls-Universität Heidelberg, Heidelberg; [(b)] Physikalisches Institut, Ruprecht-Karls-Universität Heidelberg, Heidelberg, Germany
[62] Faculty of Applied Information Science, Hiroshima Institute of Technology, Hiroshima, Japan
[63] [(a)] Department of Physics, Chinese University of Hong Kong, Shatin, N.T., Hong Kong; [(b)] Department of Physics, University of Hong Kong, Hong Kong; [(c)] Department of Physics and Institute for Advanced Study, Hong Kong University of Science and Technology, Clear Water Bay, Kowloon, Hong Kong, China
[64] Department of Physics, National Tsing Hua University, Hsinchu, Taiwan
[65] IJCLab, Université Paris-Saclay, CNRS/IN2P3, 91405, Orsay, France
[66] Department of Physics, Indiana University, Bloomington IN, United States of America
[67] [(a)] INFN Gruppo Collegato di Udine, Sezione di Trieste, Udine; [(b)] ICTP, Trieste; [(c)] Dipartimento Politecnico di Ingegneria e Architettura, Università di Udine, Udine, Italy
[68] [(a)] INFN Sezione di Lecce; [(b)] Dipartimento di Matematica e Fisica, Università del Salento, Lecce, Italy
[69] [(a)] INFN Sezione di Milano; [(b)] Dipartimento di Fisica, Università di Milano, Milano, Italy
[70] [(a)] INFN Sezione di Napoli; [(b)] Dipartimento di Fisica, Università di Napoli, Napoli, Italy
[71] [(a)] INFN Sezione di Pavia; [(b)] Dipartimento di Fisica, Università di Pavia, Pavia, Italy
[72] [(a)] INFN Sezione di Pisa; [(b)] Dipartimento di Fisica E. Fermi, Università di Pisa, Pisa, Italy
[73] [(a)] INFN Sezione di Roma; [(b)] Dipartimento di Fisica, Sapienza Università di Roma, Roma, Italy
[74] [(a)] INFN Sezione di Roma Tor Vergata; [(b)] Dipartimento di Fisica, Università di Roma Tor Vergata, Roma, Italy
[75] [(a)] INFN Sezione di Roma Tre; [(b)] Dipartimento di Matematica e Fisica, Università Roma Tre, Roma, Italy
[76] [(a)] INFN-TIFPA; [(b)] Università degli Studi di Trento, Trento, Italy
[77] Institut für Astro und Teilchenphysik, Leopold-Franzens-Universität, Innsbruck, Austria
[78] University of Iowa, Iowa City IA, United States of America

JHEP03(2020)179

[79] Department of Physics and Astronomy, Iowa State University, Ames IA, United States of America
[80] Joint Institute for Nuclear Research, Dubna, Russia
[81] [(a)] Departamento de Engenharia Elétrica, Universidade Federal de Juiz de Fora (UFJF), Juiz de Fora; [(b)] Universidade Federal do Rio De Janeiro COPPE/EE/IF, Rio de Janeiro; [(c)] Universidade Federal de São João del Rei (UFSJ), São João del Rei; [(d)] Instituto de Física, Universidade de São Paulo, São Paulo, Brazil
[82] KEK, High Energy Accelerator Research Organization, Tsukuba, Japan
[83] Graduate School of Science, Kobe University, Kobe, Japan
[84] [(a)] AGH University of Science and Technology, Faculty of Physics and Applied Computer Science, Krakow; [(b)] Marian Smoluchowski Institute of Physics, Jagiellonian University, Krakow, Poland
[85] Institute of Nuclear Physics Polish Academy of Sciences, Krakow, Poland
[86] Faculty of Science, Kyoto University, Kyoto, Japan
[87] Kyoto University of Education, Kyoto, Japan
[88] Research Center for Advanced Particle Physics and Department of Physics, Kyushu University, Fukuoka , Japan
[89] Instituto de Física La Plata, Universidad Nacional de La Plata and CONICET, La Plata, Argentina
[90] Physics Department, Lancaster University, Lancaster, United Kingdom
[91] Oliver Lodge Laboratory, University of Liverpool, Liverpool, United Kingdom
[92] Department of Experimental Particle Physics, Jožef Stefan Institute and Department of Physics, University of Ljubljana, Ljubljana, Slovenia
[93] School of Physics and Astronomy, Queen Mary University of London, London, United Kingdom
[94] Department of Physics, Royal Holloway University of London, Egham, United Kingdom
[95] Department of Physics and Astronomy, University College London, London, United Kingdom
[96] Louisiana Tech University, Ruston LA, United States of America
[97] Fysiska institutionen, Lunds universitet, Lund, Sweden
[98] Centre de Calcul de l'Institut National de Physique Nucléaire et de Physique des Particules (IN2P3), Villeurbanne, France
[99] Departamento de Física Teorica C-15 and CIAFF, Universidad Autónoma de Madrid, Madrid, Spain
[100] Institut für Physik, Universität Mainz, Mainz, Germany
[101] School of Physics and Astronomy, University of Manchester, Manchester, United Kingdom
[102] CPPM, Aix-Marseille Université, CNRS/IN2P3, Marseille, France
[103] Department of Physics, University of Massachusetts, Amherst MA, United States of America
[104] Department of Physics, McGill University, Montreal QC, Canada
[105] School of Physics, University of Melbourne, Victoria, Australia
[106] Department of Physics, University of Michigan, Ann Arbor MI, United States of America
[107] Department of Physics and Astronomy, Michigan State University, East Lansing MI, United States of America
[108] B.I. Stepanov Institute of Physics, National Academy of Sciences of Belarus, Minsk, Belarus
[109] Research Institute for Nuclear Problems of Byelorussian State University, Minsk, Belarus
[110] Group of Particle Physics, University of Montreal, Montreal QC, Canada
[111] P.N. Lebedev Physical Institute of the Russian Academy of Sciences, Moscow, Russia
[112] National Research Nuclear University MEPhI, Moscow, Russia
[113] D.V. Skobeltsyn Institute of Nuclear Physics, M.V. Lomonosov Moscow State University, Moscow, Russia
[114] Fakultät für Physik, Ludwig-Maximilians-Universität München, München, Germany
[115] Max-Planck-Institut für Physik (Werner-Heisenberg-Institut), München, Germany
[116] Nagasaki Institute of Applied Science, Nagasaki, Japan
[117] Graduate School of Science and Kobayashi-Maskawa Institute, Nagoya University, Nagoya, Japan
[118] Department of Physics and Astronomy, University of New Mexico, Albuquerque NM, United States of America
[119] Institute for Mathematics, Astrophysics and Particle Physics, Radboud University Nijmegen/Nikhef, Nijmegen, Netherlands

JHEP03(2020)179

[120] Nikhef National Institute for Subatomic Physics and University of Amsterdam, Amsterdam, Netherlands
[121] Department of Physics, Northern Illinois University, DeKalb IL, United States of America
[122] [(a)] Budker Institute of Nuclear Physics and NSU, SB RAS, Novosibirsk; [(b)] Novosibirsk State University Novosibirsk, Russia
[123] Institute for High Energy Physics of the National Research Centre Kurchatov Institute, Protvino, Russia
[124] Institute for Theoretical and Experimental Physics named by A.I. Alikhanov of National Research Centre "Kurchatov Institute", Moscow, Russia
[125] Department of Physics, New York University, New York NY, United States of America
[126] Ochanomizu University, Otsuka, Bunkyo-ku, Tokyo, Japan
[127] Ohio State University, Columbus OH, United States of America
[128] Faculty of Science, Okayama University, Okayama, Japan
[129] Homer L. Dodge Department of Physics and Astronomy, University of Oklahoma, Norman OK, United States of America
[130] Department of Physics, Oklahoma State University, Stillwater OK, United States of America
[131] Palacký University, RCPTM, Joint Laboratory of Optics, Olomouc, Czech Republic
[132] Center for High Energy Physics, University of Oregon, Eugene OR, United States of America
[133] Graduate School of Science, Osaka University, Osaka, Japan
[134] Department of Physics, University of Oslo, Oslo, Norway
[135] Department of Physics, Oxford University, Oxford, United Kingdom
[136] LPNHE, Sorbonne Université, Université de Paris, CNRS/IN2P3, Paris, France
[137] Department of Physics, University of Pennsylvania, Philadelphia PA, United States of America
[138] Konstantinov Nuclear Physics Institute of National Research Centre "Kurchatov Institute", PNPI, St. Petersburg, Russia
[139] Department of Physics and Astronomy, University of Pittsburgh, Pittsburgh PA, United States of America
[140] [(a)] Laboratório de Instrumentação e Física Experimental de Partículas — LIP, Lisboa; [(b)] Departamento de Física, Faculdade de Ciências, Universidade de Lisboa, Lisboa; [(c)] Departamento de Física, Universidade de Coimbra, Coimbra; [(d)] Centro de Física Nuclear da Universidade de Lisboa, Lisboa; [(e)] Departamento de Física, Universidade do Minho, Braga; [(f)] Departamento de Física Teórica y del Cosmos, Universidad de Granada, Granada (Spain); [(g)] Departamento de Física and CEFITEC of Faculdade de Ciências e Tecnologia, Universidade Nova de Lisboa, Caparica; [(h)] Instituto Superior Técnico, Universidade de Lisboa, Lisboa, Portugal
[141] Institute of Physics of the Czech Academy of Sciences, Prague, Czech Republic
[142] Czech Technical University in Prague, Prague, Czech Republic
[143] Charles University, Faculty of Mathematics and Physics, Prague, Czech Republic
[144] Particle Physics Department, Rutherford Appleton Laboratory, Didcot, United Kingdom
[145] IRFU, CEA, Université Paris-Saclay, Gif-sur-Yvette, France
[146] Santa Cruz Institute for Particle Physics, University of California Santa Cruz, Santa Cruz CA, United States of America
[147] [(a)] Departamento de Física, Pontificia Universidad Católica de Chile, Santiago; [(b)] Universidad Andres Bello, Department of Physics, Santiago; [(c)] Departamento de Física, Universidad Técnica Federico Santa María, Valparaíso, Chile
[148] Department of Physics, University of Washington, Seattle WA, United States of America
[149] Department of Physics and Astronomy, University of Sheffield, Sheffield, United Kingdom
[150] Department of Physics, Shinshu University, Nagano, Japan
[151] Department Physik, Universität Siegen, Siegen, Germany
[152] Department of Physics, Simon Fraser University, Burnaby BC, Canada
[153] SLAC National Accelerator Laboratory, Stanford CA, United States of America
[154] Physics Department, Royal Institute of Technology, Stockholm, Sweden
[155] Departments of Physics and Astronomy, Stony Brook University, Stony Brook NY, United States of America

JHEP03(2020)179

[156] Department of Physics and Astronomy, University of Sussex, Brighton, United Kingdom
[157] School of Physics, University of Sydney, Sydney, Australia
[158] Institute of Physics, Academia Sinica, Taipei, Taiwan
[159] [(a)] E. Andronikashvili Institute of Physics, Iv. Javakhishvili Tbilisi State University, Tbilisi; [(b)] High Energy Physics Institute, Tbilisi State University, Tbilisi, Georgia
[160] Department of Physics, Technion, Israel Institute of Technology, Haifa, Israel
[161] Raymond and Beverly Sackler School of Physics and Astronomy, Tel Aviv University, Tel Aviv, Israel
[162] Department of Physics, Aristotle University of Thessaloniki, Thessaloniki, Greece
[163] International Center for Elementary Particle Physics and Department of Physics, University of Tokyo, Tokyo, Japan
[164] Graduate School of Science and Technology, Tokyo Metropolitan University, Tokyo, Japan
[165] Department of Physics, Tokyo Institute of Technology, Tokyo, Japan
[166] Tomsk State University, Tomsk, Russia
[167] Department of Physics, University of Toronto, Toronto ON, Canada
[168] [(a)] TRIUMF, Vancouver BC; [(b)] Department of Physics and Astronomy, York University, Toronto ON, Canada
[169] Division of Physics and Tomonaga Center for the History of the Universe, Faculty of Pure and Applied Sciences, University of Tsukuba, Tsukuba, Japan
[170] Department of Physics and Astronomy, Tufts University, Medford MA, United States of America
[171] Department of Physics and Astronomy, University of California Irvine, Irvine CA, United States of America
[172] Department of Physics and Astronomy, University of Uppsala, Uppsala, Sweden
[173] Department of Physics, University of Illinois, Urbana IL, United States of America
[174] Instituto de Física Corpuscular (IFIC), Centro Mixto Universidad de Valencia — CSIC, Valencia, Spain
[175] Department of Physics, University of British Columbia, Vancouver BC, Canada
[176] Department of Physics and Astronomy, University of Victoria, Victoria BC, Canada
[177] Fakultät für Physik und Astronomie, Julius-Maximilians-Universität Würzburg, Würzburg, Germany
[178] Department of Physics, University of Warwick, Coventry, United Kingdom
[179] Waseda University, Tokyo, Japan
[180] Department of Particle Physics, Weizmann Institute of Science, Rehovot, Israel
[181] Department of Physics, University of Wisconsin, Madison WI, United States of America
[182] Fakultät für Mathematik und Naturwissenschaften, Fachgruppe Physik, Bergische Universität Wuppertal, Wuppertal, Germany
[183] Department of Physics, Yale University, New Haven CT, United States of America
[184] Yerevan Physics Institute, Yerevan, Armenia

[a] Also at Borough of Manhattan Community College, City University of New York, New York NY, United States of America
[b] Also at CERN, Geneva, Switzerland
[c] Also at CPPM, Aix-Marseille Université, CNRS/IN2P3, Marseille, France
[d] Also at Département de Physique Nucléaire et Corpusculaire, Université de Genève, Genève, Switzerland
[e] Also at Departament de Fisica de la Universitat Autonoma de Barcelona, Barcelona, Spain
[f] Also at Departamento de Física, Instituto Superior Técnico, Universidade de Lisboa, Lisboa, Portugal
[g] Also at Department of Applied Physics and Astronomy, University of Sharjah, Sharjah, United Arab Emirates
[h] Also at Department of Financial and Management Engineering, University of the Aegean, Chios, Greece

JHEP03(2020)179

[i] Also at Department of Physics and Astronomy, Michigan State University, East Lansing MI, United States of America
[j] Also at Department of Physics and Astronomy, University of Louisville, Louisville, KY, United States of America
[k] Also at Department of Physics, Ben Gurion University of the Negev, Beer Sheva, Israel
[l] Also at Department of Physics, California State University, East Bay, United States of America
[m] Also at Department of Physics, California State University, Fresno, United States of America
[n] Also at Department of Physics, California State University, Sacramento, United States of America
[o] Also at Department of Physics, King's College London, London, United Kingdom
[p] Also at Department of Physics, St. Petersburg State Polytechnical University, St. Petersburg, Russia
[q] Also at Department of Physics, Stanford University, Stanford CA, United States of America
[r] Also at Department of Physics, University of Adelaide, Adelaide, Australia
[s] Also at Department of Physics, University of Fribourg, Fribourg, Switzerland
[t] Also at Department of Physics, University of Michigan, Ann Arbor MI, United States of America
[u] Also at Dipartimento di Matematica, Informatica e Fisica, Università di Udine, Udine, Italy
[v] Also at Faculty of Physics, M.V. Lomonosov Moscow State University, Moscow, Russia
[w] Also at Giresun University, Faculty of Engineering, Giresun, Turkey
[x] Also at Graduate School of Science, Osaka University, Osaka, Japan
[y] Also at Hellenic Open University, Patras, Greece
[z] Also at IJCLab, Université Paris-Saclay, CNRS/IN2P3, 91405, Orsay, France
[aa] Also at Institucio Catalana de Recerca i Estudis Avancats, ICREA, Barcelona, Spain
[ab] Also at Institut für Experimentalphysik, Universität Hamburg, Hamburg, Germany
[ac] Also at Institute for Mathematics, Astrophysics and Particle Physics, Radboud University Nijmegen/Nikhef, Nijmegen, Netherlands
[ad] Also at Institute for Nuclear Research and Nuclear Energy (INRNE) of the Bulgarian Academy of Sciences, Sofia, Bulgaria
[ae] Also at Institute for Particle and Nuclear Physics, Wigner Research Centre for Physics, Budapest, Hungary
[af] Also at Institute of Particle Physics (IPP), Vancouver, Canada
[ag] Also at Institute of Physics, Academia Sinica, Taipei, Taiwan
[ah] Also at Institute of Physics, Azerbaijan Academy of Sciences, Baku, Azerbaijan
[ai] Also at Institute of Theoretical Physics, Ilia State University, Tbilisi, Georgia
[aj] Also at Instituto de Fisica Teorica, IFT-UAM/CSIC, Madrid, Spain
[ak] Also at Joint Institute for Nuclear Research, Dubna, Russia
[al] Also at Louisiana Tech University, Ruston LA, United States of America
[am] Also at LPNHE, Sorbonne Université, Université de Paris, CNRS/IN2P3, Paris, France
[an] Also at Manhattan College, New York NY, United States of America
[ao] Also at Moscow Institute of Physics and Technology State University, Dolgoprudny, Russia
[ap] Also at National Research Nuclear University MEPhI, Moscow, Russia
[aq] Also at Physics Department, An-Najah National University, Nablus, Palestine
[ar] Also at Physics Dept, University of South Africa, Pretoria, South Africa
[as] Also at Physikalisches Institut, Albert-Ludwigs-Universität Freiburg, Freiburg, Germany
[at] Also at School of Physics, Sun Yat-sen University, Guangzhou, China
[au] Also at The City College of New York, New York NY, United States of America
[av] Also at The Collaborative Innovation Center of Quantum Matter (CICQM), Beijing, China
[aw] Also at Tomsk State University, Tomsk, and Moscow Institute of Physics and Technology State University, Dolgoprudny, Russia
[ax] Also at TRIUMF, Vancouver BC, Canada
[ay] Also at Universita di Napoli Parthenope, Napoli, Italy
[*] Deceased

JHEP03(2020)179